Manganese Toxicity in Yeast and Plants

Wannapisit Thammakul

A Thesis Submitted in Partial Fulfillment of the Requirements for the Degree of

Master of Science in Technology and Environmental Management

Prince of Songkla University

2019

Manganese Toxicity in Yeast and Plants

Wannapisit Thammakul

A Thesis Submitted in Partial Fulfillment of the Requirements for the Degree of

Master of Science in Technology and Environmental Management

Prince of Songkla University

2019

Thesis Title	Manganese Toxicity in Yeast and Plants
Author	Mr. Wannapisit Thammakul
Major Program	Technology and Environmental Management

Major Advisor

.....

(Assoc. Prof. Dr. Raymond J. Ritchie)

Co-advisor

.....

(Assist. Prof. Dr. Sutsawat Duangsrisai)

Examining Committee:

.....Chairperson

(Assoc. Prof. Dr. Aree Choodum)

.....Committee

(Assoc. Prof. Dr. Raymond J. Ritchie)

.....Committee

(Assist. Prof. Dr. Sutsawat Duangsrisai)

.....Committee

(Assoc. Prof. Dr. Srunya Vajrodaya)

The Graduate School, Prince of Songkla University, has approved this thesis as partial fulfillment of the requirements for the Master of Science in Technology and Environment Degree in Technology and Environmental Management.

…….

(Prof. Dr. Damrongsak Faroongsarng)

Dean of Graduate School

This is to certify that the work here submitted is the result of the candidate's own investigations. Due acknowledgement has been made of any assistance received.

……..…….Signature

(Assoc. Prof. Dr. Raymond J. Ritchie)

Major Advisor

……..…….Signature

(Mr. Wannapisit Thammakul)

Candidate

I hereby certify that this work has not been accepted in substance for any degree, and is not being currently submitted in candidature for any degree.

……..…….Signature

(Mr. Wannapisit Thammakul)

Candidate

Thesis Title Manganese Toxicity in Yeast and Plants

Author Mr. Wannapisit Thammakul

Major Program Technology and Environmental Management

Academic Year 2018

ABSTRACT

Manganese (Mn) is normally present in soils as the insoluble, harmless MnO_2. Toxic Mn^{2+} of manganese is formed in acid soils but there is little consensus on the physiological basis of Mn toxicity in plants. Yeast, algae and vascular plants share similar membrane transport mechanisms and so yeast (*Saccharomyces cerevisiae*) and *Chlorella vulgaris* provides a convenient model system for studies of Mn–toxicity. Early effects upon Mn toxicity in *S. cerevisiae* in the exponential growth phase over of 24 hours was examined in culture tubes and for 6 days in the freshwater aquatic angiosperm *Lemna minor* in petri dishes at various Mn concentrations (10, 30, 100, 300, 1000, 3000 mmol m^{-3}). While *C. vulgaris* was examined with oxygenic photosynthesis after incubated 2 hours in 1, 2, 3, 5, 7 and 10 mol m^{-3} Mn concentration. *S. cerevisiae* grew exponentially and growth was followed by measuring optic density (OD). *C. vulgaris* was followed oxygenic photosynthesis using junior PAM machine. Growth of *L. minor* was followed using leaf count, Chlorophyll *a* content and absorptance of the plants. Mn has toxic effects on the *S. cerevisiae* cells (K_i = 1.884 ± 0.673 mol m^{-3}) and *L. minor* (K_i = 1.154 ± 0.282 mol m^{-3}). Mn^{2+} toxicity was reversible in *S. cerevisiae* by a chelation agent (EDTA), but not in the case of *L. minor*. Therefore, our results showed that Mn is toxic to *S. cerevisiae* and *L. minor* (greater than or equal to 1.000 and 0.100 mol m^{-3}, respectively) and inhibited growth at higher concentration (more than 3.000 and 1.000 mol m^{-3}, respectively). Chelation of Mn did not consistently reduce the toxicity of Mn in *L. minor* and so Mn toxicity in *L. minor* is different to that found in *S. cerevisiae*. However, effect of Mn did not reduce oxygenic photosynthesis *C. vulgaris* (less than 10 mol m^{-3}).

Keywords: *Saccharomyces cerevisiae*, *Chlorella vulgaris, Lemna minor*, Manganese, Mn–toxicity

ชื่อวิทยานิพนธ์ ความเป็นพิษของแมงกานีสในยีสต์ และพืช
ผู้เขียน นายวรรณพิสิฏฐ์ ธรรมกูล
สาขาวิชา เทคโนโลยีและการจัดการสิ่งแวดล้อม
ปีการศึกษา 2018

บทคัดย่อ

แมงกานีสที่พบทั่วไปในดิน อยู่ในรูป MnO_2 ไม่ละลายน้ำและไม่เป็นอันตราย แมงกานีสที่เป็นพิษพบได้ในดินกรดอยู่ในรูปของแมงกานีสไอออน อย่างไรก็ตาม ยังไม่มีรายงานเกี่ยวกับความเป็นพิษของ Mn^{2+} ในพืชมากนัก ยีสต์ สาหร่าย และพืชมีระบบการลำเลียงสารที่เยื่อหุ้มเซลล์ที่คล้ายคลึงกัน ดังนั้นจึงนำยีสต์และสาหร่ายมาเป็นแบบจำลองในการศึกษาความเป็นพิษของแมงกานีส ในยีสต์ (*Saccharomyces cerevisiae*) ศึกษาโดยติดตามการเติบโตแบบเลขชี้กำลังด้วยการวัดค่า optical density (OD) ภายในถาดหลุมเพาะเชื้อเป็นเวลา 24 ชม. และวัดอัตราการเติบโตของ *Lemna minor* โดยการนับจำนวนใบ ปริมาณคลอโรฟิลล์เอ และการดูดกลืนแสงของพืชที่เพาะเลี้ยงในจานเพาะเชื้อเป็นเวลา 6 วัน ที่ระดับความเข้มข้นต่างๆของแมงกานีสที่ (10, 30, 100, 1000, และ 3000 mmol m^{-3}) ในขณะที่ *Chlorella vulgaris* ถูกตรวจสอบด้วยการวัดการสังเคราะห์ด้วยแสงแบบใช้ ออกซิเจนด้วยเครื่องมือ junior PAM โดยการเพาะเลี้ยงในความเข้มข้นต่างกันของแมงกานีส (1, 2, 3, 5, 7 และ 10 mmol m^{-3}) เป็นเวลา 2 ชม. ผลการทดลองพบว่า แมงกานีสมีผลกับ *S. cerevisiae* (K_i = 1.884 ± 0.673 mol m^{-3}) และ *L. minor* (K_i = 1.154 ± 0.282 mol m^{-3}) โดยความเป็นพิษเกิดจากไอออนของ Mn^{2+} และใน *S. cerevisiae* สารคีเลต (EDTA) สามารถลดความเป็นพิษของแมงกานีสลงได้ แต่ไม่ลดความเป็นพิษของแมงกานีสลงในผลของ *L. minor* ผลการศึกษาในครั้งนี้แสดงให้เห็นว่าแมงกานีสมีความเป็นพิษต่อ *S. cerevisiae* และ *L. minor* (มากกว่าหรือเท่ากับ 1 และ 0.1 mol m^{-3} ตามลำดับ) และยับยั้งการเติบโตที่ความเข้มข้นที่สูง (มากกว่า 3 และ 1 mol m^{-3} ตามลำดับ) การใช้สารคีเลตไม่ช่วยลดความเป็นพิษของแมงกานีสใน *L. minor* ดังนั้นความเป็นพิษของแมงกานีสใน *L. minor* นั้นแตกต่างจากที่พบใน *S. cerevisiae* อย่างไรก็ตามแมงกานีสไม่มีผลให้เกิดการลดอัตราการสังเคราะห์ด้วยแสงแบบใช้ออกซิเจนของ *C. vulgaris* (น้อยกว่า 10 mol m^{-3})

คำสำคัญ: *Saccharomyces cerevisiae*, *Chlorella vulgaris, Lemna minor*, แมงกานีส, ความเป็นพิษของแมงกานีส

ACKNOWLEDGMENTS

I would like to dedicate this dissertation to the following people and institute who support has been critical to the completion of this study.

Firstly, the Faculty of Technology and Environment at Prince of Songkla University, Phuket campus which provided me with the research scholarship.

Secondly, I am deeply grateful to my advisor Assoc. Prof. Dr. Raymond J. Ritchie, who has given me the best chance, guidance, advice and given taught me many new skills. To my co-advisor Assist. Prof. Dr. Sutsawat Duangsrisai, who suggested useful recommend and help me with many things.

Thirdly, my family, who are always there for me and love me unconditionally and there are support the living budget and cheered me up.

Finally, I would like to thank the examination committees, for their time and reconditions.

Wannapisit Thammakul

CONTENTS

CONTENTS (Cont.)

CONTENTS (Cont.)

LIST OF TABLES

LIST OF TABLES (Cont.)

LIST OF TABLES (Cont.)

LIST OF FIGURES

LIST OF FIGURES (Cont.)

LIST OF FIGURES (Cont.)

LIST OF ABBREVIATIONS AND SYMBOLS

Chl *a*	Chlorophyll *a*
E_{opt}	Optimum irradiance
ETR	Electron Transport Rate (through PSII)
Mn	Manganese
NPQ	Non–Photochemical Quenching
P_{max}	Maximum Photosynthesis
PAM	Pulse Amplitude Modeling
PSI	Photosystem I (one)
PSII	Photosystem II (two)
RAT	Reflectance – Absorptance – Transmission
RGR	Relative Growth Rate
Y	Yield

CHAPTER 1

Introduction

1.1 Background and Rational

Manganese (Mn) is one of the most abundant metals in soils (7–9,000 ppm Mn, average ≈ 440 ppm (Emsley, 2001). In soil it occurs as oxides and hydroxides, and it cycles through its various oxidation states as a consequence of the redox state of the soils and microbial activity. Mn is a common element but is usually present in soils as the virtually insoluble MnO_2 and so concentrations of Mn^{2+} in free solution are usually very low (1 mmol m^{-3} or less) (Atwell *et al*., 1999; Kennedy, 1992; Marschner, 1995). An excess of the element in plants and animals is toxic.

The "manganese–oxidizing group" of microbes is a phylogenetically diverse assemblage characterized by the ability to catalyze the oxidation of divalent, soluble Mn^{2+} to insoluble manganese oxides of the general formula MnO_x (where x is some number between 1 and 2) the organisms include a diverse array of bacteria, fungi, cyanobacteria, eukaryotic algae, and other eukaryotic microbes (Nealson, 2006). Accumulations of Mn–oxides are noticeable as a dark brown–black precipitate. The relative abundance of different forms on Mn are a function of the redox potential and oxygen levels.

Manganese is essential to iron and aluminium alloys, steel and stainless steel production and so it finds its way into industrial locations and industrial waste and leachates from waste dumps (Dastur and Leslie, 1981; Fernandes and Woodhouse, 2008; Kaufman, 2000). Manganese dioxide is also an important industrial catalyst (Rancke–Madsen, 1975; Myers, 2003) and is a common component of industrial wastewater from the chemical industry.

Manganese is an essential element for all species because it is a non–replaceable component of key enzymes. Some organisms also accumulate Mn. It has particular importance as an essential nutrient for photosynthetic oxygen evolution cyanobacteria and in chloroplasts in plants and algae. It is an essential trace element in higher animals, in which it participates in the action of

many other enzymes not directly involved in photosynthesis. Fish can have up to 5 ppm and mammals up to 3 ppm Mn in their tissue, although normally they have around 1 ppm.

It is an essential component of two key enzymes in photosynthetic organisms: the oxygen–evolving complex of photosystem II and superoxide dismutase and much more extensively Mn acts as a redox cofactor for many enzymes (Marschner, 1995; Umena *et al.*, 2011). Plants normally obtain the trace amounts of Mn they require by secreting chelating compounds to dissolve carefully regulated amounts of Mn from soils or by dissolving MnO_2 by H^+–extrusion. Plants use these two processes to mobilize regulated amounts of Mn. Increased acidity in soils causes mobilization of Mn and so can reach toxic levels particularly in waterlogged soils (Atwell *et al.*, 1999; Kennedy, 1992; Marschner, 1995; Reichman, 2002). The conditions that mobilize Mn are also responsible for the mobilization of toxic Al^{3+} and so the toxic effects of acid soils are often a combination of Al and Mn–toxicity (Kennedy, 1992). Acid soils limit crop production, particularly of cereals in much of the tropics and subtropics of Australia and Asia. Infertile acids soils is often primarily an unrecognized consequence of Al and Mn–toxicity. The combination of acid soils and waterlogging exacerbates Mn toxicity in the growing of plants and so paddy rice is particularly vulnerable to Mn–toxicity (Reichman, 2002).

Manganese is an important element for human health, essential for development, metabolism, and antioxidant biochemistry. However, excessive exposure or intake may lead to a condition known as Manganism. Effects of excessive Manganese effects occur mainly in the respiratory tract and in the brain, manganism is a neurodegenerative disorder that causes dopaminergic neuronal death and symptoms similar to Parkinson's disease. Manganism is typically an industry–related disease. In humans lack of Mn causes testicular atrophy. Mn deficiency and toxicity effects in human occur mainly in the respiratory tract and in the brain and nervous system.

In plants, Mn–toxicity symptoms include burning of the leaf margins and tips or as reddish–brown spot across older leaves. Chronic toxicity increases the severity of the symptoms (Bloodnick, 2018; Horst and Marschner, 1978; Kennedy, 1992; Wu, 1994).

Figure 1.1 Mn–toxicity symptoms in plants (from Bloodnick (2018) and Pasian (2016))

The elemental composition of higher plants growing in soils does not necessarily point to an element being an essential element in the plants. The criterion for an element being essential for a plant is not simply whether or not a plant grows better in the presence of an element. The crucial criterion is that the plant requires an element in order to complete its life cycle (Marschner 1995). For example, silica is an essential element for aquatic diatoms because they cannot complete their life cycle without it: whereas many terrestrial vascular plants do benefit from the presence of silica but nevertheless can complete their life cycle in hydroponic culture without silica and so silica is not regarded as an essential element for terrestrial vascular plants.

The protocol used to identify essential elements involved Media culture, acid–washed sand and water experiments were implemented in which plants were deprived of distinct elements and the consequent effects on growth and development studied using the "completion of life cycle criterion". Early work showed that there were two fairly distinct groups of nutrients, the macronutrients which are needed and are present in rather high concentrations, and the micronutrients which are requisite in plants, but present in lower concentrations. Often micronutrients are toxic at excessive concentrations. For higher plants, the essentiality of 14 elements is now well established but some are needed at very low concentrations where very pure chemicals are needed to demonstrate that they are essential. Sodium is essential for some vascular plants but not others: the essential nature of the micronutrients chlorine and nickel has been demonstrated in only a few species. Progress in micronutrient research was intimately related to the development of analytical chemistry, especially in the purification of chemicals. The time course of identification of essential elements closely reflects progressive improvements in analytical chemistry (Table 1.1) (Marschner, 1995). The smaller the amount of a micronutrient

required by a plants the longer it took analytical methods to reach the level of technology to demonstrate that the element was essential. Elements that are chemically very similar to macronutrients are particularly difficult to demonstrate to be essential elements. The list of essential elements for plants and animals is closely similar, however, there are some exceptions: selenium is an essential element for mammals but has not (yet) been demonstrated to be essential for vascular plants. The primary reason is that Selenium is chemically very similar to Sulphur and so sulphates are contaminated with trace amounts of Selenium as selenite.

Table 1.1 Discovery of the essentiality of elements for higher plants

Element (chemical symbol)	Discovered by	Year
Fe	Sachs	1860
Mn	McHargue	1922
B	Warington	1923
Zn	Sommer and Lipman	1926
Cu	Lipman and MacKenney	1931
Mo	Arnon and Stout	1938
Cl	Broter *et al.*	1954
Ni	Brown *et al.*	1987

Note: Form Marschner (1995)

Manganese is a common element but is usually present in soils as the virtually insoluble MnO_2 and so concentrations of Mn^{2+} in solution are usually very low (1 mmol m^{-3} g^{-1} and 50 mg kg^{-1} or less). Iron is typically contaminated with Mn and so Mn–deficiency can be difficult to demonstrate without very pure iron sources (Marschner, 1995). Mn is not only an essential nutrient for plants because it is an essential component the oxygen–evolving complex of photosystem II and superoxide dismutase but much more extensively Mn acts as a redox cofactor for many enzymes, balancing anions and controlling membrane permeability and electrochemical potentials. Mn has a non–specific function in establishing osmotic potential that may be related to effects of Mn on aquaporin function (Atwell *et al*., 1999). The ability of Mn to form chelates means that its chemistry and biochemistry closely resembles those of the trace metals, Cu, Fe, Mo and Zn,

which are widely present in plants in chelated form. Another consequence of this is that trace elements, not only iron, may be contaminated with manganese. An important function of these latter elements is involvement in electron transport across cell membranes and in redox reactions. (Clarkson, 1996; Atwell *et al*., 1999).

1.2 Review of Literature

1.2.1 Yeast (*Saccharomyces cerevisiae*)

S. cerevisiae is known as – Baker's yeast (oxygenic varieties) and Brewer's yeast (varieties that are very good fermenters). It was the first eukaryotic genome to be sequenced. It is a single cell organism with a short doubling time of about 1.5 hours to 2 hours. Sex differentiation exists in haploid cells. Yeast is may be found as a harmless and transient digestive commensal and colonization of mucosal surfaces of normal people. The budding yeast phase suffers from replicative senescence in which each mother cell can only divide a limited amount of times to produce daughter cells; the number of divisions by the mother cell is thus used to determine lifespan (Cornely *et al.*, 2014; Johnson and Echavarri–Erasun, 2010; Sinclair and Guarente, 1997). Purely vegetative reproduction can only occur a limited number of times before a sexual stage needs to take place and so the vegetative stage has a determinant lifespan.

1.2.1.1 Yeast (*Saccharomyces cerevisiae*) Taxonomy

Kingdom Fungi

Phylum Ascomycota

Class Saccharomycetes

Order Saccharomycetales

Family Saccharomycetaceae

Genus *Saccharomyces*

Species *S. cerevisiae*

1.2.1.2 Yeast: Ion uptake

In yeast, under non–stressful conditions, when Mn is adequately available, the intracellular and uptake diffusion of the metal ion relies heavily on Smf2p, a Nramp Mn transporter (Culotta *et al.*, 2005). A very attractive feature of yeast is that many of its transport systems are analogous or homologous to transport mechanisms found in green algae and in vascular plants. Mn toxicity studies are worthwhile in yeast not only in themselves but seem to offer a simple system in which to study Mn–toxicity in plants. When *S. cerevisiae* cells are grown under normal laboratory growth conditions in standard enriched or minimal medium containing about to 5 mmol m^{-3} Mn, the metal ion is taken up via the Nramp metal transporter Smf1p and also by another, as–yet–unknown metal transporter(s) at the cell surface. Once inside the cell the Mn is compartmentalized into Smf2p containing vesicles that may represent transient intracellular transport of the metal or as an Mn–storage mechanism. The Smf2p–transported Mn can then move to either the Golgi apparatus or mitochondria (mito). The Pmr1p protein pumps Mn into the Golgi apparatus for activation of sialytransferase (STase) enzymes. Although the means by which mitochondria take up Mn is still unknown, Mtm1p in the inner membrane of mitochondria facilitates insertion of the metal into the mitochondrial gene SOD2 (Fig. 1.2).

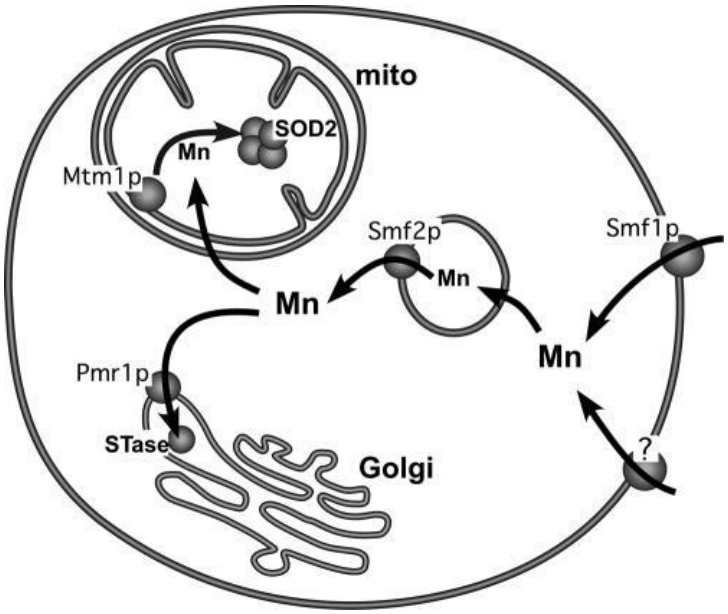

Figure 1.2 A model for intracellular trafficking of Mn in yeast under physiological growth conditions (from Culotta *et al*., 2005).

Culotta *et al.* (2005) explains the sequence of events in yeast cells with sufficient and insufficient Mn.

"*When cells are faced with Mn starvation, they may respond to changes in Mn availability by shifting localization of the Smf1p Mn transporter. When cells have extensive Mn (Fig. 1.3) (e.g., grown in medium enhance with more than 1 mmol* m^{-3} *manganese [+*Mn*]), Smf1p in the secretory pathway is thought to interact with Mn and adopt a conformation that is recognized by membrane bound Bsd2p. Bsd2p recruits the E3 ubiquitin ligase Rsp5, and Smf1p becomes tagged with ubiquitin (*Ub*), resulting in movement of Smf1p to the vacuole for degeneration by vacuolar proteases. The bottom of Figure 1.3 shows that when cells are starved for Mn (extracellular Mn concentration of < 1.0 mmol* m^{-3} *[–*Mn*]), Smf1p adopts a conformation that is not recognized by Bsd2p (1*st *step). This lack of recognition by Bsd2p is not enough to move Smf1p to the cell surface, and in a 2*nd *step, Free Mn Smf1p may be recognized by another protein trafficking factor (unknown; "?") that helps direct Smf1p to the cell surface for the uptake of Mn from the growth medium. (Figure 1.3). The mechanism by which cells sense Mn and respond by shifting localization of the Nramp transporters is an area of current investigation."*

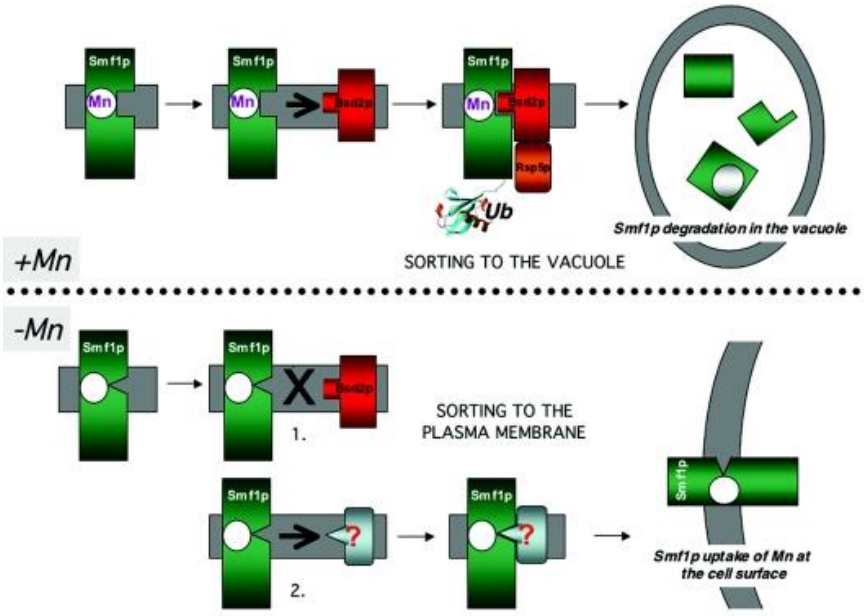

Figure 1.3 Manganese control of Smf1p at the level of protein sorting in the secretory pathway (from Culotta *et al.,* 2005).

When cells are exposed to toxic levels of Mn, the Smfp transporters are not expressed. When *Saccharomyces cerevisiae* cells are grown in the presence of excess Mn (about 10 to 100 mmol m^{-3}), the metal is taken up mostly in the form of Mn–phosphate complexes via the Pho84p phosphate transporter. The excess Mn is eliminated from the cell by two major Mn detoxification systems. A bulk of the excess Mn is pumped into the Golgi apparatus via Pmr1p and the metal then exits the cell via the secretory pathway. Mn is also delivered into the vacuole by Ccc1p and perhaps by Cos16p as well. The action of vacuolar Mam3p is not known, but it helps contribute to the symptoms of Mn–toxicity (Fig. 1.4). The role of the secretory pathway in Mn homeostasis and detoxification is likely to be conserved among eukaryotes (Culotta *et al*., 2005; Reddi *et al*., 2009). This suggests that interactions between Mn and P status of yeast cells would be found under conditions of high Mn.

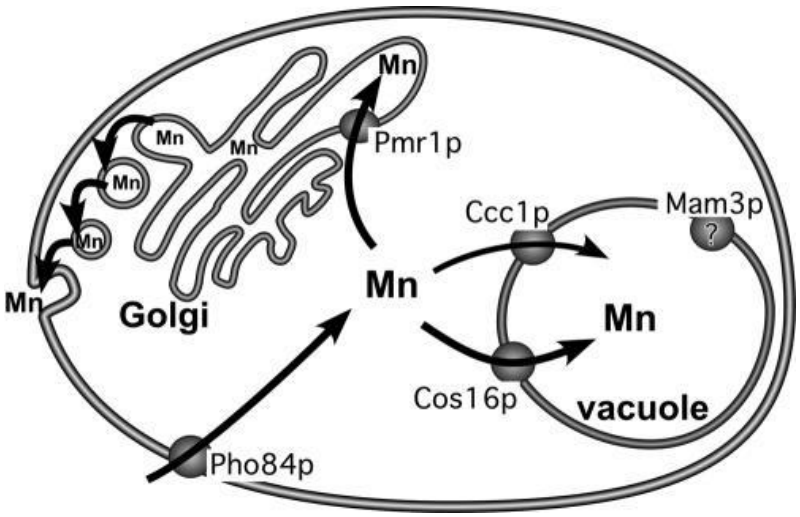

Figure 1.4 Manganese trafficking under excess Mn or toxicity conditions (from Culotta *et al*., 2005). The excretory mechanism for excess Mn in yeast is a vesicular excretion mechanism.

In preliminary work, we have already established that it is possible to demonstrate Mn–toxicity in yeast (Figure 1.5). We have shown that Mn is toxic in yeast, but it is not nearly as toxic is Al and Ga. Its K_i is ≈ 1 mol m^{-3} and the toxicity/dosage response appears to obey Michaelis–Menten type kinetics. It needs to be established how rapidly the toxicity effects of Mn set in. This will provide an important clue whether rapid cell membrane surface effects are involved or whether

Mn has to penetrate the cells or whether there is a membrane surface effect, for example, channel blocking.

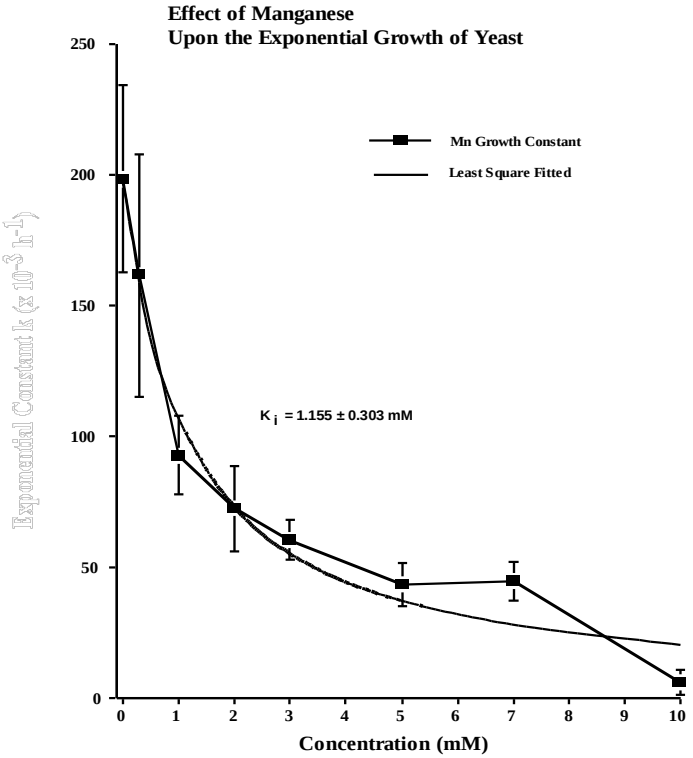

Figure 1.5 Manganese is toxic to aerobic yeast at pH 3 but is considerably less toxic than Aluminium ($K_i \approx 1$ mM). Unpublished material from Ritchie (PSU–Phuket).

Preliminary experiments on the effects of citrate on Mn toxicity show that citrate is not very effective in protecting yeast cells from Mn–toxicity (cf Al–toxicity in yeast (Ritchie and Raghupathi, 2008). Citrate is readily metabolised by cells and so the less metabolizable ethylenediaminetetraacetic (EDTA) was used as the chelation agent in the present study.

In preliminary work growth kinetics have been routinely used to measure toxicity effects in yeast. This is a rather slow method and does not provide information on the possibly quite rapid toxicity effects of Mn. Fluorescent Ca–sensitive dyes appear to be a promising alternative avenue. In a recent study of aluminium toxicity in yeast only a small effect of aluminium upon respiration could be detected using an oxygen electrode (Ritchie unpublished). It is possible that more dramatic effects might be found in the case of Mn, but this was not part of the present study. PAM (pulse–amplitude–modulation) fluorescence monitoring of stress physiology of plants can be

used on both algal and vascular plant systems (Ritchie and Larkum, 2012; Ritchie, 2012; Ritchie and Bunthawin, 2010a; 2010b; Ritchie, 2014) but cannot be used on yeast because it is not photosynthetic. The green alga *Chlorella* is very suitable for PAM studies (Ritchie, 2014).

1.2.2 Plants

1.2.2.1 *Chlorella vulgaris*

C. vulgaris is a single–celled green alga belonging to the division Chlorophyta. It is spherical shape, does not have flagella or cilia. *C. vulgaris* has chlorophyll *a* + *b* (Scheffler, 2007). *C. vulgaris* can serve as a potential source of food and energy and can be grown on an industrial scale (Zelitch, 1971). *C. vulgaris* is high nutrient food, because it has high levels of protein and other essential nutrients and most people know in "single–cell protein". when dried, it is about 45% protein, 20% fat, 20% (high in polyunsaturated fats), carbohydrate, 5% fiber, and 10% minerals and vitamins (Belasco, 2006; Yongmanitchai and Ward, 1991). *C. vulgaris* is therefore an important biotechnology organism. With due caution because *Chlorella* is greatly separated from vascular plants by evolutionary divergence, *C. vulgaris* can be a useful model organism for studies of mineral nutrition in vascular plants.

1.2.2.1.1 *C. vulgaris* Taxonomy

Kingdom Plantae

Division Chlorophyta

Subdivision Chlorophytina

Class Trebouxiophyceae

Order Chlorellales

Family Oocystaceae

Genus *Chlorella*

Species *C. vulgaris* (Beyerinck, 1980)

1.2.2.2 *Lemna minor*

L. minor is a genus of free–floating aquatic plants in the Araceae family. Common name is "Duckweed". These rapidly growing vascular aquatic plants are routinely used as a model system for nutrient studies and also used as a source of animal feeds for agriculture and aquaculture. *L. minor* is grown as a simple free–floating plant on the water surface. Most strains of duckweed are small, not exceeding 5 mm. in length. Duckweeds are flowering vascular plants with sexual and vegetative reproduction. The rapid growth of duckweeds are sometimes a cause of environmental concern in waterways. Duckweed finds application in bioremediation of polluted waters and as an organism for experimental environmental studies. It is also being used for economical production of complex biopharmaceuticals (Kabir *et al.*, 1970; The Angiosperm Phylogeny Group, 2003).

1.2.2.2.1 *L. minor* Taxonomy

Kingdom Plantae

Subkingdom Viridiplantae

Division Tracheophyta

Subdivision Spermatophytina

Class Magnoliopsida

Superorder Lilianae

Order Alismatales

Family Araceae

Genus *Lemna*

Species *L. minor*

1.2.2.3 Plants: Ion uptake

In plants, Manganese has a role in many biochemical processes. However, unlike other essential trace elements such as Cu, Zn, Fe and Molybdenum which are usually integral components of enzymes, Mn usually acts as an activator of enzymes and is often able to be at least partially replaced by other metal ions as a cofactor. In this respect Mn resembles Mg in its biochemical function and is involved in activating enzyme–catalyzed reactions including phosphorylations, decarboxylations, reductions and hydrolysis reactions and therefore affects

processes such as respiration, amino acid synthesis, lignin biosynthesis and the level of hormones in plants (Campbell and Nable, 1988; Kong *et al*., 2010). Mn is however, essential, and not replaceable even in part, for the oxygen evolving complex of photosystem II in photosynthetic organisms. Perhaps its most crucial biological role of Mn is in the oxygen–evolving complex which catalases the reaction of two water molecules ($2H_20$) to form $4H^+ + 4e^-$ to provide the electron source to support photosynthetic electron transport.

Manganese (Mn) is an important plant micronutrient for other metabolic functions and of the trace elements, it is required by plants in the second greatest quantity compared to iron. Like many other trace elements, it can have a limiting factor on plant growth if it is deficient but at elevated levels it can be toxic in plant tissue. Chemically it is similar to iron in many ways, including the critical importance of the redox state of the Mn, and Mn deficiency or toxicity is often mistaken for iron deficiency or toxicity. Environmental conditions that induce iron deficiency usually induce Mn deficiency as well.

Manganese is a common element but is usually present in soils as the virtually insoluble MnO_2 and so concentrations of Mn^{2+} in solution are usually very low (1 mmol m^{-3} or less) (Atwell *et al*., 1999; Marschner, 1995). Plants normally obtain the trace amounts of Mn they require by secreting chelating compounds or by dissolving MnO_2 by H^+–extrusion. Plants use these two processes to mobilize carefully regulated amounts of Mn. This mechanism is rather different to that found in yeast (the Smf1p system: Culotta *et al*., 2005). The manganese/phosphate uptake mechanisms found in yeast seems to be of less importance (Culotta *et al*., 2005). Increased acidity in soils causes mobilization of Mn and so can reach toxic levels particularly in waterlogged soils because of redox reactions of Mn, hence the importance of Mn-toxicity in paddy rice (Atwell *et al*., 1999; Kennedy, 1992; Marschner, 1995). The same conditions that mobilize Mn are also responsible for mobilization of toxic Al^{3+} and so the toxic effects of acid soils are often a combination of Al and Mn–toxicity (Kennedy, 1992). Acid soils limit crop production, particularly of cereals in much of the tropics and subtropics of Australia and Asia. The combination of acid soils and waterlogging exacerbates Mn toxicity in the growing of paddy rice (*Oryza sativa*) because of the combination of acidic and anoxic conditions. Kennedy (1992) points out that many tropical soils appear to be infertile, but the apparent infertility is actually Al/Mn toxicity.

Mn is also used in plants as a major contributor to various biological systems including nitrogen, photosynthesis and respiration assimilation. Mn is also involved in pollen tube growth, root cell elongation, resistance and pollen germination to root pathogens. Thus, Mn deficiency and excess Mn result in developmental symptoms in vascular plants. Mn is also critical in nitrogen–fixation by microbes with serious consequences for N–fixation by both free–living microbes and N–fixing legumes (Kennedy, 1992).

Mn deficiency symptoms often look like those of iron deficiency, appearing as interveinal chlorosis (yellow leaves with green veins) on the young leaf and sometimes tan–colored, sunken spots that appear in the chlorotic areas between the veins. The occurrences of Mn–deficiency symptoms between viens of leaves points to limitations of intercellular transport of Mn. Plant growth may also be stunted and reduced. Mn deficiency can occur when the pH of the growing medium exceeds 6.5, because it is bound up in an insoluble form and is unavailable for uptake. Deficiency can also occur from low nutrients application rates, use of general–purpose nutrients (which typically have reduced micronutrient contents), excessive leaching or applying too many iron chelate drenches.

Symptoms of Mn toxicity in plants: Mn toxicity symptoms begin with the burning of the leaf margins and tips of older leaf or as reddish–brown spots across older leaves. Severe toxicity may result in spots becoming larger and numerous, forming patches on the older leaf. At pH levels below 5.5, Mn^{2+} is very soluble and toxicity symptoms are likely to occur, especially in marigolds, geraniums and New Guinea Impatiens. Hence Mn–toxicity is common in lateritic acid tropical soils which often also suffer from Al–toxicity (Kennedy, 1992). Mn–toxicity can occur if the fertilizer application rate is excessive (Bloodnick, 2018; Campbell and Nable, 1988) because of acidification leading to mobilization of toxic amounts of Mn ions under anoxic conditions. Careful note also needs to be taken of the interactions between Mn & phosphate uptake noted above in yeast (Culotta *et al*., 2005). It is conceivable that excessive phosphate could exacerbate Mn–toxicity in hydroponic culture. Typical vascular plant symptoms of Mn–toxicity are often not apparent in aquatic vascular plants and may have no clear analogue in unicellular algae which do not have intercellular Mn–transport. For example, the “spotting” phenomenon found in Mn–toxicity in vascular plants.

Manganese is both a nutrient and a toxic element: cells must therefore carefully control the uptake and trafficking of this ion. While the picture of Mn homeostasis in vascular plants is far from complete, many advances have been made with the baker's yeast *(S. cerevisiae)* which is a completely sequenced organism (Culotta *et al*., 2005; Kanehisa *et al*., 2017). Many of the ion transport mechanisms found in yeast are close analogues of transporters found in green algae such as *C. vulgaris* (another completely sequenced organism) and in high plants such as rice (completely sequenced). Rice also has a smaller genome than most cereals. There may, however, be no vascular plant analogue for the secretory system found in yeast (Culotta *et al*., 2005).

At the molecular level, facilitated diffusion is mediated by porins or channels. Control of uptake is mediated by the number of transporters present in the cells membranes and control mechanisms turning them on or off. Passive transporters facilitating the influx of 10 of the 14 mineral nutrients across the plasma membrane of root cells have been reported (Figure 1.6). These include K–channels, such as AtAKT1:AtKC1 of *A. thaliana*, voltage–dependent Ca–channels, cation channels, such as those encoded by the cyclic nucleotide gated channel (CNGC) and glutamate receptor (GLR) gene families, ammonium transporters encoded by the ammonium transporter (AMT) gene family, M, transporters, such as AtMGT1 and AtMGT10, members of the Zn–regulated transporter (ZRT), Fe–regulated transporter (IRT) – like protein (ZIP) family, which transport,Cu^{2+}, Zn^{2+}, Mn^{2+} and Fe^{2+}, Cu^{+} transporters encoded by CTR/COPT genes, boric acid channels, formed by plasma membrane intrinsic proteins (PIPs) and nodulin–26–like intrinsic proteins (NIPs), and in saline environments, Cl^{-} channels. However, the influx into root cells of nutrients present in the soil solution as anions (e.g., nitrate, phosphate, sulfate, molybdate, chloride) is not thought to be mediated by passive transporters because of the unfavorable electrical gradient (Clarkson, 1996).

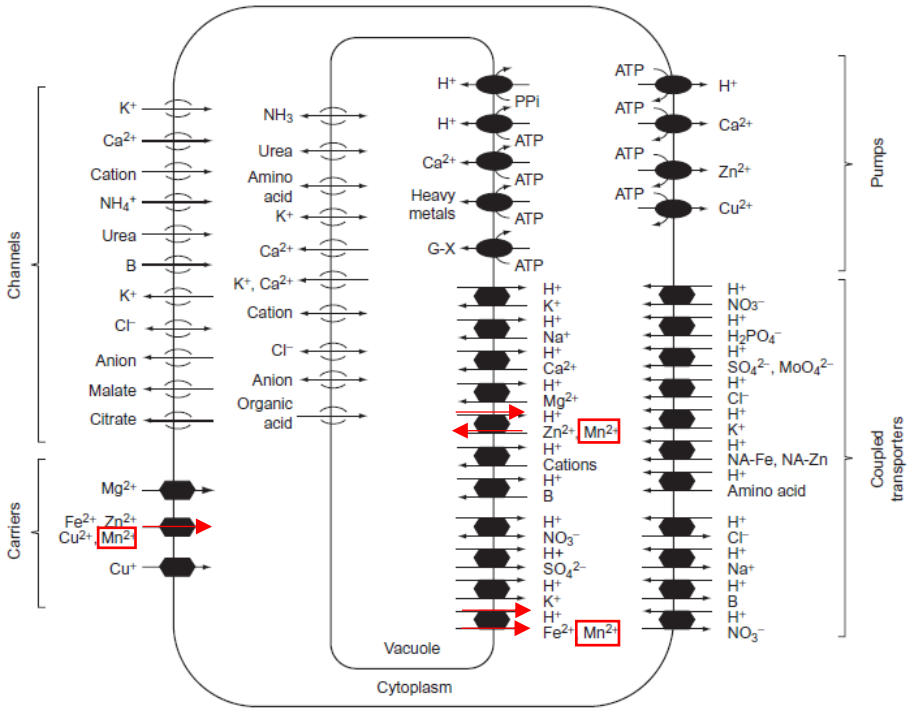

Figure 1.6 Transport proteins of the tonoplast and plasma membrane of plant cells (Modified from Clarkson (1996)).

The characterization of *Arabidopsis* Chloroplast Manganese Transporter1, an evolutionarily conserved protein in the Uncharacterized Protein Family 0016 (UPF0016). That is required for Mn buildup into the chloroplast. Chloroplast Manganese Transporter 1 is expressed primarily in tissues, and its encoded product is localized in the inner envelope membrane of the chloroplast. Disruption of Chloroplast Manganese Transporter 1 in the T–DNA insertional mutant Chloroplast Manganese Transporter 1–1 resulted in stunted plant growth, defective thylakoid stacking, and severe reduction of photosystem II complexes and photosynthetic activity. Consistent with reduced oxygen evolution capacity, the mutant chloroplasts contained less manganese than the wild–type ones. Manganese is transported from the cytosol into the chloroplast stroma through Chloroplast Manganese Transporter 1 localized in the inner envelope and further transferred to the thylakoid lumen by Photosynthesis Affected Mutant71/CCHamide1 in the thylakoid membrane where the Mn cluster is synthesized for oxygen production during photosynthesis (Figure 1.7). The results indicate that Chloroplast Manganese Transporter 1 functions as an inner envelope Mn

transporter responsible for chloroplast Mn^{2+} uptake (Zhang *et al*., 2018). This transporter would be expected to be found in both *Chorella* and in *Lemna*.

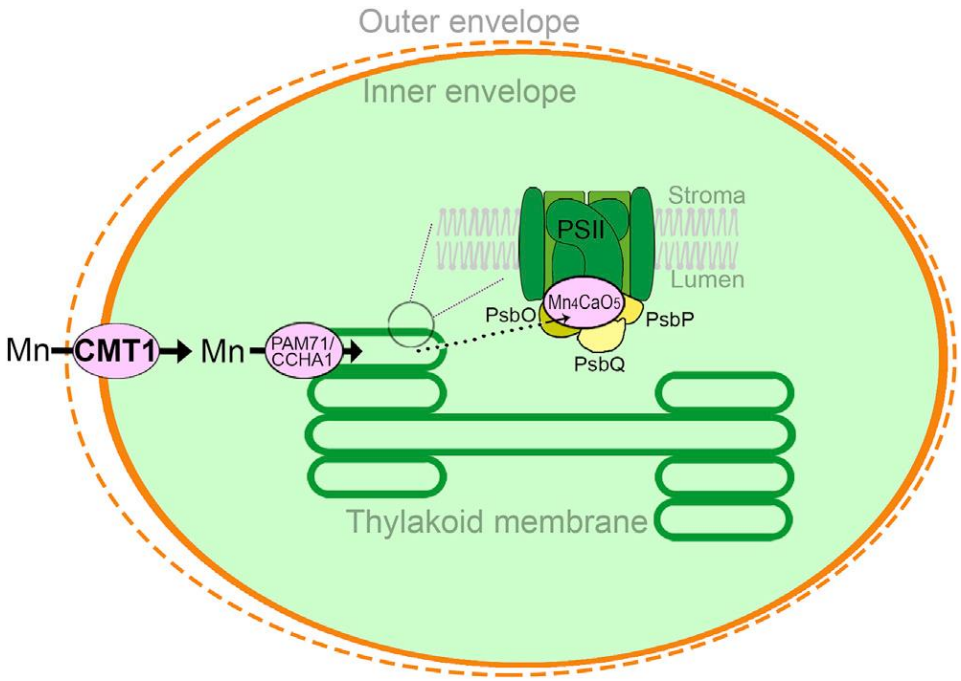

Figure 1.7 Working Model of manganese Delivery in the Chloroplast (form Zhang *et al*., 2018)).

Manganese toxicity has been studied in a variety of different plants (Table 1.2) such as Ryegrass (*Lolium perenne* L.), White clover (*Trifolium repens* L.), Barley (*Hordeum vulgare* L. cv. Obzor), Rice (*Oryza sativa* L. cv. Safari), *Juncus effusus*, Tobacco and others. Mn–toxicity in Ryegrass, White clover, Barley has been studied using plant growth criteria such as dry weight and in barley using biomass measurement. Many researchers have studied the effects of Mn uptake on plants structure, the effect of Mn stress on the enzymes and chlorophyll photosynthesis. And many research has studied the effects of chelators for reducing Mn toxicity. The results of their research show that the concentration of Mn has a variety of toxic effects in plant depending on species and cultivars (Atwell *et al*., 1999; De La Luz Mora *et al*., 2009; Demirevska–Kepova *et al*., 2004; Führs *et al*., 2008; Lei *et al*., 2007; Lidon *et al*., 2004; Marschner, 1995; Nable *et al*., 1988; Najeeb *et al*., 2009). However, Fernando and Lynch (2015) found crucial roles of light supplements on the Mn toxicity. That is an old observation that is not

yet well understood (Fernando and Lynch, 2015; Horst and Marschner, 1978). Manganese can more toxic under high light (sunshine) (Fernando and Lynch, 2015).

Table 1.2 Manganese sufficiency rang for plants

	Mn (mmol mol^{-3})
Alfalfa, Blueberry	455–1820
Apple	455–3640
Barley, Oats, Rye, Wheat	364–2730
Bell Pepper	546–1820
Bentgrass, Cucumber	455–5460
Bermudagrass, Coastal Bermuda	364–5460
Broccoli	455–2730
Cantaloupe, Muskmelon	364–1820
Celery	91–182
Corn	455–2912
Lettuce, Pear	364–3640
Ornamental Cabbage, Peanut, Poinsettia	364–4550
Pecan	1820–14560
Rice	728–13468
Soybeans	309–1820
Spinach	455–3640
Sugarcane	218–1820
Tomato	455–5460

Note: Form Campbell (2000)

1.2.3 Pulse Amplitude Modulation (PAM)

PAM machine is very useful for estimating the photosynthetic activity of plants, stress physiology. PAM machines are simple to use to measure the light reactions of photosynthesis and is a rapid method and is easy to set up in the field (Ritchie and Mekjinda, 2016). PAM directly measures photosynthetic electron transport by measuring PSII fluorescence in higher plants. It

actually measures photons of light that are emitted as far–red fluorescence from a flash of blue or red light and so the method infers how many incident photons are used for photosynthesis by subtraction (Ritchie and Bunthawin, 2010a; 2010b).

1.3 Objectives of the Study

1.3.1 To study effect of manganese toxicity and chelation in higher plants using the simple aquatic angiosperm, (*Lemna minor*) and by using yeast (*Saccharomyces cerevisiae*) and algae (*Chlorella vulgaris*) as models.

1.3.2 To study physiological responses (growth rate, chlorophyll *a* content) of *Lemna minor* exposed to manganese.

1.3.3 To study effect of chelate reduce manganese toxicity in plants (*Lemna minor*).

1.4 Scope

It is extremely improbable that Mn^{2+} enters cells simply through the lipid bilayer. However, interference with membrane function is thought to be a major factor in the toxicity of Mn^{2+} and not only its biochemical effects on enzyme function if it is in excess in the cytoplasm. Mn^{2+}, like many other polyvalent cations, is a potent channel–blocking agent (for Al–toxicity due to this effect see Kinraide and Kochian, 1993) (Ryan *et al.*, 1997). This is the likely explanation of the observation that excess Mn interferes with water relations, pointed out above (Ryan *et al.*, 1997).

Calcium is practically universally involved in cell signaling and motility in plants and animals (Atwell *et al*., 1999). Any interference with this function is likely to be toxic to cells. Manganese is known to interfere with Calcium function in vascular plants (Clarkson, 1996). Figure 1.8 shows three possible transport mechanisms that could be involved in allowing Mn to enter yeast cells. Mn–toxicity probably has much to do with the mechanism used to take up Mn as an essential trace element in both yeast and vascular plants. Note that because the cytoplasmic pH of yeast and vascular plant cells is about 7.3, both ions will form the insoluble oxide (MnO_2) in the cytoplasm.

The biologically active form of Mn in the cytoplasm would need to be a chelated form of Mn. Three possible transporters are shown. A permease protein or channel designed to transport divalent cations, that recognizes Mn^{2+} is the most likely candidate mechanism for unwanted entry of excess Mn. Cation channels are often rather non specific. Secondary active transport mechanisms, such are those driven by the proton electrochemical gradient, are also involved in Calcium uptake (McConnaughey and Whelan, 1997) and could also be targeted by Mn. An ATP–driven pump might also recognize Mn^{2+} and either transport it into the cytoplasm or its ion–carrying channel could be blocked by a Mn complex. The ubiquitous $Ca^{2+}/2H^{+}$ ATPase is an outwardly directed pump (McConnaughey and Whelan, 1997). It not likely to be involved in uptake of Mn but could be involved in extruding excess Mn that penetrates the cell. Alternatively, Mn could block this pump from the outside leading to toxic build–up of Mn as it leaks into the cell and cannot be removed.

There are no estimates of the K_m and V_{max} of protoplasmic uptake available for either yeast or vascular plant cells even though these parameters are essential in characterizing a transport system. Identification of the Mn–transport mechanism should be directly transferable to considerations of the system in rice because it is also completely sequenced. Mn–toxicity is an internationally important problem particularly for growing rice in SE Asia.

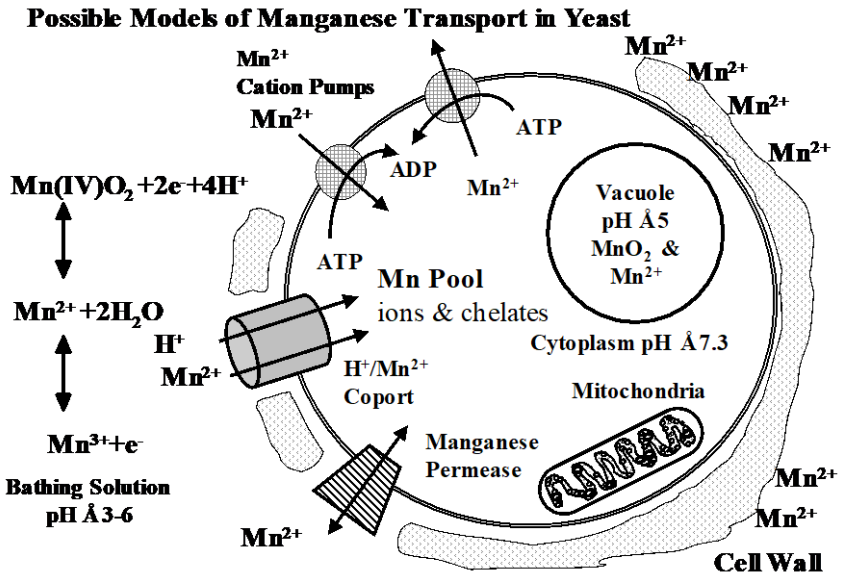

Figure 1.8 Mn is toxic to aerobic yeast at pH_o 3 but is considerably less toxic than Aluminium ($K_i \approx 1$ mM). Preliminary experiments on the effects of citrate on Mn toxicity show that citrate is

not very effective in protecting yeast cells from Mn–toxicity (cf Al–toxicity in yeast, (Ritchie and Raghupathi, 2008)). Fig. 1.5 shows an Mn toxicity curve for yeast (Ki ≈ 1 mol m^{-3}).

1.5 Expected Outcomes

Manganese toxicity is probably important in water logged acid sulphate soils that like aluminium toxicity is largely unrecognized. Characterization of Mn toxicity is hence important for growing green plants. Demonstration of Mn toxicity in simple systems such as unicellular yeast, green algae such as *C. vulgaris* and high plant such as *L. minor* have the potential for acting as a simple monitoring mechanism. Simple chemical measurements of Mn are not really satisfactory for estimating Mn toxicity because its toxicity depends on the redox potential of the soil.

CHAPTER 2

Research Methodology

2.1 Chemical toxicity for experimental design

This study used Mn in the form of manganese (II) sulfate monohydrate ($MnSO_4 \cdot H_2O$) and ethylenediaminetetraacetic acid (EDTA) in the form of disodium ethylenediaminetetraacetic dihydrate ($C_{10}H_{14}N_2Na_2O_8 \cdot 2H_2O$) for studies of the effect of toxicity on yeast (*Saccharomyces cerevisiae*) and *L. minor.* The $MnSO_4$ and EDTA solutions were prepared as stock solutions of 2, 100, and 500 mol m^{-3}.

Figure 2 is a generalized flow chart of the experiments used in the present study on Mn toxicity in yeast and in algae and plants.

2.2 Yeast, and plant culture

All of the yeast bioassay strains and the green alga *C. vulgaris* were from Assoc. Prof. Raymond J. Ritchie, Prince of Songkla University, Phuket Campus, Thailand.

2.3 Culture: Yeast (*Saccharomyces cerevisiae*) material culture condition and growth measurement

Culture–yeast: The yeast strain used was a Baker's yeast strain from Assoc. Prof. Raymond J. Ritchie, Prince of Songkla University, Phuket Campus, Thailand. Yeast was grown as stock cultures in Wickerham's chemically defined medium (Table 2) (Zonneveld, 1986). Experimental cultures were incubated for a day at a range of different concentrations of Mn (10, 30, 100, 300, 1000 and 3000 mmol m^{-3}) and 1 mol m^{-3} EDTA. The trace element and vitamin contents of the medium were as described by Zonneveld (1986). Chelators such as ethylenediaminetetraacetic acid (EDTA), citric acid, glutamic and malic were not included in the culture medium and the experimental media because they would be likely to interfere with Mn

toxicity. Chelation agents tend to bind strongly to cells, so can be difficult to remove from cells, and so can seriously interfere with experimental results.

Growth measurement: Yeast was grown in 200 µL aliquots of Wickerham's medium (pH adjusted to 7.5) and incubated at 30 °C in 96-well plates on an orbital shaker set to medium mode. The cultures were therefore grown under aerobic conditions in the present study. The 96-well titer plates were read with a standard Microplate Reader (A&E UK AMR–100, UK) at 630 nm (A_{630}). Growth curves were fitted to a logistic growth model. The exponential growth constant (k)(h^{-1}) was determined by least squares fitting (EXCEL Solver) and its asymptotic error determined by matrix inversion (Johnson and Faunt, 1992).

Table 2 Modified Wickerham's chemically defined medium (from Zonneveld, 1986)

Compound	Concentration
Glucose	55.5 mol m^{-3}
KH_2PO_4	57.792 mol m^{-3}
$MgSO_4 \cdot 7H_2O$	16.224 mol m^{-3}
$(NH_4)_2SO_4$	60.544 mol m^{-3}
H_3BO_3	8.09 mmol m^{-3}
$CaCl_2 \cdot 2H_2O$	68 mmol m^{-3}
$ZnSO_4 \cdot 7H_2O$	1.39 mmol m^{-3}
$CuSO_4 \cdot 5H_2O$	0.16 mmol m^{-3}
NaI	0.56 mmol m^{-3}
$FeCl_3 \cdot 4H_2O$	0.739 mmol m^{-3}
$NaMoO_4$	0.826 mmol m^{-3}

2.4 Algae (*Chlorella vulgaris*) material culture condition and growth measurement

Culture–*C. vulgaris*: *C. vulgaris* was kept as stock cultures in BG-11 medium (Andersen, 2005). In preparation for experiments, cells were cultured in BG–11 in a range of different concentrations of Mn (1, 2, 3, 5, 7 and 10 mol m^{-3}) and 10 mol m^{-3} EDTA in 100 ml volumes in 250 mL flasks. Cultures were grown over 7 days to obtain exponential growth phase cells temperature 30±2 °C under 24 hours light using cool–white fluorescent lamps with intensities of about 200 µmol (quanta) $m^{-2}s^{-1}$ (PAR: Photosynthetically Active Radiation, 400–700 nm) at the level of the cultures. A total volume of 200 ml of each experimental treatment was centrifuged at 5,000 rpm for 5 minutes using a Z323 K HERMLE LABORTECHNIK fitted with a swing bucket rotor. After centrifugation, the media were removed as much as possible new 150 mL of media was added to the centrifuge tube, vortexed and each 30 mL variant of the experimental media was placed in culture tube for experiments under the same conditions, pH 7.50±0.05 for 2 hours.

Photosynthesis was measured by using Pulse Amplitude Modulation (PAM) machine, Absorptance by using Blue–ray (465 nm) RAT meter (Reflectance-Absorptance-Transmission, RAT) (Aquation Pty Ltd, Australia) (Ritchie and Runcie, 2014) and chlorophyll absorbance was measured by optical density (OD) on solvent extracts of the cells. After the algae were incubated for 2 hours in an experimental medium, 4 mL samples were filtered by using vacuum filtration onto glass fiber disks using a standard Millipore filtration apparatus. Photosynthesis of the disk of filtered cells was measured using a Junior PAM (Pulse Amplitude Modulation) Fluorometer (Gademann Instruments, Germany). This PAM machine has a 1.5 mm diameter optic fiber and a blue diode light source (465 ± 40 nm) and is controlled by WinControl ver. 2.13 Software (Heinz Walz, Germany), The Yield (Y) was calculated by the WinControl software output as the effective quantum yield (Y or ΦPSII) and is defined in the range from 0 to 1:

$$Y = 1 - F_o / F_m' \quad (1)$$

where, F_o is the fluorescence in the modulated measuring light and F_m' is the fluorescence in the light acclimated state after a flash of actinic light (Brestic and Zivcak, 2013; Genty *et al*., 1989). Experimentally it is found that if Y is plotted against irradiance (E), follows a

simple exponential decay function of the form $y = e^{-kx}$ (Ritchie, 2008; Ritchie, 2013; Chandaravithoon *et al.,* 2018).

The photosynthetic electron transport rate (ETR) is proportional to the product of the yield (Y) × Irradiance (E). The relative Electron Transport Rate (rETR) was calculated by using the standard settings (default absorptance (Abt_F) = 0.84, default PSI/PSII. allocation factor (PSII/PSI = 0.5) as described by Genty *et al.* (1989), Rascher *et al.* (2000), Gademann and Ralph (2005), Ritchie, 2008; Ritchie and Larkum, 2013; Brestic and Zivcak (2013) and Chandaravithoon *et al.* (2018). The actual ETR has to be corrected for the proportion of light actually absorbed by the organism at a specified wavelength (Absorptance; $Abt\lambda_{\%}$) (Ritchie and Runcie, 2014; Chandaravithoon *et al.*, 2018). Experimentally measured absorptances of the filter disks impregnated with cells were made at 465 nm (Abt_{465nm}) using the RAT machine (Ritchie and Runcie, 2014). Many estimates of ETR in publications are actually rETR because actual absorptances were not measured.

$$rETR = Y \times E \times (PSII/PSI = 0.5) \times (Abt_F = 0.84) \quad (2)$$

$$ETR = Y \times E \times 0.5 \times Abt_{465nm}/0.84 \quad (3)$$

$$ETR = rETR \times Abt_{465nm}/0.84$$

where, *rETR* is the relative photosynthetic electron transport rate calculated by the WinControl software in default mode, *Y* is the yield calculated by the WinControl software, E is the irradiance (μmol photons m^{-2} s^{-1}), $Abt_F = 0.84$ is the default absorptance value, Abt_{645nm} is the experimentally measured absorptance measured at 465 nm, PSII/PSI = 0.5 is the default PSII/PSI allocation factor.

Water is the electron source in oxygenic photosynthesis: $2H_2O \Rightarrow 4H^+ + 4e^- + O_2$ and so the photosynthetic oxygen evolution rate (POER) from the light reactions of photosynthesis can be used as an estimate of gross photosynthesis (Pg) (1 μmol O_2 m^{-2} s^{-1} = 4 μmol e^- m^{-2} s^{-1}) (Apichatmeta *et al.,* 2017; Quinnell *et al.,* 2017; Chandaravithoon *et al.*, 2018). The POER estimate of oxygenic photosynthesis does not take photorespiration into account and so is a high estimate of gross photosynthesis.

2.4.1 Determination of Photosynthesis of *C. vulgaris* on a Chlorophyll *a* basis

The PAM machine calculates photosynthesis on a surface area basis as mol e^- m^{-2} s^{-1}. It is conventional to standardize photosynthesis on a chlorophyll *a* basis and so ETR as mol e^- m^{-2} s^{-1} needs to be converted to mol e^- g^{-1} Chl *a* s^{-1}. *C. vulgaris* was filtered onto glass fiber disks using a standard Millipore filtration apparatus and so the uniform disk of algae had a surface are of 206.12 × 10^{-3} m^2 (diameter 16.2 mm). Measuring the Chl *a* extracted from an algal disk combined with the known surface area of the disk allowed the calculation of Chl *a* m^{-2} and hence it was possible to calculate ETR on a chlorophyll *a* basis (Ritchie 2008; Chandaravithoon *et al.*, 2018). The algal disk samples were then put in 10 mL centrifuge tube and 3 mL of pure ethanol was added. The samples were incubated in refrigerator at -10 ºC for about 12 hours. After that the extracts were equilibrated to room temperature in a dark box, vortexed, and centrifuged. 1 mL of supernatant was used for chlorophyll determination in narrow glass cuvettes by using spectrophotometer (SHIMADZU UV–1601, Japan) at 750, 665 and 649 nm and the equations of Ritchie (2006) were used to estimate the chlorophyll *a* quantity as µg/mL of solvent and hence mg Chl *a* m^{-2} of the disk surface area could be calculated. This figure could then be used to convert ETR as mol e^- m^{-2} s^{-1} into mol e^- g^{-1} Chl *a* s^{-1}.

$$\text{Chl } a \text{ (µg/mL)} = 11.867 \text{ x } (A_{665\text{ nm}} - A_{750\text{ nm}}) - 5.201 \text{ x } (A_{649\text{ nm}} - A_{750\text{ nm}}) \quad (4)$$

2.5 Plant (*Lemna minor*) material culture condition and growth measurement

L. minor plants were cultured by using 10% BG–11 medium (Andersen, 2005) in plastic cups. Experiments were started with a single plant or a few plants and the growth was measured for 3-7 days under a temperature of 30 ± 2 ºC under 24 h light using cool-white fluorescence light as described for growing *C. vulgaris* above. After setting up a starter culture, *L. minor* plants were separated in 30 mL 10% BG–11 variant media in petri dishes for an experiment under the same growth conditions, pH 7.50 ± 0.05 for 7 days under different concentrations of Mn (10, 30, 100, 300 and 1000 mmol m^{-3}) and ± 10 mmol m^{-3} EDTA where the effect of a chelator was to be measured. In the case of *L. minor,* EDTA by itself was found to be relatively non-toxic but was found to very toxic in the presence of elevated levels of Mn. This was a very different result to that found in the case of yeast and *C. vulgaris* in the present study

Growth measurements: *L. minor* growth was easily measured by counting leaf number. Numbers of leaf were counted as a simple measure of the plant growth. Growth analysis is a widely used analytical tool for characterizing plant growth. Of the parameters typically calculated, the most important is the relative growth rate (RGR), defined as the parameter r in Equation 5.

$$RGR = \frac{\ln(\overline{W})_2 - \ln(\overline{W})_1}{t_2 - t_1} \quad (5)$$

where, W_1 and W_2 are plants leaves number at time t_1 and t_2.

In each of the *L. minor* growth experiment the leaves were counted, the leaf number on the first count date and the leaf count on the second date were recorded. RGR was then calculated for each experimental treatment, and the values were averaged for the overall experiment. Alternatively, where growth was being followed over several days, a curve was fitted to the ln–transformed plant leaf number through time and RGR at a particular time is calculated as the slope of the curve. When applied to counts made at only two points in time, the results are algebraically identical to the RGR estimator (Equation 5) (Hoffmann and Poorter, 2002).

Photosynthesis measurement: *L. minor* plants were filtered by using vacuum filtration onto glass fiber membrane filters. The photosynthesis of the flattened sample was measured using a PAM machine and Walz software (Waltz, Germany) as relative photosynthetic Electron Transport Rate (rETR) as described above for algal disks. Absorptance of the leaves was measured using the blue–ray RAT meter (Ritchie and Runcie, 2014; Quinnell *et al*., 2017; Chandaravithoon *et al.*, 2018) to calculate ETR from the rETR measurements calculated by the Walz software.

2.5.1 Expressing Photosynthesis of *Lemna minor* on a Chlorophyll *a* basis

PAM machines measure photosynthesis on a surface area basis (mol e^- m^{-2} s^{-1}). Photosynthesis measurements expressed on a leaf surface area basis have some uses in plant science, particularly in plant ecology, but as in the case of algae, it is conventional to standardize photosynthetic rates on a Chlorophyll *a* basis. Chlorophyll *a* was estimated on a leaf surface area basis using optical density (OD) measurements on solvent extracts using a 7:2 mixture of acetone and ethanol because pure ethanol was not found to be a satisfactory extractant for *L. minor* (Ritchie, 2018). The leaf samples were put in 10 mL centrifuge tubes and 3 mL 7:2 acetone/ethanol

was added. The samples were incubated in the refrigerator at -10 ºC for about 12 h in the dark. After removal from the refrigerator, the samples were kept at room temperature in a dark box and then vortexed before being centrifuged to clear the Chlorophyll extract solution. One mL of cleared supernatant was used for chlorophyll *a* determination using the Shimadzu spectrophotometer at 850, 665 and 648 nm using the equations of Ritchie (2018) for estimating the quantity of chlorophyll *a* (Equation 6) in 7:2 acetone:ethanol solvent. Using the Chl *a*/leaf surface area relationship it was possible to recalculate ETR as mol e^{-} g^{-1} Chl *a* s^{-1}.

Chl *a* (µg/mL) = 2.34435 x ($A_{648\ nm} - A_{850\ nm}$) + 12.4552 x ($A_{665\ nm} - A_{850\ nm}$) (6)

2.6 Statistics

All results presented in this thesis are means ±95% confidence limits. Significantly different results were identified using simple *t*–tests and ANOVA using the Tukey test interval (TTI) at the $p < 0.05$ level. Cochran and Snedecor and Cochran (1989) was used as the standard statistical reference text.

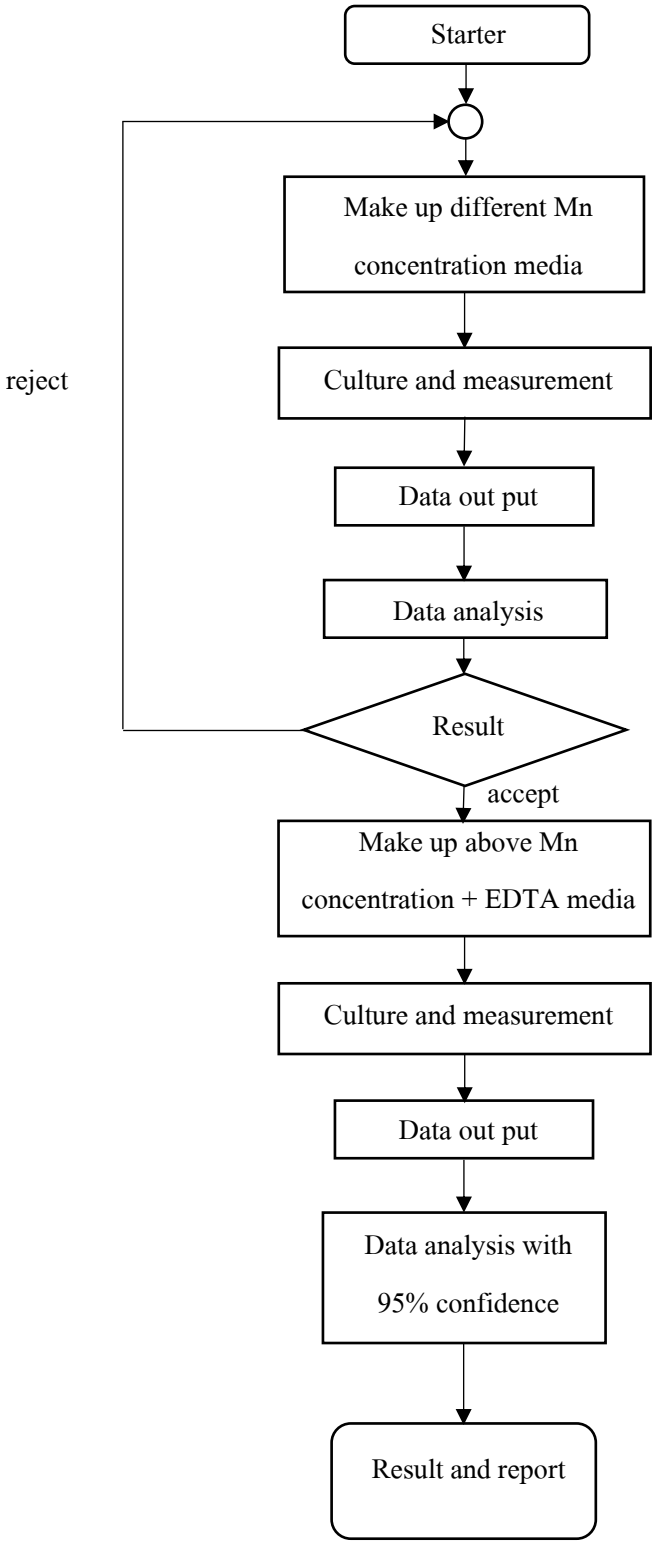

Figure 2 General Flow chart of experimental design in the project

CHAPTER 3

Results

The results of all experiment data are fully documented in the Appendices.

3.1 Determination of the effects of Mn upon growth in yeast

In present study, Yeast manganese toxicity was measured by comparing the growth rate as changes in optical density: OD (A_{630}). Analyzed data are shown in Table I1–I4 [Exponential growth rate (k h^{-1}), exponential growth doubling time: t_2 (hour), initial velocity for OD: V_0, Pearson r & P–value] (Ritchie and Raghupathi, 2008).

Growth of the yeast was measured by following the optical density (OD) at 630 nm in a time course of 24 h. If the A_{630} was greater than 1.0, the cell sample was diluted and the density of the culture calculated from the diluent. Optical density is usually only directly proportional to cell numbers up to an OD of about 1 or 1.5. Growth of a control culture was included in each experiment. Growth was then followed for at least 24 h. In the example shown, the effect of Mn upon exponential growth of yeast was determined at pH 7.5. Chelation agents such as EDTA are often reported to control metal toxicity (Ryan *et al*., 1995a; 1995b; Ritchie and Raghupathi, 2008; MacDiarmid and Gardner, 1996, Rengel and Zhang, 2003). The growth curves of yeast in the conditions containing Mn and Mn plus EDTA are shown in Figures 1 and 2, respectively. The results show that the conditions of 1 mol m^{-3} Mn (Figure 3.1a) and 3 mol m^{-3} Mn + 1 mol m^{-3} EDTA (Figure 3.1b), had almost identical inhibitory effects upon growth. The condition of 3 mol m^{-3} Mn almost halted growth. Inhibitory effects were noticeable within 8 h of exposure (see Table. I1, 3).

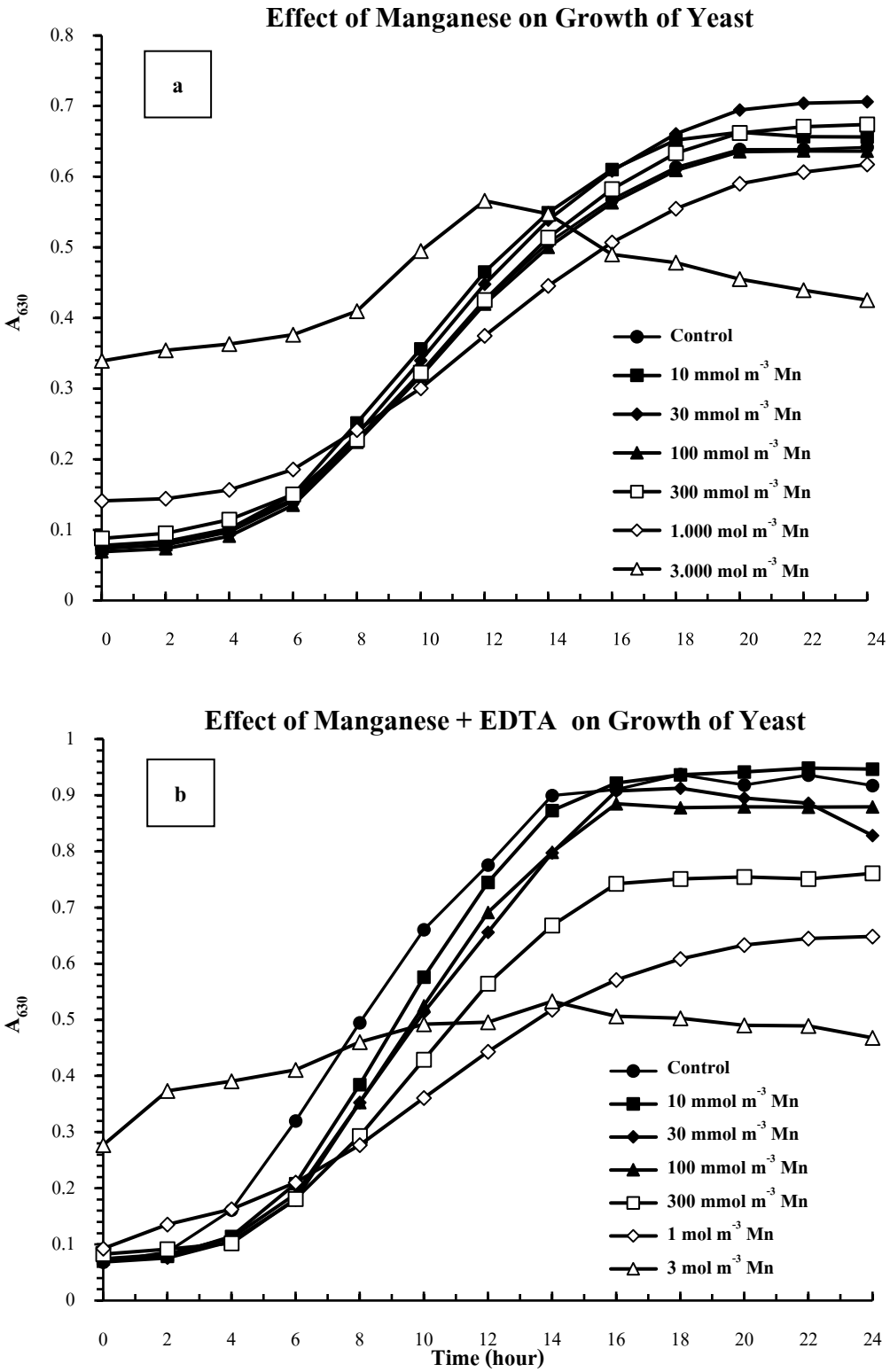

Figure 3.1 The effects of Mn **(a)** and Mn + 1 mol m^{-3} EDTA **(b)** on the exponential growth of yeast over a time course of 24 h. Cells were grown in modified Wickerham's medium at pH 7.5.

Figure 3.1: Fig. 3.1a shows that 1 mol m^{-3} Mn and Fig. 3.1b shows that 3 mol m^{-3} Mn + 1 mol m^{-3} EDTA had almost identical inhibitory effects upon growth. 3 mol m^{-3} Mn almost halted growth. Inhibitory effects of 3 mol m^{-3} Mn absence and presence EDTA were noticeable within 8 hours of exposure.

Logistic exponential growth constant could be calculated using non–linear least squares fitting methods using the Mn data shown in Figure 3.1. A logistic modelling curve was fitted which took the lag–phase into account. In the experimental conditions containing added Mn, the growth constants (h^{-1}) (Fig. 3.1a) were: control, 0.0672 ± 0.0080; 10 mmol m^{-3} Mn, 0.0646 ± 0.085; 30 mmol m^{-3} Mn, 0.0693 ± 0.0084; 100 mmol m^{-3} Mn, 0.0679 ± 0.0084; 300 mmol m^{-3} Mn, 0.0676 ± 0.0082, 1.000 mol m^{-3} Mn, 0.0603 ± 0.0050; 3.000 mol m^{-3} Mn, 0.0104 ± 0.0053 (see Table I2). The Mn + 1.000 mol m^{-3} EDTA growth data is shown in Fig. 3.1b**.** The growth constants (h^{-1}) were: control, 0.0558 ± 0.0095; 10 mmol m^{-3} Mn, 0.0631 ± 0.0107; 30 mmol m^{-3} Mn, 0.0628 ± 0.0120; 100 mmol m^{-3} Mn, 0.0630 ± 0.0100; 300 mmol m^{-3} Mn, 0.0626 ± 0.0091, 1.000 mol m^{-3} Mn, 0.0582 ± 0.0059; 3.000 mol m^{-3} Mn, 0.0141 ± 0.0041 (see Table I4).

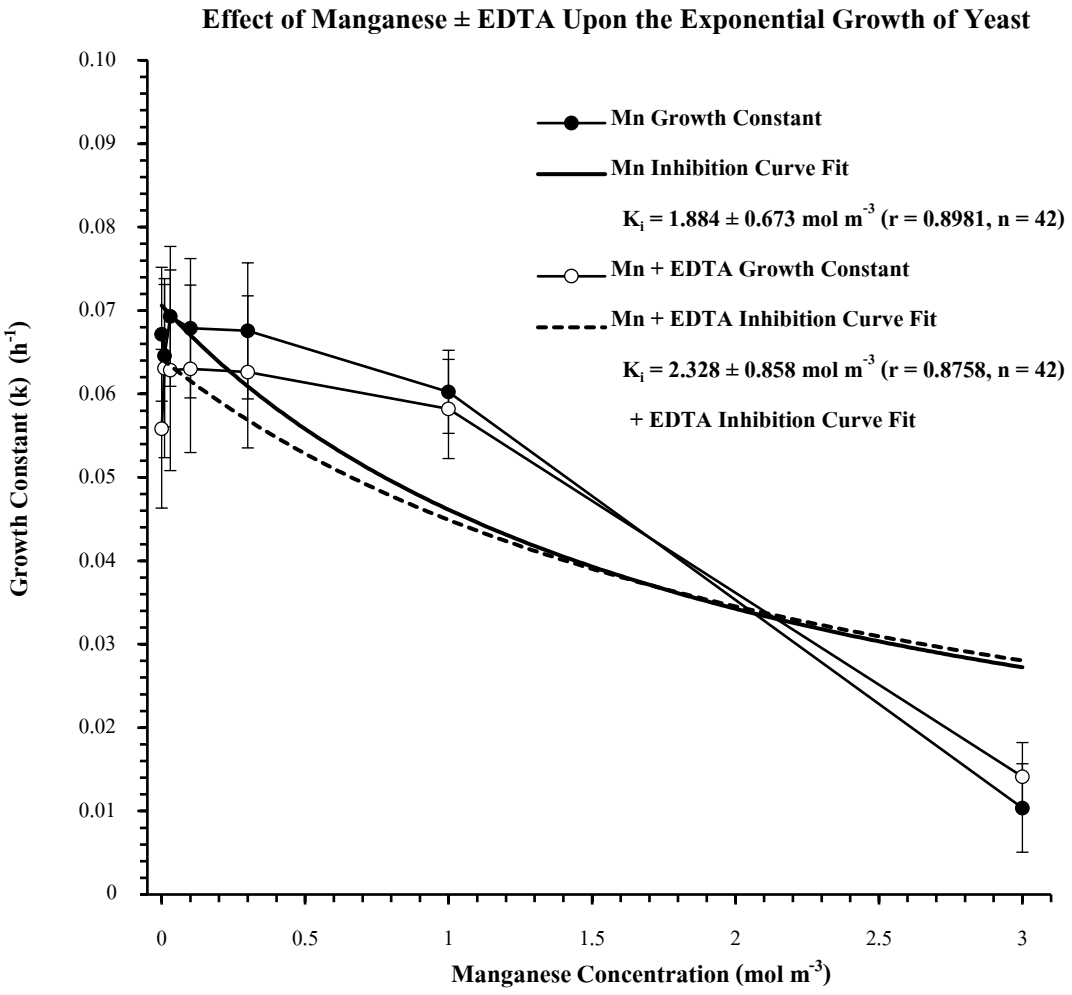

Figure 3.2 Effect of manganese upon exponential growth of yeast in the presence and absence of EDTA at pH 7.5. Growth constants are based on growth at 7 time points. The inhibition constant (K_i) for manganese in the presence and absence of EDTA were no significantly different so are K_i could be calculated.

Figure 3.2 shows the logistic exponential constants determined in an experiment similar to that shown in Figure 3.1 plotted against the concentration of Mn ions in the absence and presence of EDTA. The inhibition constant (K_i) for Mn and Mn + 1 mol m^{-3} EDTA were determined using non–linear least squares fitting. A student's *t*–test showed that the results were no significantly different. The K_i of the Mn growth inhibition was 1.884 ± 0.673 mmol m^{-3} (r = 0.8981, n = 42) and that of the Mn plus EDTA condition K_i was 2.328 ± 0.858 mol m^{-3} (r = 0.8758, n = 42).

3.2 Determination of the effects of Mn upon oxygenic photosynthesis in *Chlorella vulgaris*

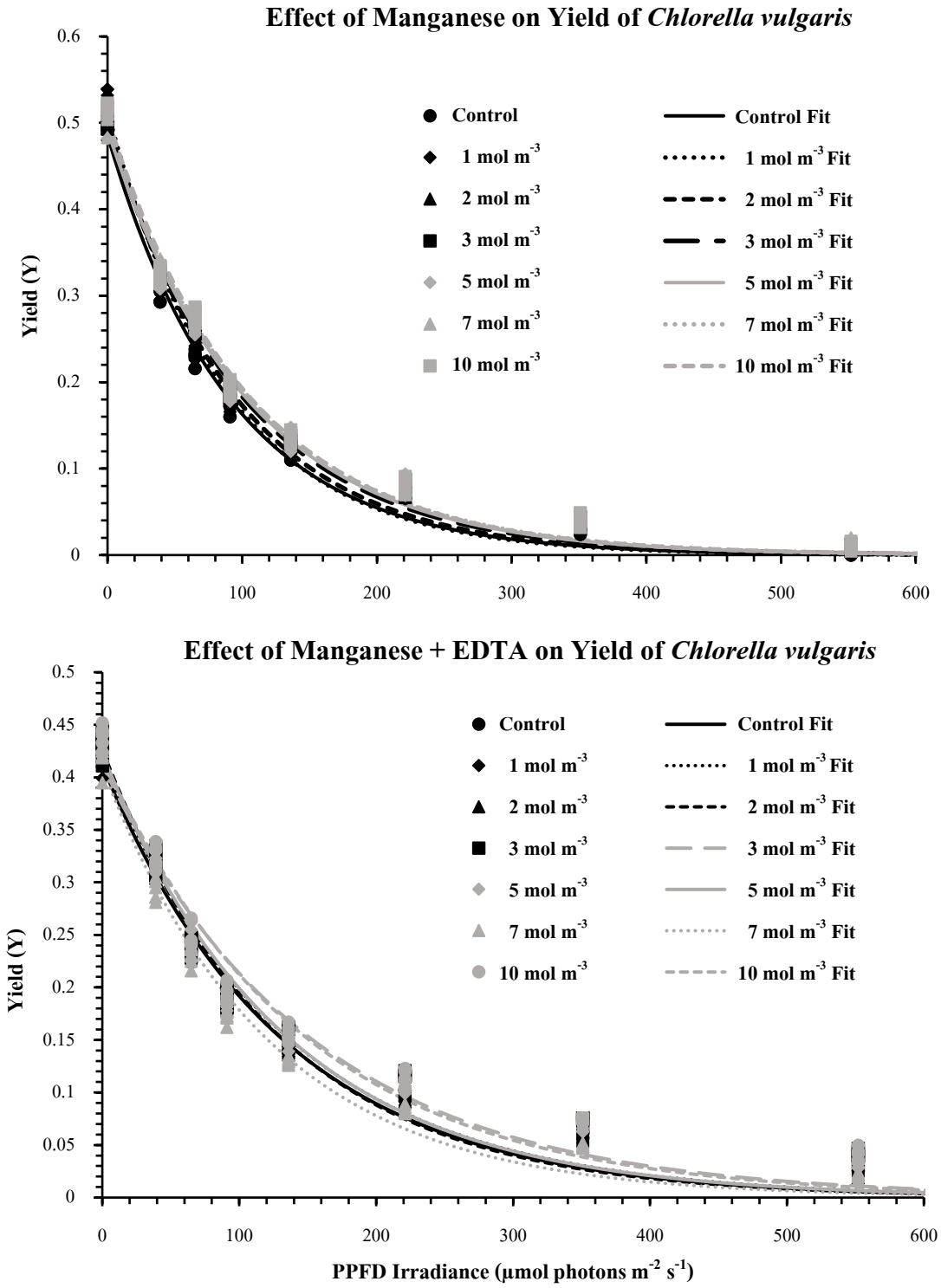

Figure 3.3 Plots of yield of *C. vulgaris* (Chl *a* + *b*) *vs.* irradiance for control cells and cells incubated 2 h in different Mn concentrations in the presence and absence of EDTA at pH 7.5. **(a)** Yield *vs.*

irradiance fits a simple exponential curve for the control (manganese conditions) cells (r = 0.9955, n = 54) and **(b)** Yield *vs*. irradiance also fits a simple exponential curve for the control (manganese + EDTA conditions) cells (r = 0.9907, n = 54). Overall both experiments show no significant effects on photochemical yield (Y).

In present study, *C. vulgaris* was used as the model organism to estimate manganese toxicity on oxygenic photosynthesis. *C. vulgaris* data analysis is shown in Table I5–I12 [maximum yield: Y, k constant for Yield: Y_k, half saturation point for yield: $Y_{0.5}$ (µmol photo m^{-2} s^{-1}), optimum irradiance: E_{opt} (µmol photo m^{-2} s^{-1}), maximum photosynthesis: P_{max}, maximum non–photochemical quenching: NPQ_{max}, Pearson r & P–value] (Brestic and Zivcak, 2013).

Both *C. vulgaris* experiments to measure photosynthetic performance was done in 6 replicates. But chlorophyll *a* and absoptance with RAT machine measurement was done using 4 replicates (Ritchie, 2012; Ritchie and Mekjinda, 2016). By the PAM machine was setting calibration in 130 and the actually absorptance was first used to calculate actual ETR from relative ETR and Chl *a* content was used to calculate photosynthesis on a chlorophyll *a* basis. So ETR quoted here is actual ETR not relative ETR (rETR) calculated by the Walz software.

Figure 3.3a shows plots of yield of *C. vulgaris* (Chl *a* + *b*) *vs*. irradiance for control cells and cells incubated 2 h in 1, 2, 3, 5, 7 and 10 mol m^{-3} Mn. Yield *vs*. irradiance fits a simple exponential decay curve for the manganese control cells (r = 0.9955, n = 54) and Figure 3.3b in manganese + 10.000 mol m^{-3} EDTA control cells (r = 0.9907, n = 54). Overall manganese in the presence and absence EDTA have no significant effect on photochemical yield.

Yield *vs*. irradiance fits a simple exponential decay curve for Mn data shown in Fig. 3.3. The maximum yield (Y_{max}) (Fig. 3.3a) were: control, 0.4852 ± 0.0128; 1 mol m^{-3} Mn, 0.5132 ± 0.0143; 2 mol m^{-3} Mn, 0.5051 ± 0.0128; 3 mol m^{-3} Mn, 0.4965 ± 0.0105; 5 mol m^{-3} Mn, 0.4917 ± 0.0115, 7 mol m^{-3} Mn, 0.4935 ± 0.108; 10 mol m^{-3} Mn, 0.5046 ± 0.0116 (see Table I5). The Mn + 10 mol m^{-3} EDTA growth data is shown in Fig. 3.3b**.** The maximum yield (Y_{max}) were: control, 0.4116 ± 0.0147; 1 mol m^{-3} Mn, 0.4184 ± 0.0131; 2 mol m^{-3} Mn, 0.4263 ± 0.0135; 3 mol m^{-3} Mn, 0.4117 ± 0.0166; 5 mol m^{-3} Mn, 0.4221 ± 0.0150, 7 mol m^{-3} Mn, 0.4088 ± 0.0058; 10 mol m^{-3} Mn, 0.4189 ± 0.0170 (see Table I9).

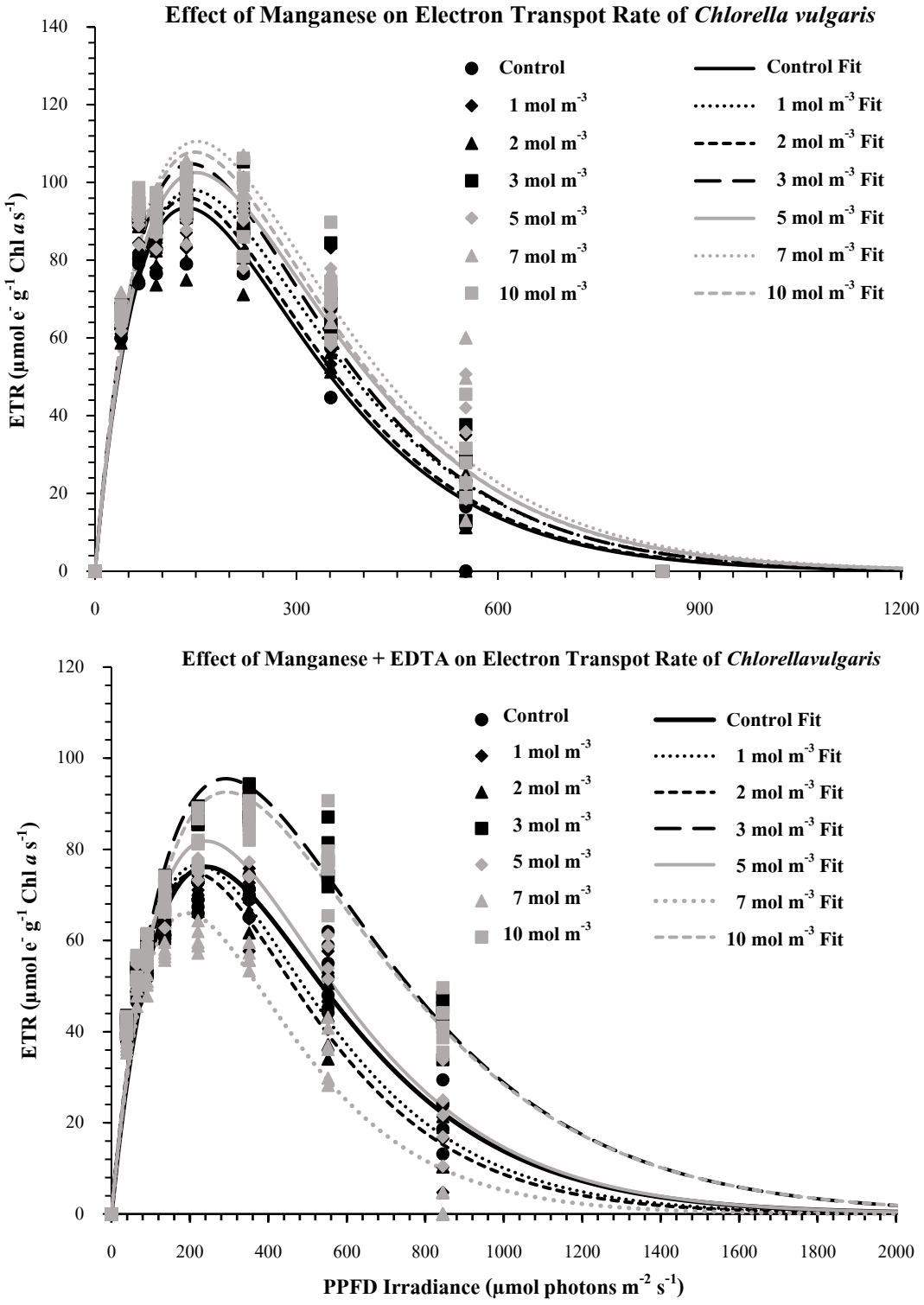

Figure 3.4 Photosynthetic electron transport rate (ETR) *vs*. irradiance for *C. vulgaris* in different manganese concentrations presence and absence of EDTA. **(a)** The ETR *vs*. irradiance curves for the manganese absence EDTA control *C. vulgaris* cells fits the waiting–inline equation very well

in (r = 0.9772, n = 54) and **(b)** manganese presence EDTA control (r = 0.9706, n = 54). Manganese low concentration (<10 mol m^{-3}) cannot eliminated oxygenic photosynthetic electron transport.

Figure 3.4 shows photosynthetic Electron Transport Rate (ETR) *vs*. irradiance for *C. vulgaris* in the manganese presence and absence 10 mol m^{-3} EDTA, respectively. The ETR *vs*. irradiance curves for the control *C. vulgaris* cells fits the waiting–in–line equation very well (r = 0.9772, n = 54) and (r = 0.9706, n = 54) in presence 10 mol m^{-3} EDTA. Overall both experiments have significant effect eliminates photochemical electron transport. But manganese low concentration (<10 mol m^{-3}) did not inhibit oxygenic photosynthetic electron transport.

ETR *vs*. irradiance fits the waiting–in–line model for Mn data shown in Fig. 3.4. The Maximum photosynthesis (P_{max} or ETR_{max}) (Fig. 3.4a) were: control, 93.4898 ± 1.5693; 1 mol m^{-3} Mn, 98.0627 ± 3.3616; 2 mol m^{-3} Mn, 96.0630 ± 3.6722; 3 mol m^{-3} Mn, 104.8134 ± 3.4389; 5 mol m^{-3} Mn, 102.5483 ± 3.8035, 7 mol m^{-3} Mn, 110.6171 ± 4.2319; 10 mol m^{-3} Mn, 107.8323 ± 3.7522 (see Table I6). The Mn + 10 mol m^{-3} EDTA growth data is shown in Fig. 3.4b**.** The Maximum photosynthesis (P_{max} or ETR_{max}) were: control, 57.117 ± 1.8087; 1 mol m^{-3} Mn, 57.4432 ± 2.0125; 2 mol m^{-3} Mn, 71.3020 ± 1.8562; 3 mol m^{-3} Mn, 61.3561 ± 1.9343; 5 mol m^{-3} Mn, 49.4940 ± 1.8446, 7 mol m^{-3} Mn, 69.4317 ± 2.1786; 10 mol m^{-3} Mn, 57.1170 ± 1.8087 (see Table I10).

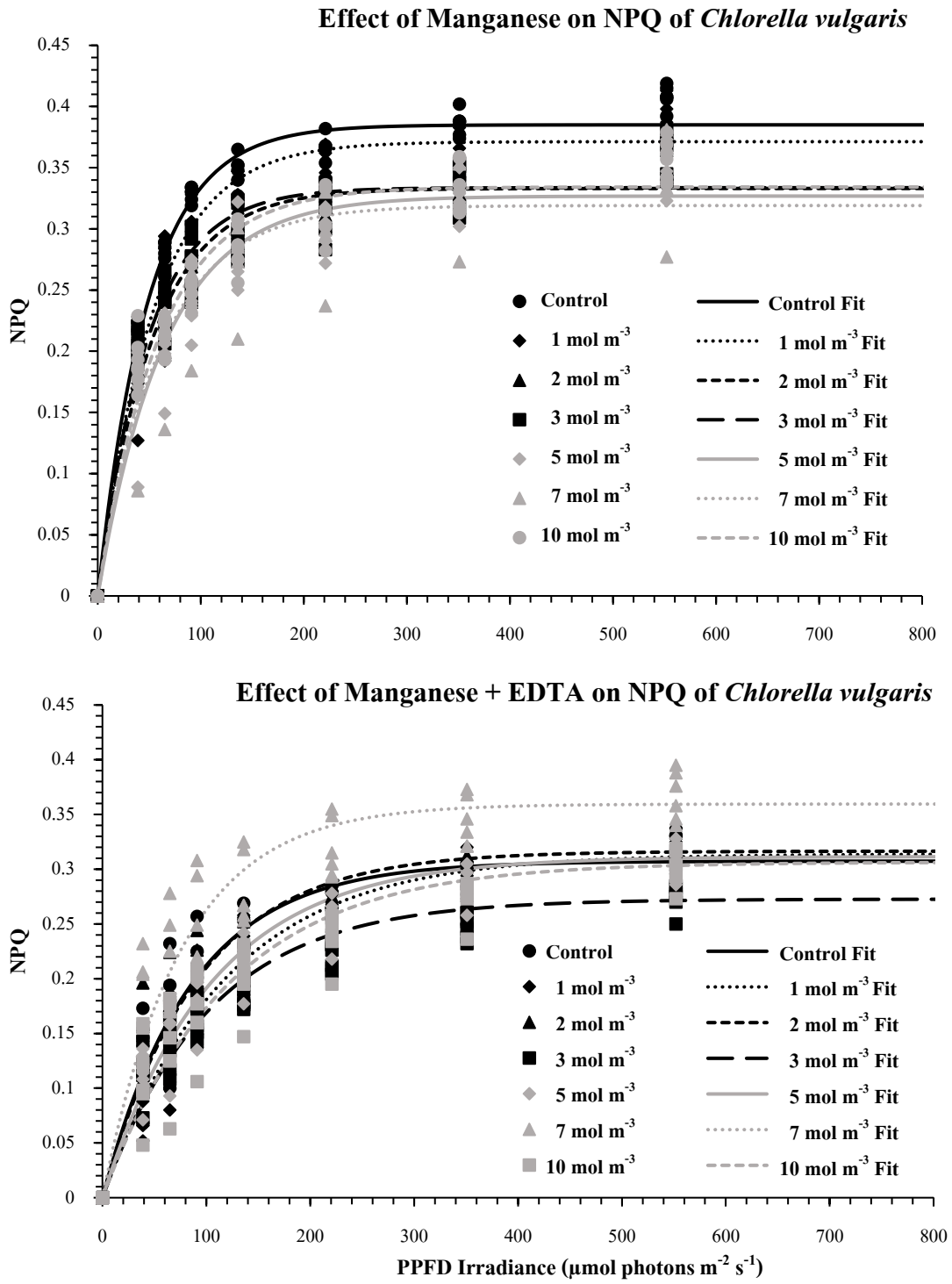

Figure 3.5 Non–photochemical quenching (NPQ) *vs*. irradiance for *C. vulgaris* in different manganese concentrations presence and absence of EDTA. **(a)** The NPQ *vs*. irradiance curves for the manganese in the absence of EDTA (control) in *C. vulgaris* cells fits a simple exponential

saturation curve very well in (r = 0.9925, n = 54) and **(b)** manganese presence EDTA control (r = 0.9907, n = 54).

Figure 3.5 shows non–photochemical quenching (NPQ) *vs*. irradiance for *C. vulgaris* in the manganese presence and absence 10 mol m^{-3} EDTA, respectively. The NPQ *vs*. irradiance curves for the control *C. vulgaris* cells fits (r = 0.9925, n = 54) and (r = 0.9907, n = 54) in presence 10 mol m^{-3} EDTA. Overall both experiments have significant effect eliminates on quenching of Chlorophyll fluorescence.

NPQ *vs*. irradiance fits a simple exponential saturation curve for Mn data shown in Fig. 3.4. The maximum non–photochemical quench (NPQ_{max}) (Fig. 3.4a) were: control, 0.4116 ± 0.0147; 1 mol m^{-3} Mn, 0.3139 ± 0.0154; 2 mol m^{-3} Mn, 0.3165 ± 0.0135; 3 mol m^{-3} Mn, 0.2727 ± 0.0108; 5 mol m^{-3} Mn, 0.3115 ± 0.0117, 7 mol m^{-3} Mn, 0.3595 ± 0.0156; 10 mol m^{-3} Mn, 0.3064 ± 0.0166 (see Table I7). The Mn + 10 mol m^{-3} EDTA growth data is shown in Fig. 3.4b**.** The maximum non–photochemical quench (NPQ_{max}) were: control, 0.3850 ± 0.0072; 1 mol m^{-3} Mn, 0.3713 ± 0.0128; 2 mol m^{-3} Mn, 0.3330 ± 0.0096; 3 mol m^{-3} Mn, 0.3337 ± 0.0103; 5 mol m^{-3} Mn, 0.3268 ± 0.0130, 7 mol m^{-3} Mn, 0.3191 ± 0.0159; 10 mol m^{-3} Mn, 0.3342 ± 0.0114 (see Table I11).

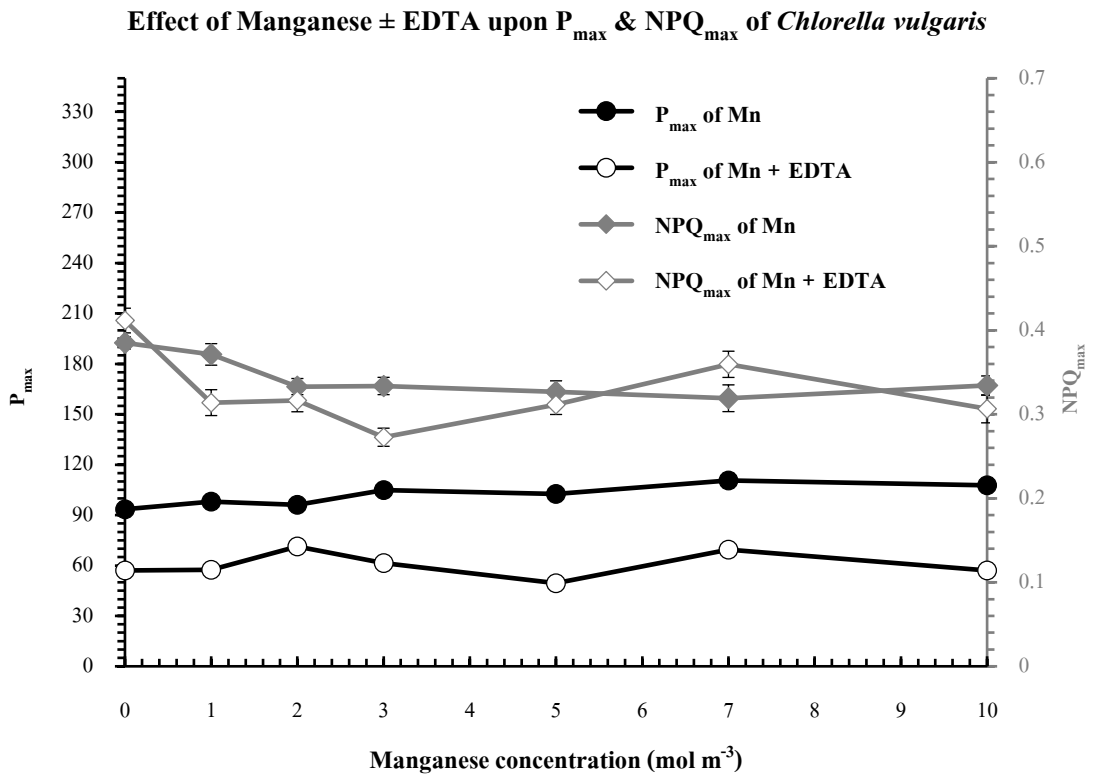

Figure 3.6 Effect of manganese upon P_{max} and NPQ_{max} of *C. vulgaris* in the presence and absence of EDTA at pH 7.5. P_{max} and NPQ_{max} are based on incubated 2 hours.

Figure 3.6 shows the P_{max} and NPQ_{max} determined in all the experiments plotted against the concentration of manganese ions in the presence and absence of EDTA. The P_{max} and NPQ_{max} for manganese and manganese + 10 mol m^{-3} EDTA were not different. So, this study the manganese low concentration (<10 mol m^{-3}) cannot eliminated oxygenic photosynthetic *C. vulgaris*. Chelation does not reduce manganese toxicity in *C. vulgaris*.

3.3 Determination of the effects of Mn upon growth in *Lemna minor*

Growth of the *L. minor* was measured by following the count leaf number over time (Fig. 3.19). Growth of a control culture was included in each experiment. Growth was then followed for at least 6 days. In the example shown, the effect of manganese in the presence and absence of EDTA upon exponential growth of leaf number of *L. minor* was determined at pH 7.5. *L. minor* analyzed data are shown in appendix, Table I13–I20: Leaf number (n), Exponential growth rate (k h^{-1}), exponential growth doubling time: t_2 (day), initial velocity for leaf number: V_0 (n), leaf surface (10^{-6} m^{-2}), chlorophyll *a* content: Chl *a* (µg), absorptance for leaf (%), relative growth rate: RGR (n n^{-1} d^{-1}), Pearson r & P–value] (Hoffmann and Poorter, 2002; Ritchie and Raghupathi, 2008).

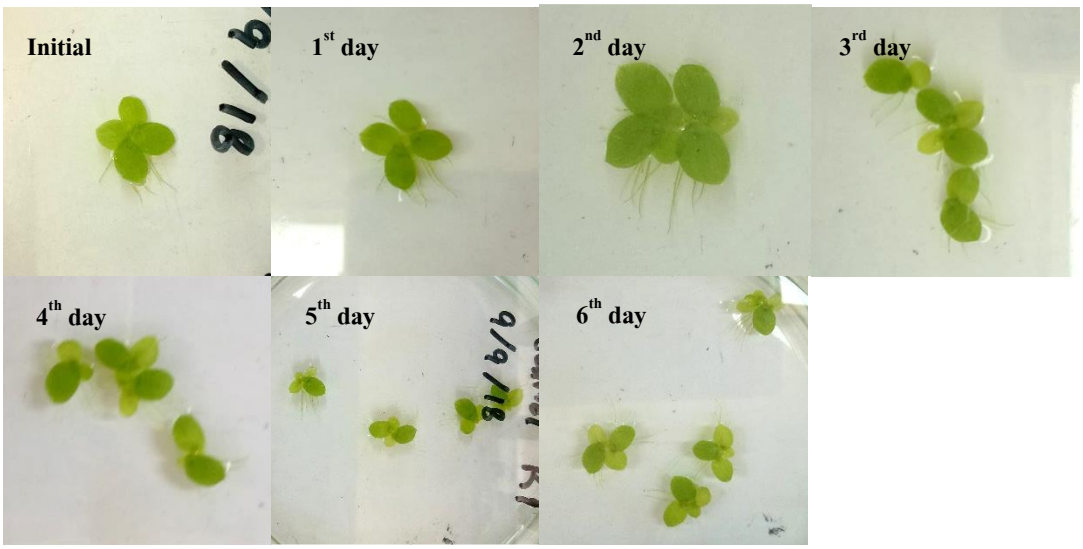

Figure 3.7 Photo of *L. minor* growth in 10% BG–11 – Control (Mn) on 6 day (Initial to 6th day).

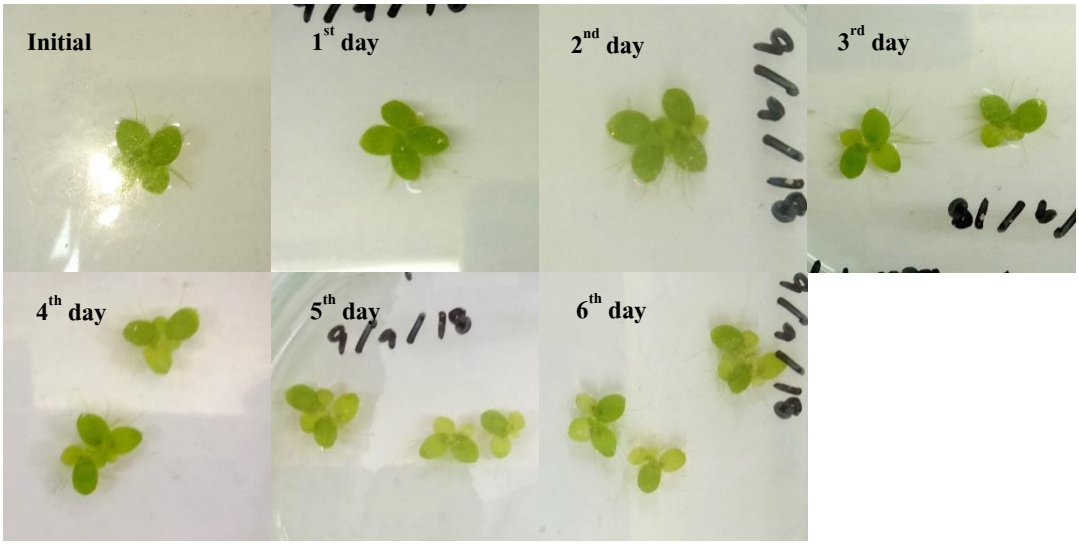

Figure 3.8 Photo of *L. minor* growth in 10% BG–11 – 10 mmol m^{-3} Mn on day 6.

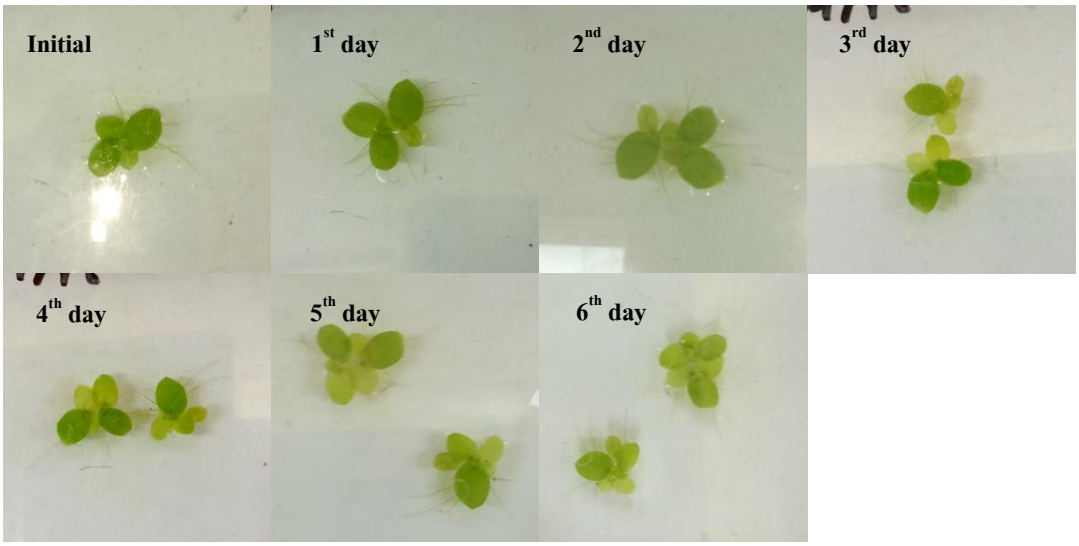

Figure 3.9 Photo of *L. minor* growth in 10% BG–11 – 30 mmol m^{-3} Mn on day 6.

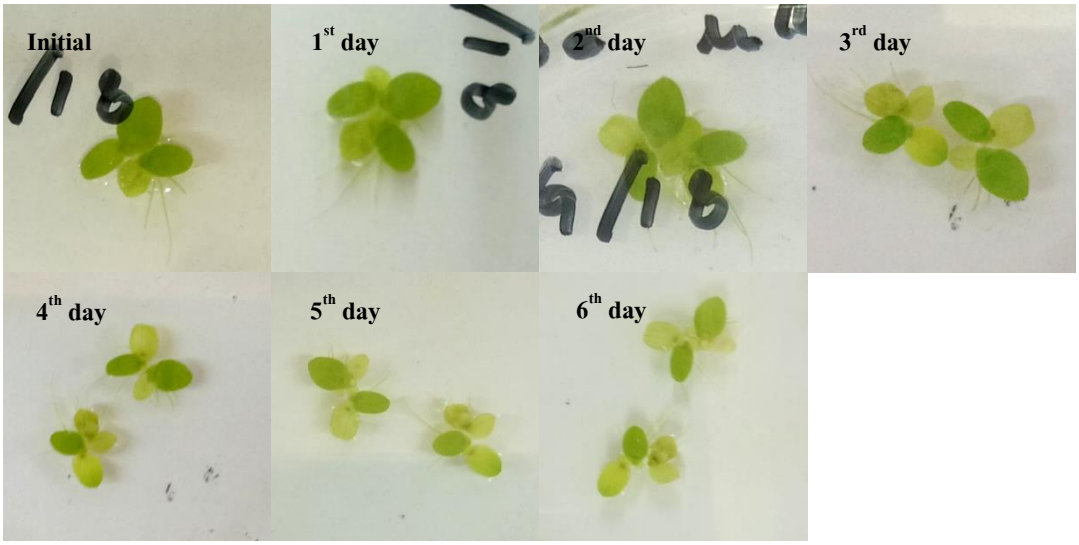

Figure 3.10 Photo of *L. minor* growth in 10% BG–11 – 100 mmol m^{-3} Mn on day 6.

Figure 3.11 Photo of *L. minor* growth in 10% BG–11 – 300 mmol m^{-3} Mn on day 6.

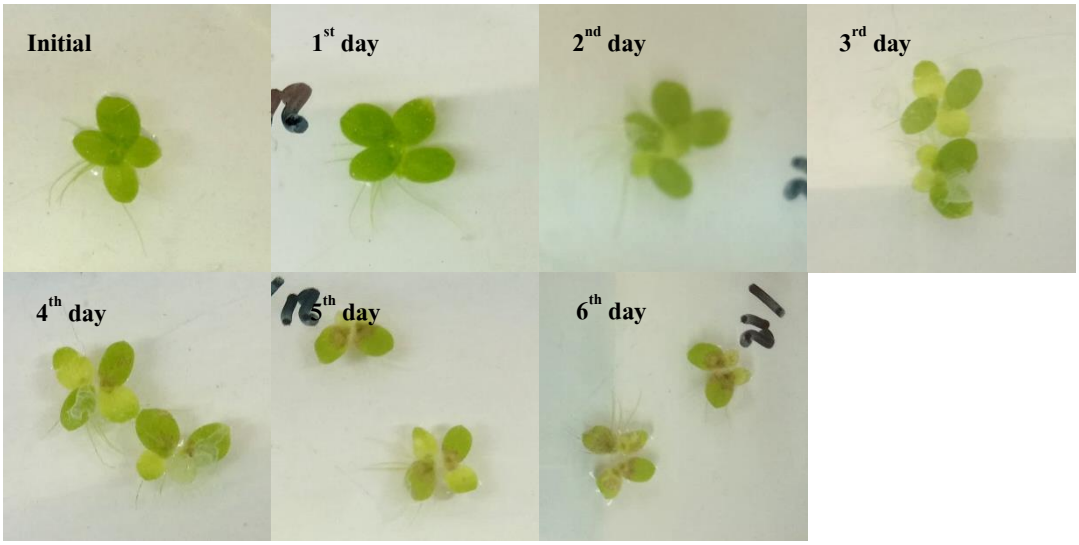

Figure 3.12 Photo of *L. minor* growth in 10% BG–11 – 1 mol m^{-3} Mn on day 6. Since 3rd day can find brown spot on the leaf of *L. minor*.

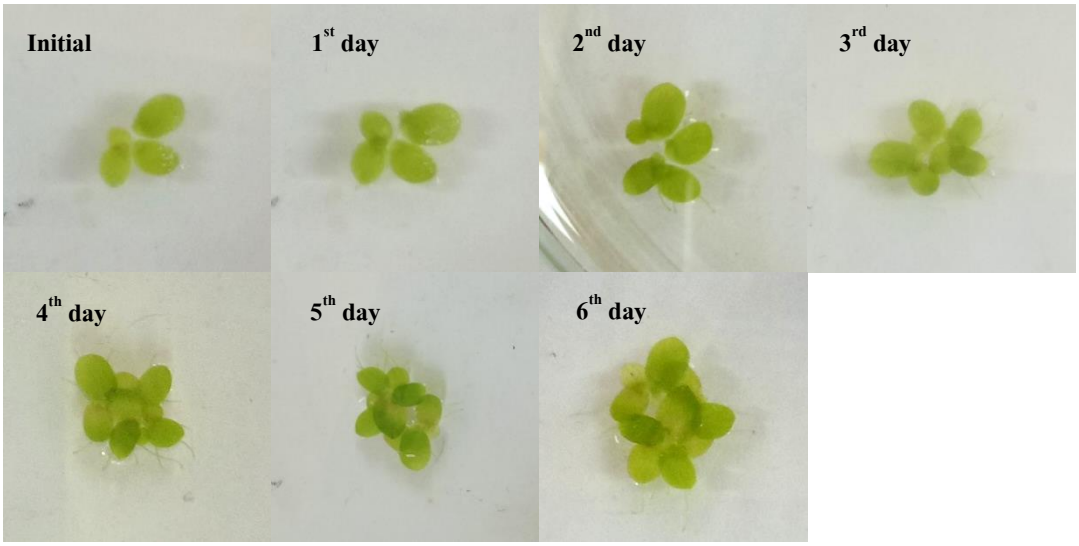

Figure 3.13 Photo of *L. minor* growth in 10% BG–11 presence 10 mmol m^{-3}EDTA – Control on day 6.

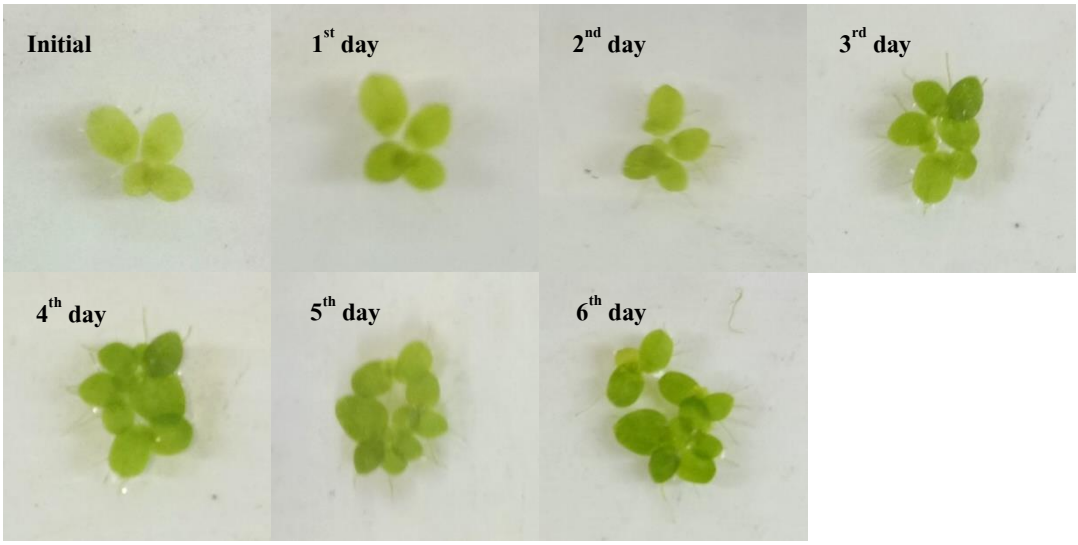

Figure 3.14 Photo of *L. minor* growth in 10% BG–11 presence EDTA – 10 mmol m^{-3} Mn on day 6.

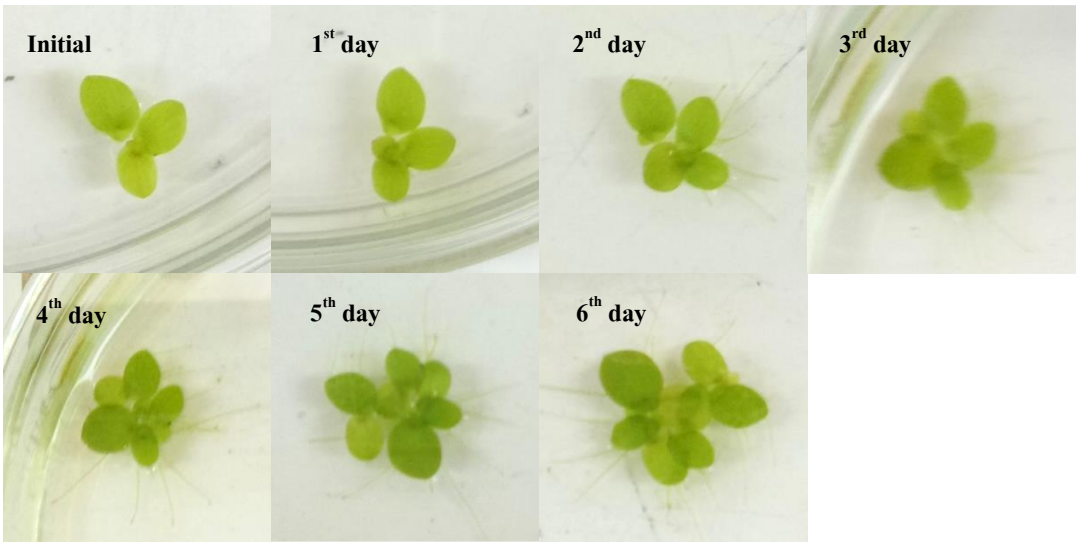

Figure 3.15 Photo of *L. minor* growth in 10% BG–11 presence EDTA – 30 mmol m^{-3} Mn on day 6.

Figure 3.16 Photo of *L. minor* growth in 10% BG–11 presence EDTA – 100 mmol m^{-3} Mn on day 6.

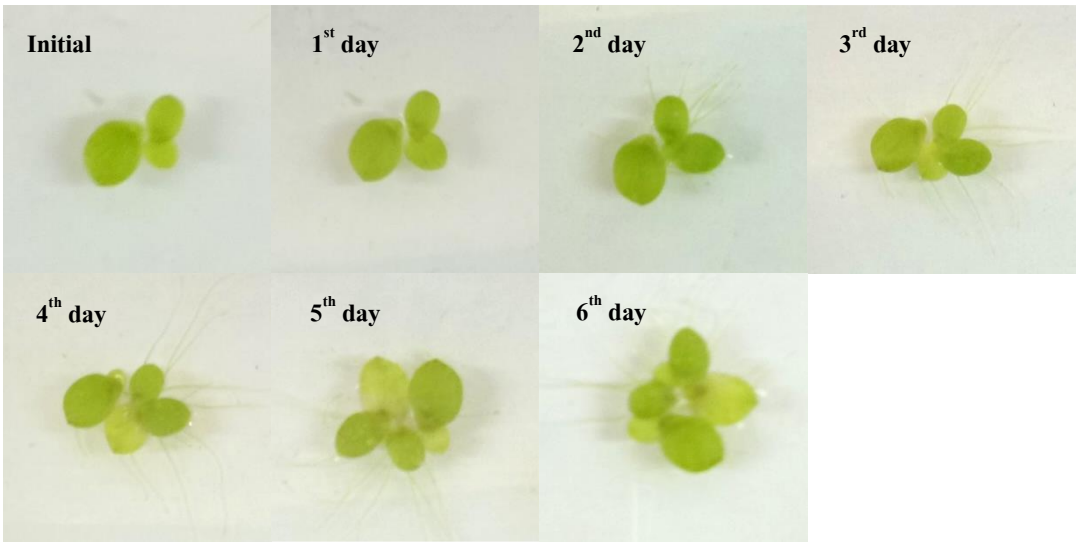

Figure 3.17 Photo of *L. minor* growth in 10% BG–11 presence EDTA – 300 mmol m^{-3} Mn on day 6.

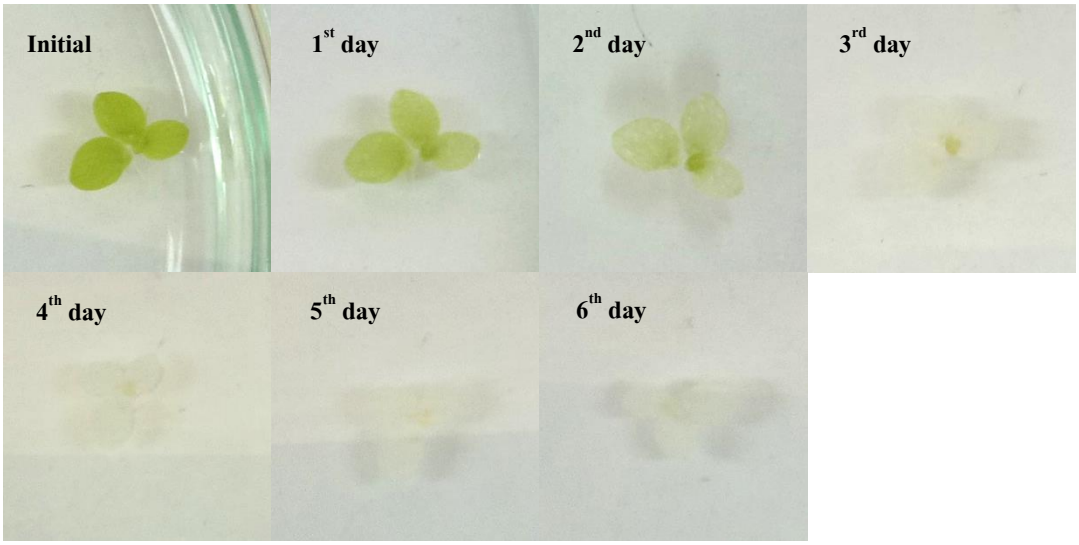

Figure 3.18 Photo of *L. minor* growth in 10% BG–11 presence EDTA – 1 mol m^{-3} Mn on day 6.

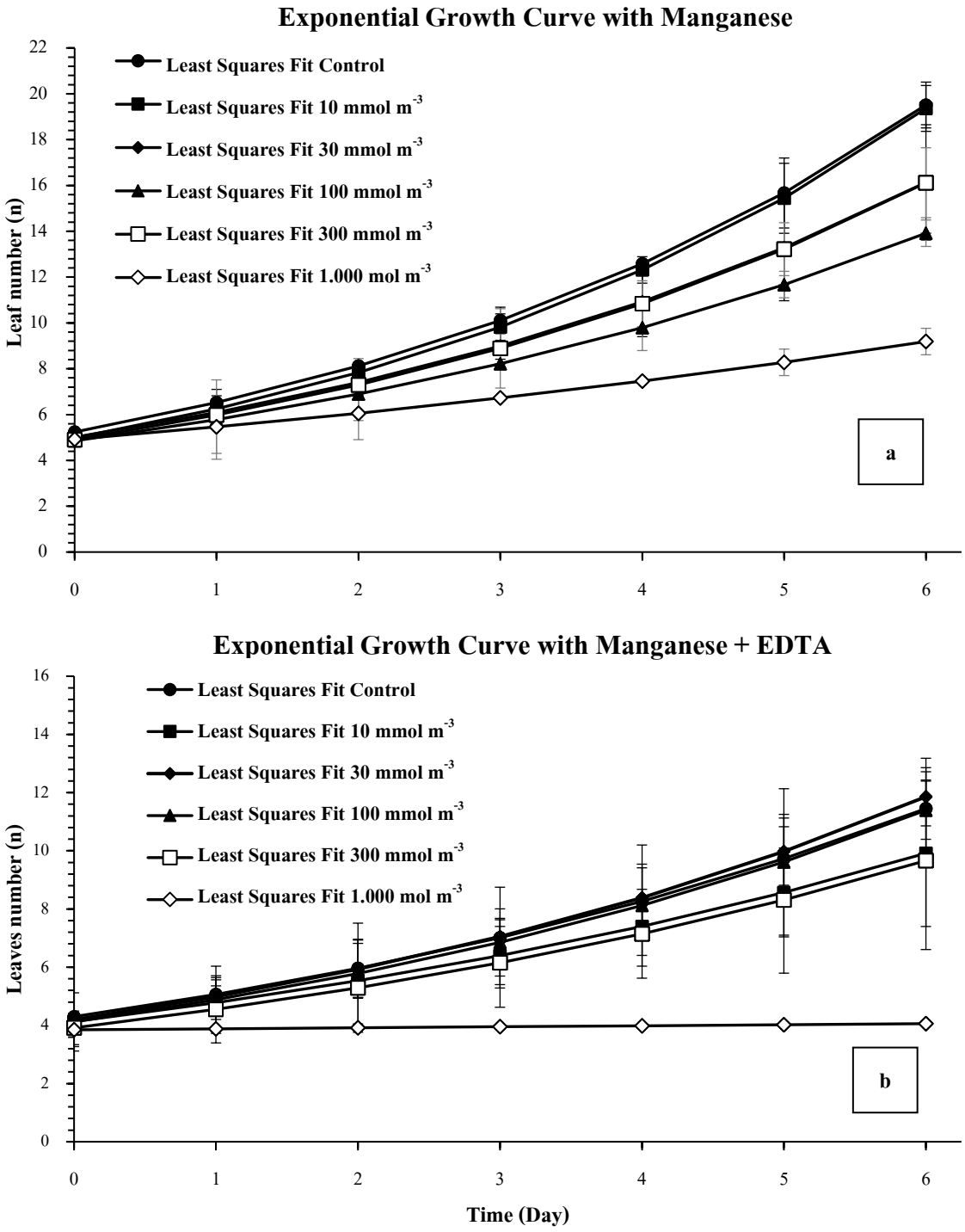

Figure 3.19 *L. minor* was grown in 10%BG–11 at pH 7.5. Exponential curves for the **(a)** control had r = 0.9670, n = 21 and the **(b)** control had r = 0.9070, n = 21. The highest Mn concentration (1 mol m^{-3}) coupled with the presence of EDTA was toxic.

Figure 3.19 shows growth of the *L. minor* was measured by following the count leaf number over time. Growth of a control culture was included in each experiment. Growth was followed for at least 6 days. In the examples shown, the effect of Mn in the absence and presence of EDTA upon exponential growth of leaf number of *L. minor* was determined at pH 7.5 as seen in Figures 3.19a and 3.19b, respectively. Figure 3.19a shows that 100 mmol m^{-3} in Mn had some inhibitory effects upon growth and statistically significant. Growth of the *L. minor* in 100 mmol m^{-3} Mn was almost halved and 1 mol m^{-3} Mn inhibited nearly all growth. Inhibitory effects were visually noticeable within 2 and 1 days of exposure, respectively. Figure 3.19b shows that Growth of the *L. minor* in 1 mol m^{-3} Mn plus 10 mmol m^{-3} EDTA was inhibited all growth. Inhibitory effects were visually noticeable 1 days of exposure.

Exponential growth constant could be calculated using non–linear least squares fitting methods using the data shown in Figure 3.19. The exponential growth constants (h^{-1}) were: (Fig. 3.19a) control, 0.219 ± 0.0320; 10 mmol m^{-3} Mn, 0.2263 ± 0.0342; 30 mmol m^{-3} Mn, 0.1948 ± 0.0386; 100 mmol m^{-3} Mn, 0.1756 ± 0.0273; 300 mmol m^{-3} Mn, 0.1984 ± 0.0328; 1.000 mol m^{-3} Mn, 0.1040 ± 0.0353 (see Table. I14) and (Fig. 3.19b) control, 0.1632 ± 0.0395; 10 mmol m^{-3} Mn, 0.1459 ± 0.0424; 30 mmol m^{-3} Mn, 0.1731 ± 0.0282; 100 mmol m^{-3} Mn, 0.1696 ± 0.0508; 300 mmol m^{-3} Mn, 0.1505 ± 0.0620; 1.000 mol m^{-3} Mn, 0.0089 ± 0.0122 (see Table I18).

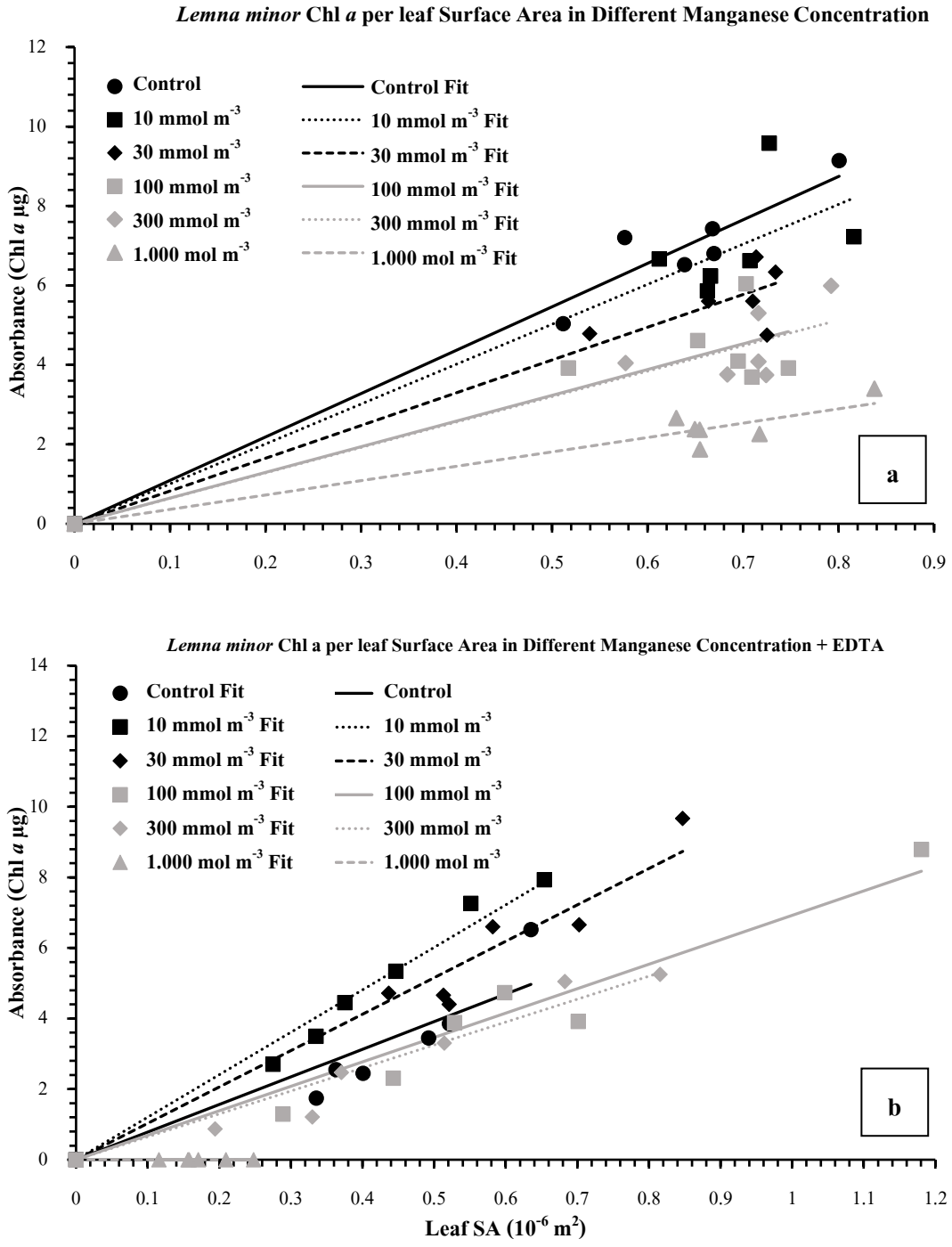

Figure 3.20 Comparison of the toxicity of Mn in experiments under the conditions containing Mn **(a)** and Mn plus EDTA **(b)**. The condition containing 1 mol m^{-3} Mn had chlorophyll *a* content half less than the control plants. The condition containing 10 mmol m^{-3} EDTA and 1 mol m^{-3} Mn had no chlorophyll *a* content in the leaves because the plants were killed. Chlorophyll a in each experiment was measured by using chlorophyll *a* content (µg) on a leaf surface area (10^{-6} m^2) basis.

Figure 3.20 shows chlorophyll *a* content of *L. minor* measured as chlorophyll *a* content (μg) per unit surface area (10^{-6} m^2) (see Table I12, I15). Figure 3.20a shows that the 1 mol m^{-3} Mn treatment had a chlorophyll *a* content half less than the control condition. In Figure 3.20b, the condition of 1 mol m^{-3} Mn + 10 mmol m^{-3} EDTA was found to be toxic to the plant (*L. minor* died see Fig II15).

In the comparison of the toxicity of Mn experiments, growth constants were also determined, which were based on growth after 6 days including day (0) (total 7 time points). Growth of a control culture was also measured in each experiment.

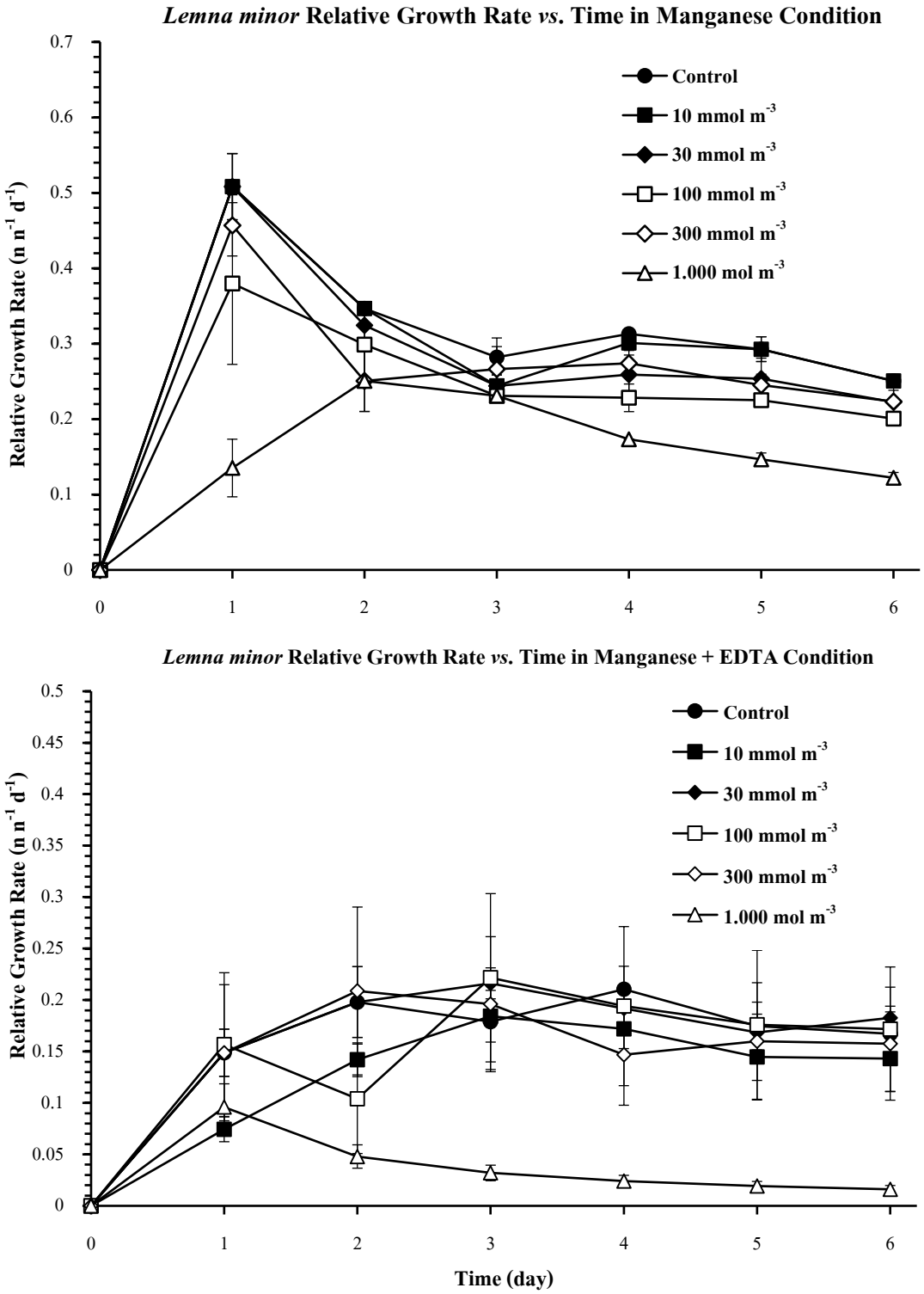

Figure 3.21 Relative growth rate for *L. minor* in the conditions containing Mn **(a)** and Mn plus EDTA **(b)**. Growth constants are based on growth at 7 time points. Growth of a control culture was

cultured in each experiment. Growth was then followed for 6 days. Plants were grown in 10% BG–11 medium at pH 7.5.

Figure 3.21 shows relative growth rate for *L. minor.* Figure 3.21a shows that the plant growths in the conditions containing 10 to 300 mmol m^{-3} Mn were not significantly different (ANOVA, ratio; chl *a*/Leaf SA). In the example shown, the effect of Mn (Fig. 3.21a) and (Fig. 3.21b) Mn + 10 mmol m^{-3} EDTA upon relative growth rate of *L. minor* was followed. Plants were grown in 10% BG–11 medium at pH 7.5. For Figs 3.21 a and b, relative growth rates were calculated using RGR-equation 2 plotting over time using data shown in Figure 3.19.

The RGR (n n^{-1} d^{-1}) in Fig. 3.21a were: control, 0.2505 ± 0.0230; 10 mmol m^{-3} Mn, 0.2505 ± 0.0230; 30 mmol m^{-3} Mn, 0.2225 ± 0.0675; 100 mmol m^{-3} Mn, 0.2006 ± 0.0177; 300 mmol m^{-3} Mn, 0.2234 ± 0.0407; 1.000 mol m^{-3} Mn, 0.1465 ± 0.0282 (see Table I16). The RGR (n n^{-1} d^{-1}) in Fig. 3.21b were: control, 0.1671 ± 0.0688; 10 mmol m^{-3} Mn, 0.1430 ± 0.1135; 30 mmol m^{-3} Mn, 0.1827 ± 0.0346; 100 mmol m^{-3} Mn 0.1717 ± 0.1125; 300 mmol m^{-3} Mn, 0.1576 ± 0.1461; 1.000 mmol m^{-3} Mn, 0.0160 ± 0.0688 (see Table I20).

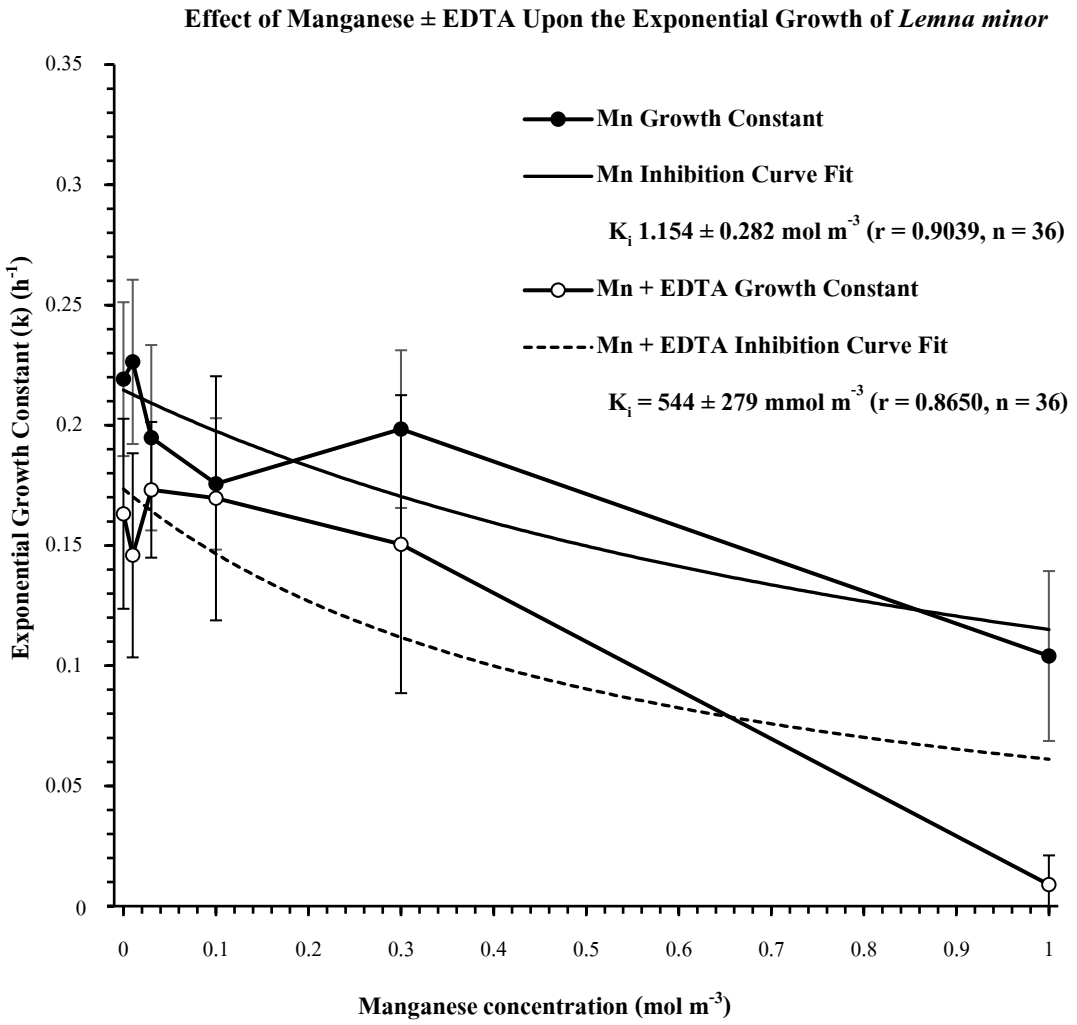

Figure 3.22 Effect of Mn on the exponential growth of *L. minor* in the absence and presence of EDTA at pH 7.5. Growth constants were based on growth at 6 days. The inhibition constants (K_i) for Mn in the absence and presence of EDTA were significantly different so K_i could be calculated for Mn toxicity ± EDTA.

Figure 3.22 shows the exponential constants determined in an experiment similar to that shown in Fig. 3.19 plotted against the concentration of Mn ions in the absence and presence of EDTA. The inhibition constant (K_i) for Mn and Mn + 10 mmol m^{-3} EDTA were determined using non–linear least squares fitting. A student's *t*–test showed that the results were significantly different. The Mn, $K_i = 1.154 \pm 0.282$ mol m^{-3} ($r = 0.9039$, $n = 36$) and Mn + 10 mmol m^{-3} EDTA, $K_i = 544 \pm 279$ mmol m^{-3} ($r = 0.8650$, $n = 36$).

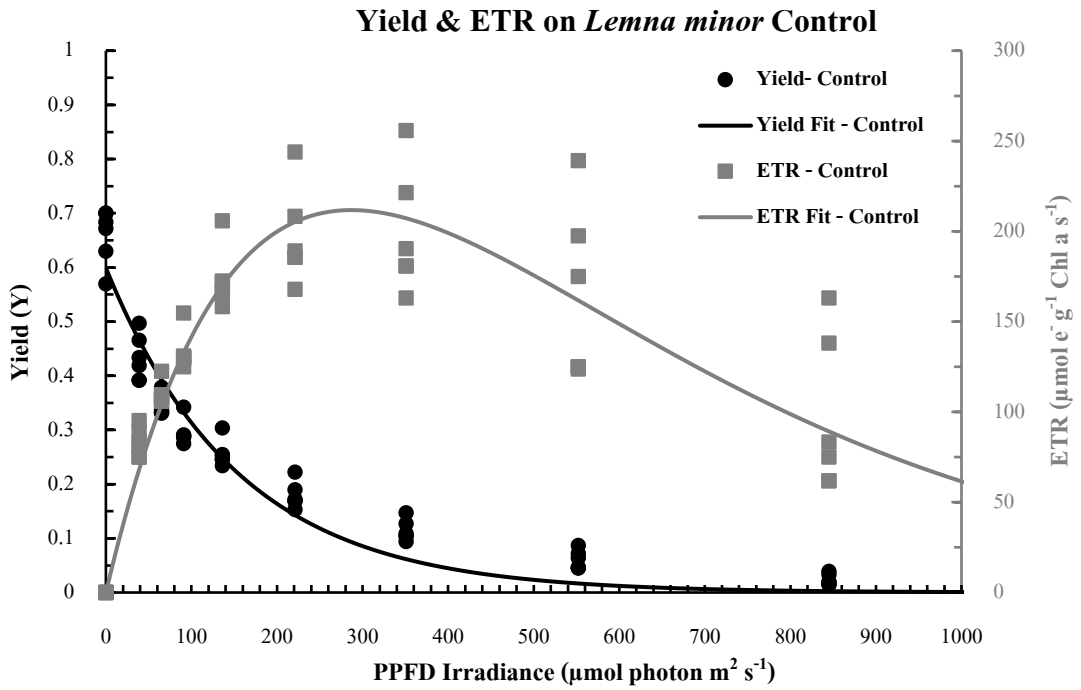

Figure 3.23 Photosynthesis of *L. minor* measured using PAM methods (n = 6). The Yield decays exponentially with increased irradiance (Y_{max} = 0.5992 ± 0.0334, ½ Y_{max} at 107 ± 13.1 µmol photon m^{-2} s^{-1}; Optimum irradiance = 287 ± 21.3 µmol photon m^{-2} s^{-1} and ETR_{max} = 212 ± 10.6 µmol e^- g^{-1} Chl *a* s^{-1}.

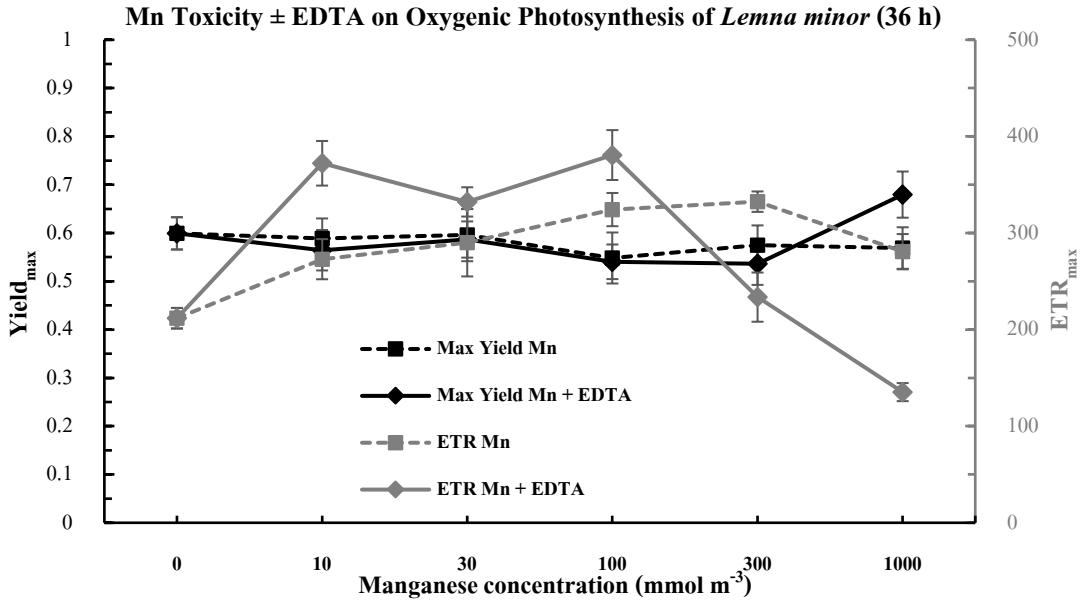

Figure 3.24 Photosynthesis of *L. minor* measured using PAM methods under a range of Mn concentrations ± EDTA (10 mmol m^{-3}). Plants were incubated for 36h. The Y_{max} without EDTA

was almost independent of Mn concentrations. EDTA increased Y_{max} at the highest Mn concentration. ETR_{max} tended to increase as Mn concentrations increased without EDTA and was inhibitory only at the highest concentration of Mn. Mn + EDTA inhibited ETR_{max} at 300 and 1000 mmol m^{-3} Mn.

Figure 3.23 shows a rapid light curve for control *L. minor* plants. This light saturation curve is typical of plants grown under low light conditions (Quinnell *et al*., 2017). Photosynthetic ETR measured on a leaf surface area basis were converted to a chlorophyll *a* basis (mol e^{-} g^{-1} Chl *a* s^{-1}) using measurements of Chl *a* per unit leaf surface area. The optimum irradiance (E_{opt}) was about 300 µmol photon m^{-2} s^{-1} which is rather similar to the conditions under which the plants were grown. The maximum photosynthetic electron transport rate is also typical of plants grown under low–light conditions. Figure 3.24 shows the maximum photosynthetic yield (Y_{max}) and ETRmax for *L. minor* grown in a range of Mn concentration for 36 h with and without 10 mmol m^{-3} EDTA. The very low EDTA concentration had to be used because of the toxicity of EDTA shown in Figures 3.19–3.22. The range of Mn concentrations did not show a high degree of toxicity to photosynthesis for the incubation time (36 h) used. EDTA did not protect *L. minor* from Mn and seemed to exacerbate Mn toxicity at higher Mn concentration. This confirms the observations made in the growth experiments.

In the condition containing Mn, the maximum photosynthetic yield (Y_{max}) are shown in Fig. 3.24 were: control, 0.5992 ± 0.0334; 10 mmol m^{-3} Mn, 0.5889 ± 0.0412; 30 mmol m^{-3} Mn, 0.5957 ± 0.0542; 100 mmol m^{-3} Mn, 0.5482 ± 0.0528; 300 mmol m^{-3} Mn, 0.5751 ± 0.0406; 1000 mmol m^{-3} Mn, 0.5688 ± 0.0430 (see Table I21). In the condition containing Mn and EDTA, the Y_{max} of control, 0.5992 ± 0.0334; 10 mmol m^{-3} Mn, 0.5650 ± 0.0419; 30 mmol m^{-3} Mn, 0.5865 ± 0.0375; 100 mmol m^{-3} Mn, 0.5403 ± 0.0358 mmol m^{-3} Mn, 0.5362 ± 0.0437; 1000 mmol m^{-3} Mn, 0.6795 ± 0.0478 (see Table I24).

In the condition containing Mn, the maximum photosynthetic ETR (ETR_{max}) are shown in Fig. 3.24 were: control, 212 ± 10.6; 10 mmol m^{-3} Mn, 273 ± 20.8; 30 mmol m^{-3} Mn, 290 ± 34.9; 100 mmol m^{-3} Mn, 324 ± 17.2; 300 mmol m^{-3} Mn, 332 ± 10.6; 1000 mmol m^{-3} Mn, 281 ± 18.2 (see Table I22). In the condition containing Mn and EDTA, the ETR_{max} of control,

212 ± 10.6; 10 mmol m^{-3} Mn, 372 ± 23.1; 30 mmol m^{-3} Mn, 332 ± 15.1; 100 mmol m^{-3} Mn, 381 ± 25.8; 300 mmol m^{-3} Mn, 234 ± 25.5; 1000 mmol m^{-3} Mn, 135 ± 9.35 (see Table I25).

CHAPTER 4

Discussion

In the present study, attempts were also made to demonstrate reversal of Mn–toxicity in yeast (*Saccharomyces cerevisiae*) and plants (*C. vulgaris* and *L. minor*) using Ethylene diamine tetra acetic acid (EDTA) (Lindsay and Norvell, 1978; Najeeb *et al*., 2009; Reichman, 2002).

4.1 Effect of manganese toxicity on growth of yeast

Manganese toxicity in yeast appears to be the same syndrome as Al–toxicity. In yeast, Mn toxicity can be conveniently measured by the effects of these metals on growth. The K_i of Mn was found to be about 100 mmol m^{-3}; toxicities of both metals could be reversed by EDTA (Ritchie and Raghupathi, 2008).

S. cerevisiae was grown in modified Wickerham's medium without any extra added vitamin (Table 2) in pH 7.5. The growth rate (measured as A_{630}) of *S. cerevisiae* exposed to Mn (0, 10, 30, 100, 300, 1,000 and 3,000 mmol m^{-3}) absence and presence 1 mol m^{-3} EDTA showed that there was significant difference in 3 mol m^{-3} Mn ($P < 0.05$ see Table III1 and III2). The growth rate of the yeast was found in Mn absence and presence EDTA 3 mol m^{-3} Mn (0.0101 ± 0.0053 and 0.0141 ± 0.0041 h^{-1}, respectively). When growth rate control was 0.0672 ± 0.0080 and 0.0558 ± 0.0095 h^{-1}, respectively. Hence, EDTA will reverse the Mn–toxicity syndrome in yeast if it is not used at toxic concentrations. Figures 3.1 and 3.2 show that the effect of chelation alleviated Mn toxicity uptake in yeast but did not completely reverse Mn–toxicity. Mn toxicity in yeast is not a simple function of the abundance of the divalent forms of metal ions in the bulk medium.

4.2 Effect of manganese toxicity on the light reactions of photosynthesis in *Chlorella vulgaris* (Yield, ETR and NPQ)

In this study, Mn–toxicity in *C. vulgaris* was measured at a range of different manganese concentrations (0, 1, 2, 3, 5, 7 and 10 mol m^{-3}) and in the absence and presence 10 mol m^{-3} EDTA using PAM fluorometry to measure photosynthetic yield, electron transport (ETR) and non–photochemical quenching. *C. vulgaris* was growth in BG–11 6 day in light intensities = 200 µmol (quanta) $m^{-2}s^{-1}$, pH 7.5 and 30±2 ˚C.

The photosynthetic yield of *C. vulgaris* exposed Mn (Fig. 3.3) showed that maximum yield (Y_{max}) that was significantly different (control, 1 and 5 mol m^{-3}; $P < 0.05$ see Table III4 and III5) and presence EDTA had no significant effect at different concentrations ($P < 0.05$). The highest Y_{max} was found in 1 mol m^{-3} Mn (0.5132 ± 0.0143), 2 mol m^{-3} + EDTA (0.4263 ± 0.0135) and lowest Y_{max} was in Mn control (0.4852 ± 0.0128), 7 mol m^{-3} + EDTA (0.4088 ± 0.0058) (Table I5 and I9).

The photosynthetic electron transport of *C. vulgaris* in the presence of Mn and in the absence and presence EDTA (Fig. 3.4) showed effects on the maximum photosynthetic electron transport rate (P_{max} or ETR_{max}) that was significant different among concentrations ($P < 0.05$ see Table III6 and III7). The highest P_{max} was found in 7 mol m^{-3} Mn (110.6171 ± 4.2319), 2 mol m^{-3} Mn + EDTA (71.3020 ± 1.8562) and lowest P_{max} was in Mn control (93.4898 ± 1.5693), 5 mol m^{-3} Mn + EDTA (49.4940 ± 1.8446) (Table I6 and I10).

The photosynthetic non–photochemical quenching (NPQ) of *C. vulgaris* exposed to Mn in the absence and presence EDTA (Fig. 3.5) showed in maximum non–photochemical quenching (NPQ_{max}) rate that was significantly different among concentrations ($P < 0.05$ see Table III8 and III9). The highest NPQ_{max} was found in Mn control (0.3850 ± 0.0072), 2 mol m^{-3} Mn + EDTA control (0.4116 ± 0.0147) and lowest NPQ_{max} was in 7 mol m^{-3} Mn (0.3191 ± 0.0159), 2 mol m^{-3} Mn + EDTA (0.2727 ± 0.0108) (Table I7 and I11).

Although *C. vulgaris* exposed to Mn showed effects in yield, ETR and NPQ were significant different ($P < 0.05$) the effects on photosynthesis was not very severe. *C. vulgaris* is quite resistant to Mn–toxicity. Hence, *C. vulgaris* is very resistant to Mn when the concentration is

lower than 10 mmol m^{-3} but chelation with EDTA cannot alleviate Mn toxicity uptake in *C. vulgaris*.

4.3 Effect of manganese toxicity on *Lemna minor*

L. minor is a freshwater aquatic angiosperm and was used to study the effect of different manganese concentrations (0, 10, 30, 100, 300 and 1,000 mmol m^{-3}) and absence and presence 10 mmol m^{-3} EDTA in relative growth rate, chlorophyll *a* content per leaf surface area of a vascular plant. *L. minor* was grown in 10% BG–11 for 6 days in light intensities = 200 µmol (quanta) $m^{-2}s^{-1}$, pH 7.5 and 30±2 ˚C.

In study, the growth rate, relative growth rate (RGR) and Chlorophyll *a* content per leaf surface of *L. minor* showed that there was a reduction in growth by Mn. The manganese effects of absence and presence EDTA was significantly different in every concentration of Mn ($P < 0.05$ see Table III10 – III15). This is a different result to that found in *C. vulgaris*.

The growth rate of *L. minor* exposed to Mn is shown in Fig. 3.19. The highest k constant was found in 10 mol m^{-3} Mn (0.2263 ± 0.0342 h^{-1}), 30 mmol m^{-3} Mn + EDTA control (0.1731 ± 0.0282 h^{-1}) and lowest k constant was in 1 mol m^{-3} Mn (0.1040 ± 0.0353 h^{-1}), 1 mol m^{-3} Mn + EDTA (0.0089 ± 0.0122 h^{-1}) (Table I14 and I18). The RGR of *L. minor* (Fig. 3.21) exposed to different levels of Mn were tested at $P < 0.05$. The highest RGR were found in Mn control and 10 mol m^{-3} Mn (0.2505 ± 0.0230 n n^{-1} d^{-1}), 30 mmol m^{-3} Mn + EDTA control (0.1827 ± 0.0346 n n^{-1} d^{-1}) and lowest RGR was in 1 mol m^{-3} Mn (0.1221 ± 0.0282 n n^{-1} d^{-1}), 1 mol m^{-3} Mn + EDTA (0.0160 ± 0.0688 n n^{-1} d^{-1}) ($P < 0.05$) (Table I16 and I20). Both experiments have similar results.

The chlorophyll *a* content per leaf surface area of *L. minor* (µg/m^2) exposed Mn is shown in Fig. 3.20. The slope (m) was found in Mn control (10.9288 ± 0.8367), 10 mmol m^{-3} Mn + EDTA control (12.0373 ± 0.9151) and lowest slope was in 1 mol m^{-3} Mn (3.6160 ± 0.4712), 1 mol m^{-3} Mn + EDTA (0) ($P < 0.05$) (Table I15 and I19). Finally, since 4^{th} day for 1 mol m^{-3} Mn experiments was found brown spot symptom from Mn on the leaf (Fig. 3.12) and 1 mol m^{-3} Mn + 10 mmol m^{-3} EDTA was found to kill *L. minor* on the 1^{st} day (Fig. 3.18).

The photosynthesis of *L. minor* in Fig. 3.24. The comparison between Mn and Mn + 10 mmol m^{-3} EDTA conditions on Y_{max} were significant in 1 mol m^{-3} Mn only. But the comparison between Mn and Mn + 10 mmol m^{-3} EDTA conditions on ETR_{max} were significant in all Mn concentrations (*t*–test, $P < 0.05$).

It is thought that in vascular plants only the Mn^{2+} form is toxic (Kennedy, 1992). However, toxicity in plants is claimed to be reversible by chelation by organic acids such as malic, glutamic, oxalic and citric acids and synthetic chelation agents such as EDTA. Whether the observations that Mn toxicity is reversed by the presence of different types of chelation agents such as citric acid in agreement with previous findings by MacDiarmid and Gardner (1996) in yeast or not has not been firmly established in this study. Citric acid is a naturally occurring chelation agent that is secreted by roots. This needs further study because some of the results using EDTA in the present study were not consistent with reports where citric acid was used.

Mn–resistant varieties of ryegrass (*Populus cathayana*) are known to secrete carboxylates (Lei *et al.*, 2007; Rengel and Zhang, 2003; Ryan *et al*., 1995a; 1995b). In the present study it was found that Mn was only toxic to *C. vulgaris* at high concentrations (<10 mol m^{-3}) (Fig. 3.3–3.6). However, in the present study about *C. vulgaris*, we studied the effect of Mn toxicity on oxygenic photosynthesis only and over a short term. Longer exposure times might have had different effects on photosynthesis and on growth rates. The studies on *L. minor* involved much longer exposure times and the apparent resistance of *C. vulgaris* to Mn might be a reflection of the short incubation times not allowing enough Mn to accumulate in cells for toxic effects to be observed.

Interference with membrane function is thought to be a major factor in the toxicity of Mn^{2+} along with its biochemical effects on enzyme function if it is in excess in the cytoplasm. Mn^{2+}, like many other polyvalent cations, is a potent channel–blocking agent due to the effects of Al and Mn on aquaporin function and on calcium metabolism. Calcium is practically universally involved in cell signaling and motility in plants and animals (Atwell *et al*., 1999). Any interference with this function is likely to be toxic to cells. Manganese is known to interfere with calcium function in vascular plants (Marschner, 1995).

The low rates of uptake of Mn into the cytoplasm of cells is not a water–tight argument against the idea that much of the toxicity of Mn is due to Mn that actually enters the

cytoplasm of cells. Transport of Mn ions within the xylem of land plants is essentially driven by mass upward flow of water created by the transpiration stream and transport in the phloem is thought to occur via the positive hydrostatic pressure gradient developed from the loading of sucrose into the phloem from mature actively photosynthesizing leaves and unloading of sucrose into the sink tissues such as rapidly growing tissues, apical root zones and reproductive organs (Hocking, 1980; MacRobbie, 1971; Reichman, 2002; Reid, 2001; Welch, 1995). *L. minor* is a small freshwater aquatic, but it still has roots and so there is a transportation stream from the roots to the leaves and then out through the stomata by transpiration. The transpiration rate of water has a large effect on macronutrient translocation rate, however at low supply, processes such as xylem loading and unloading and transfer between xylem and phloem have been shown to be more important for the rate of nutrient supply (Reichman, 2002; Welch, 1995). Mn in the xylem fluid exists in the uncompleted, free–ion form. Thus, in computer speciation studies, 37% of the Mn in *Glycine max* (Soybean) xylem sap and 72% of Mn in *L. esculentum* (tomato) xylem sap was found as Mn^{2+}. Manganese was also found complexed to organic acids (such as citrate) rather than by amino acids (White *et al*., 1981). In another study, Mn in the xylem exudate of *Helianthus annuus* (sunflower) was mainly present as Mn^{2+} at ranges of Mn supply from deficient to toxic (Graham, 1979; Reichman, 2002). Hence, the opportunity exists for high concentrations of harmful Mn^{2+} in the xylem fluid at excess Mn supply. Mn is predominately transported throughout the plant within the xylem rather than the phloem (Pearson *et al.*, 2008; Reichman, 2002). In another study, The metal toxicity may have an effect on the rate of xylem transport, possibly by reducing transpiration (Brune *et al.*, 1994; Reichman, 2002; Rousos *et al*., 1989). This could have effects on the concentrations of other nutrients reaching the shoots. As in the xylem, the pH, redox potential, ionic strength and organic constituents of the phloem sap will determine the loading, transport and unloading of metals in the phloem. However, unlike xylem cells, phloem cells are alive and metabolically active. Hence, metabolic reactions within the phloem have the potential to make the phloem sap more responsive to changes in the internal plant environment than the xylem sap (Reichman, 2002; Welch, 1995). Manganese mobility within the phloem is generally considered to variable and is dependent on the Mn status of the plant species as well as the source and sink organs. Excess Mn supply reduced phloem transport of Mn and the authors suggested loading from the xylem into the phloem may have been the rate limiting process (Pearson *et al.*, 2008;

Reichman, 2002). *L. minor* has a limited growth of roots and probably much nutrient uptake occurs on the underside of the floating leaves however, the leaves do have stomata and so there is significant transpiration effects in *L. minor* just as in non–aquatic vascular plants.

Mn^{2+} toxicity has been shown in the present study to be reversible in yeast by a chelation agent (EDTA). This consistent with other studies, the chelation has the effect of reducing Mn toxicity (Lei *et al*., 2007; Rengel and Zhang, 2003; ca; 1995b). However, in the present study it was surprising how tolerant, yeast, *C. vulgaris* and *L. minor* were to Mn. Toxic effects were only observed at much higher concentrations than expected (Atwell *et al*., 1999; Marschner, 1995). In soil, Mn is present in Mn(II) form as Manganese (II) bicarbonate ($Mn(HCO_3)_2$), soluble in Mn^{2+} and Mn^{3+}. When it occurs as oxides and hydroxides it is transformed to Mn^{4+} (MnIV). Mn^{4+} is present as a dark brown–sediment (MnO_2) which is insoluble but can be mobilized by changes in the redox potential (Atwell *et al*., 1999; Marschner, 1995; Reichman, 2002; Scholz, 2016). EDTA has the effect of stabilizing solutions to prevent catalytic oxidative decoloration, which is catalyzed by metal ions. The solubilization of Mn^{2+} ions can be accomplished using EDTA (Norvell and Lindsay, 1969; Reichman, 2002; Taylor, 1998). That may explain why EDTA reduced Mn–toxicity in yeast (anaerobic conditions) and but could not reduce Mn–toxicity in *C. vulgaris* or *L. minor* (under aerobic conditions). A more thorough study of Mn–toxicity in yeast grown under aerobic *vs.* anaerobic conditions is needed. From the results of this study it appears likely that Baker's and Brewer's yeast strains are likely to have different sensitivities to Mn.

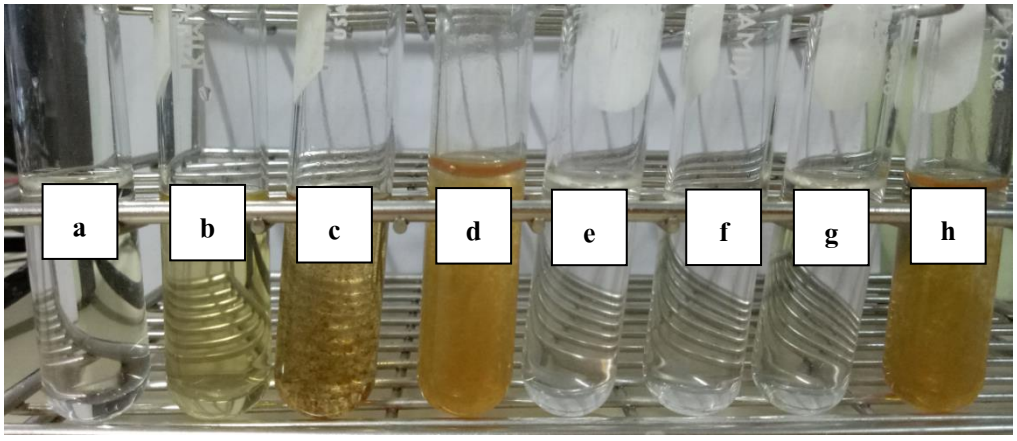

Figure 4.1 The various (low–high, respectively) of $MnSO_4$ solution. a–d are pH 7.5 and e–h are low pH.

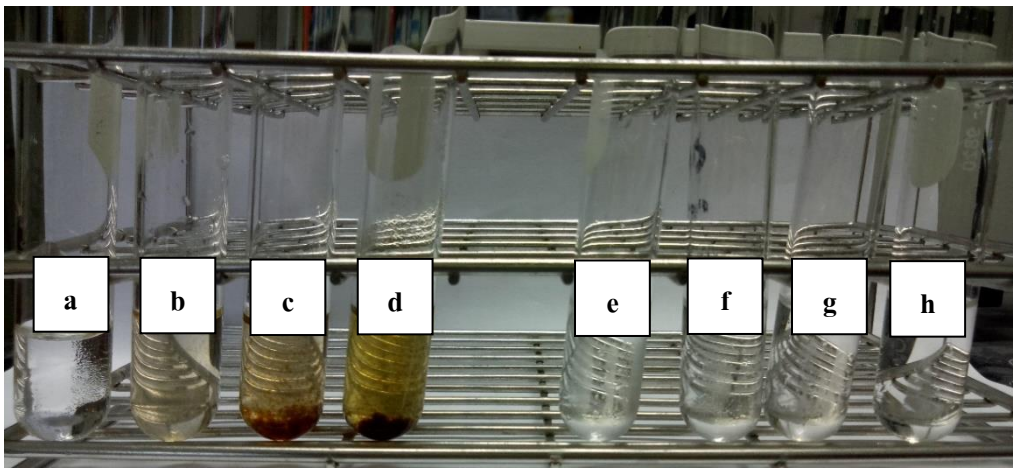

Figure 4.2 The various (low–high pH, respectively) of pH in $MnSO_4$ solution. a–d are $MnSO_4$ absence EDTA and e–h are $MnSO_4$ presence EDTA.

Figure 4.1 and 4.2 shows the Mn oxidation state at different pH and Fig. 4.1(a–d) shows the various states (low–high concentrations of Mn, respectively) of $MnSO_4$ in pH 7.5. The solution has more sediment when the Mn^{2+} has been oxidized: the Mn^{2+} has been transformed to Mn^{4+} forming insoluble MnO_2 which is non–toxic to *L. minor.* In contrast, Fig. 4.1(e–h) shows the same concentration of $MnSO_4$ in low pH.

Sediment is present in high Mn concentrations only. That means that Mn^{2+} is non–oxidized and the solutions are toxic to *L. minor* plants. However, this is a preliminary test and needs to be followed up. It might explain why chelation did not reduce Mn toxicity in *C. vulgaris* and *L. minor*.

CHAPTER 5

Conclusions

5.1 Conclusions

Preliminary experiments showed manganese had toxic effects on yeast growth (1 and 3 mol m^{-3}). Mn was toxic (1 and 3 mol m^{-3}) to yeast. We found that yeast grew equally well on Mn + EDTA. We found that EDTA–grown yeast was found to be insensitive to Mn when tested in a modified Wickerham's medium without any extra added vitamin (Table 2). The *C. vulgaris* oxygenic photosynthesis data on yield, ETR and NPQ showed only small effects of manganese when the alga was incubated for 2 hours in the Mn toxic BG–11 medium. The *L. minor* experiments show toxic effect of exposure to manganese since 300 mmol m^{-3} and 1 mol m^{-3} Mn *L. minor* show the brown spot symptom on the leaves (Campbell and Nable, 1988) and this effect was noticeable on the 4^{th} day (Fig. 3.12). The chelation agent (EDTA) alleviated manganese toxicty very well on *L. minor* growth and noticeable effects were apparent in 300 mmol m^{-3} Mn + 10 mmol m^{-3} EDTA. But EDTA itself was toxic at higher manganese concentrations (1 mol m^{-3}) and *L. minor* died (Fig. 3.18).

5.2 Future direction

In preliminary results can't still clearly investigating the cause of effect of manganese toxicity on yeast, *C. vulgaris* and *L. minor*. The yeast and *L. minor* results were more consistent with one another than for *C. vulgaris*. This might reflect a difference in the time required for toxicity to manifest itself in *C. vulgaris*. Hence, the future direction will investigate the Mn content in plants cell after removing the sediment and specific the sediment after adjusting the pH for medium. Dicot and monocot plants need to be investigated.

REFERENCES

Andersen, R. A. (2005). *Algal Culturing Techniques*. (1st ed.). Academic Press, United States.

Apichatmeta, K., Sudsiri, C. J., and Ritchie, R. J. (2017). "Photosynthesis of Oil Palm (*Elaeis guineensis*)." *Scientia Horticulturae*, 214, 34–40.

Atwell, J. B., Kreidemann, E. P., Turnbull, G. N. C., Eamus, D., Bieleski, L. R., and Farquhar, G. (1999). *Plants in Action*. Macmillan Education Australia, Australia.

Avila, D. S., Puntel, R. L., and Aschner, M. (2013). "Manganese in health and disease". *Metal Ions in Life Sciences*, 13, 199–227.

Belasco, W. (2006). "Algae Burgers for a Hungry World? The Rise and Fall of *Chlorella* Cuisine." *Technology and Culture*, 38(3), 608–634.

Beyerinck, M. W. (1980). "Culturversuche mit Zoochlorellen, Lichenengonidien und anderen niederen Algen." *Botanische Zeitung*, 47, 725–785.

Bloodnick, E. (2018). "Role of Manganese in Plant Culture" (Online) Available on https://www.pthorticulture.com/en/training-center/role-of-manganese-in-plant-culture/ (19 June 2018).

Brestic, M., and Zivcak, M. (2013). PSII fluorescence techniques for measurement of drought and high temperature stress signal in crop plants: Protocols and applications. In Rout, G. R., and Des, A. B. (Eds.), *Molecular Stress Physiology of Plants* (pp. 87–131). Springer India, India.

Brune, A., Urbach, W., and Dietz, K. J. (1994). "Compartmentation and transport of zinc in barley primary leaves as basic mechanisms involved in zinc tolerance." *Plant, Cell & Environment*, 17(2), 153–162.

Campbell, L. C., and Nable, R. O. (1988). Physiological Functions of Manganese in Plants. In Graham, R. D., Hannam, R. J., and Uren, N. C. (Eds.), *Manganese in Soils and Plants*, (pp. 139–154). Springer, Netherlands.

Campbell, R. C. (2000). *Reference sufficiency ranges for plant analysis in the Southern region of the United states*. Southern Region Agricultural Experiment Station, United states.

Chandaravithoon, P., Nakphet, S., and Ritchie, R. J. (2018). "Oxygenic and anoxygenic photosynthesis in a sewage pond." *Journal of Applied Phycology*, 30(6), 3089–3102.

Charle, D. G., and van Willigen, R. T. (2006). Manganese: The Oxygen–Evolving Complex & Models. In Scott, R. A. (Ed.), *Encyclopedia of Inorganic Chemistry* (1st ed., pp. 28). John Wiley & Sons, Ltd, United Kingdom.

Clarkson, D. (1996). "Mineral nutrition of higher plants." *Annals of Botany*, 78(4), 527–528.

Cornely, O. A., Cuenca–Estrella, M., Meis, J. F., and Ullmann, A. J. (2014). "European society of clinical microbiology and infectious diseases (ESCMID) fungal infection study group (EFISG) and European confederation of medical mycology (ECMM) 2013 joint guidelines on diagnosis and management of rare and emerging fungal diseases." *Clinical Microbiology and Infection*, 20, 1–4.

Culotta, V. C., Yang, M., and Hall, M. D. (2005). "Manganese transport and trafficking: Lessons learned from *Saccharomyces cerevisiae*." *Eukaryotic Cell*, 4(7), 1159–1165.

Dastur, Y. N., and Leslie, W. C. (1981). "Mechanism of work hardening in Hadfield manganese steel." Metallurgical Transactions. A, *Physical Metallurgy and Materials Science*. 12(5), 749–759.

De La Luz Mora, M., Rosas, A., Ribera, A., and Rengel, Z. (2009). "Differential tolerance to Mn toxicity in perennial ryegrass genotypes: Involvement of anti–oxidative enzymes and root exudation of carboxylates." *Plant and Soil*, 320(1–2), 79–89

Demirevska–Kepova, K., Simova–Stoilova, L., Stoyanova, Z., Hölzer, R., and Feller, U. (2004). "Biochemical changes in barley plants after excessive supply of copper and manganese." *Environmental and Experimental Botany*, 52(3), 253–266.

Emsley, J. (2001). *Nature's building blocks: An A–Z guide to the elements*. Oxford University Press, England.

Fernandes, L. A. de O., and Woodhouse, P. J. (2008). "Family farm sustainability in southern Brazil: An application of agri–environmental indicators." *Ecological Economics*, 66(2–3), 243–257.

Fernando, D. R., and Lynch, J. P. (2015). "Manganese phytotoxicity: New light on an old problem." *Annals of Botany*, 166(3), 313–319.

Führs, H., Hartwig, M., Molina, L. E. B., Heintz, D., Van Dorsselaer, A., Braun, H. P., and Horst, W. J. (2008). "Early manganese–toxicity response in *Vigna unguiculata* L. – A proteomic and transcriptomic study." *Proteomics*, 8(1), 149–159.

Gademann, R., and Ralph, P. J. (2005). "Rapid light curves: A powerful tool to assess photosynthetic activity." *Aquatic Botany*, 82(3), 222–237.

Genty, B., Briantais, J. M., and Baker, N. R. (1989). "The relationship between the quantum yield of photosynthetic electron transport and quenching of chlorophyll fluorescence." *Biochimica et Biophysica Acta – General Subjects*, 990(1), 87–92.

Graham, R. D. (1979). "Transport of copper and manganese to the xylem exudate of sunflower." *Plant, Cell & Environment*, 2(2), 139–143.

Hocking, P. (1980). "The composition of phloem exudate and xylem sap from tree tobacco (*Nicotiana glauca* Grah.)." *Annals of Botany*, 45(6), 633–643.

Hoffmann, W. A., and Poorter, H. (2002). "Avoiding bias in calculations of relative growth rate." *Annals of Botany*, 90(1), 37–42.

Horst, W. J., and Marschner, H. (1978). "Effect of Excessive Manganese Supply on Uptake and Translocation of Calcium in Bean Plants (*Phaseolus vulgaris* L.)." *Zeitschrift Für Pflanzenphysiologie*, 87(2), 137–148.

Johnson, E. A., amd Echavarri–Erasun, C. (2010). Yeast Biotechnology. In Kutzman, C. K., Fell, J. W., and Boekhout, T. (Eds.), *The Yeasts*, (5th ed., pp. 21–44). Elsevier, Netherlands.

Johnson, M. L., and Faunt, L. M. (1992). "Parameter estimation by least–squares methods." *Methods in Enzymology*, 210, 1–37.

Kabir, A., Hossain, M., and Rahman, M. (1970). "Use of Duckweed as Feed for Fishes in Polyculture." *Journal of Agriculture & Rural Development*, 1&2, 157–160.

Kanehisa, M., Furumichi, M., Tanabe, M., Sato, Y., and Morishima, K. (2017). "KEGG: new perspectives on genomes, pathways, diseases and drugs." *Nucleic Acids Research*, 45(1), 353–361.

Kaufman, J. G. (2000). *Introduction to Aluminum Alloys and Tempers*. ASM International, United States.

Kennedy, I. R. (1992). *Acid soil and acid rain: Research Studies in Botany and Related Applied Fields*. (2nd ed.) Research Studies Press, United Kingdom.

Kong, Q., Zhu, L., and Shen, X. (2010). "The toxicity of naphthalene to marine *C. vulgaris* under different nutrient conditions." *Journal of Hazardous Materials*, 178(1–3), 282–286.

Lei, Y., Korpelainen, H., and Li, C. (2007). "Physiological and biochemical responses to high Mn concentrations in two contrasting *Populus cathayana* populations." *Chemosphere*, 64(4), 686–694.

Lidon, F. C., Barreiro, M. G., and Ramalho, J. C. (2004). "Manganese accumulation in rice: Implications for photosynthetic functioning." *Journal of Plant Physiology*, 161(11), 1235–1244.

Lindsay, W. L., and Norvell, W. A. (1978). "Development of a DTPA Soil Test for Zinc, Iron, Manganese, and Copper." *Soil Science Society of America Journal*, 42(3), 421–428.

MacDiarmid, C. W., and Gardner, R. C. (1996). "Al toxicity in yeast (A role for Mg?)" *Plant physiology*, 112(3), 1101–1109.

MacRobbie, E. A. C. (1971). "Phloem translocation. facts and mechanisms: a comParative survey." *Biol. Review*, 46(4), 429–481.

Marschner, H. (1995). *Mineral Nutrition of Higher Plants*. (2nd ed.). Academic Press, United States.

Marschner, P. (2012). *Marschner's Mineral Nutrition of Higher Plants*. (3rd ed.). Academic Press, United States.

McConnaughey, T. A., and Whelan, J. F. (1997). "Calcification generates protons for nutrient and bicarbonate uptake." *Earth–Science Reviews*, 42(1–2), 95–117.

Myers, R. (2003). *The Basics of Chemistry*. Greenwood, United States.

Nable, R. O., Houtz, R. L., and Cheniae, G. M. (1988). "Early Inhibition of Photosynthesis during Development of Mn Toxicity in Tobacco." *Plant Physiology*, 86(4), 1136–1142.

Najeeb, U., Xu, L., Ali, S., Jilani, G., Gong, H. J., Shen, W. Q., and Zhou, W. J. (2009). "Citric acid enhances the phytoextraction of manganese and plant growth by alleviating the ultrastructural damages in *Juncus effusus* L." *Journal of Hazardous Materials*, 170(2–3), 1156–1163.

Nealson, K. H. (2006). The Manganese–Oxidizing Bacteria. In Dworkin, M., Falkow, S., Rosenberg, E., Schleifer, K. and Stackebrandt (Eds.), *The Prokaryotes* (Vol. 5, pp. 222–231). Springer New York. New York

Norvell, W. A., and Lindsay, W. L. (1969). "Reactions of EDTA Complexes of Fe, Zn, Mn, and Cu with Soils." *Soil Science Society of America Journal*, 33(1), 86–86.

Pasian, C. (2016). "Micronutrient Disorder" (Online) Available on https://u.osu.edu/greenhouse/2016/03/01/micronutrient-disorders/ (10 June 2019).

Pearson, J. N., Rengel, Z., Jenner, C. F., and Graham, R. D. (2008). "Manipulation of xylem transport affects Zn and Mn transport into developing wheat grains of cultured ears." *Physiologia Plantarum*, 98(2), 229–234.

Quinnell, R., Howell, D., and Ritchie, R. J. (2017). "Photosynthesis of an epiphytic resurrection fern *Davallia angustata* (Wall .ex Hook. & Grev.)." *Australian Journal of Botany*, 65(4), 348–356.

Rancke–Madsen, E. (1975). "The Discovery of an Element." *Centaurus*, 19(4), 299–313.

Rascher, U., Liebig, M., and Lüttge, U. (2000). "Evaluation of instant light–response curves of chlorophyll fluorescence parameters obtained with a portable chlorophyll fluorometer on site in the field." *Plant, Cell and Environment*, 23(12), 1397–1405.

Reddi, A. R., Jensen, L. T., and Culotta, V. C. (2009). "Manganese homeostasis in *Saccharomyces cerevisiae*." *Chemical Reviews*, 109(10), 4722–4732.

Reichman, S. M. (2002). *The Responses of Plants to Metal Toxicity: A review focusing on Copper, Manganese and Zinc*. Astralian Minerals & Energy Environment Foundation, Autralian.

Reid, R. J. (2001). "Mechanisms of micronutrient uptake in plants." *Aust J Plant Physiol*, 28(7), 659–666.

Rengel, Z., and Zhang, W. H. (2003). "Role of dynamics of intracellular calcium in aluminium–toxicity syndrome." *New Phytologist*, 159(2), 295–314.

Ritchie, R. J. (2006). "Consistent Sets of Spectrophotometric Chlorophyll Equations for Acetone, Methanol and Ethanol Solvents." *Photosynthesis Research*, 89(1), 27–41.

Ritchie, R. J. (2008). "Universal chlorophyll equations for estimating chlorophylls *a*, *b*, *c*, and *d* and total chlorophylls in natural assemblages of photosynthetic organisms using acetone, methanol, or ethanol solvents." *Photosynthetica*, 46(1), 115–126.

Ritchie, R. J. (2012). "Photosynthesis in the Blue Water Lily (*Nymphaea caerulea* Saligny) Using Pulse Amplitude Modulation Fluorometry." *International Journal of Plant Sciences*, 173(2), 124–136.

Ritchie, R. J. (2013). "The use of solar radiation by the photosynthetic bacterium, *Rhodopseudomonas palustris*: Model simulation of conditions found in a shallow pond or a flatbed reactor." *Photochemistry and Photobiology*. 89(5), 1143–1162.

Ritchie, R. J. (2014). "Photosynthesis in an Encrusting Lichen (*Dirinaria picta* (Sw.) Schaer.ex Clem., Physiaceae) and Its Symbiont, *Trebouxia* sp., Using Pulse Amplitude Modulation Fluorometry." *International Journal of Plant Sciences*, 175(4), 450–446.

Ritchie, R. J. (2018). "Measurement of chlorophylls *a* and *b* and bacteriochlorophyll *a* in organisms from hypereutrophic auxinic waters." *Journal of Applied Phycology*, 30(6), 1–13.

Ritchie, R. J., and Bunthawin, S. (2010a). "Photosynthesis in Pineapple (*Ananas comosus comosus* [L.] Merr) Measured Using PAM (Pulse Amplitude Modulation) Fluorometry." *Tropical Plant Biology*, 3(4), 193–203.

Ritchie, R. J., and Bunthawin, S. (2010b). "The Use of Pulse Amplitude Modulation (PAM) Fluorometry to Measure Photosynthesis in a CAM Orchid, Dendrobium spp. (*D.* cv. Viravuth Pink)." *International Journal of Plant Sciences*, 171(6), 575–585.

Ritchie, R. J., and Larkum, A. W. D. (2012). "Modelling photosynthesis in shallow algal production ponds." *Photosynthetica*, 50(4), 481–500.

Ritchie, R. J., and Mekjinda, N. (2016). "Arsenic toxicity in the water weed *Wolffia arrhiza* measured using Pulse Amplitude Modulation Fluorometry (PAM) measurements of photosynthesis." *Ecotoxicology and Environmental Safety*, 132, 178–185.

Ritchie, R. J., and Raghupathi, S. S. (2008). "Al–toxicity studies in yeast using gallium as an aluminum analogue." *BioMetals*, 21(4), 379–393.

Ritchie, R. J., and Runcie, J. W. (2014). "A portable reflectance-absorptance-transmittance meter for photosynthetic work on vascular plant leaves." *Photosynthetica*, 52(4), 614–626.

Rousos, P. A., Harrison, H. C., and Steffen, K. L. (1989). “Physiological responses of cabbage to incipient copper toxicity.” *Agris.Fao.Org*, 114, 149–152.

Ryan, P. R., Delhaize, E., and Randall, P. J. (1995a). “Characterisation of Al–stimulated efflux of malate from the apices of Al–tolerant wheat roots.” *Planta: An International Journal of Plant Biology,* 196(1), 103–110.

Ryan, P. R., Delhaize, E., and Ramdall, P. J. (1995b). “Malate efflux from root apices and tolerance to aluminium are highly correlated in wheat.” *Australian Journal of Plant Physiology,* 22(4), 531–536.

Ryan, P. R., Kinraide, T., and Kochian, L. (1993). "Al^{3+}–Ca^{2+} interactions in aluminum rhizotoxicity." *Planta*, 192(1), 98–103.

Ryan, P. R., Reid, R. J., and Smith, F. A. (1997). "Direct Evaluation of the Ca^{2+}–Displacement Hypothesis for Al Toxicity." *Plant Physiology*, 113(4), 1351–1357.

Scheffler, J. (2007). "Underwater Habitats." (Online) Available on https://illumin.usc.edu/underwaterhabitats/ (27 February 2019).

Scholz, M. (2006). *Wetlands for Water Pollution Control*, Elsevier, Netherlands.

Sinclair, D. A., and Guarente, L. (1997). "Extrachromosomal rDNA circles – A cause of aging in yeast." *Cell*, 91(7), 1033–1042.

Snedecor, G. W., and Cochran, W. G. (1989). *Statistical methods*. Iowa State University Press, Ames.

Taylor, H. (1990). “Cement chemistry”. *Cement and Concrete Composites,* 20(4), 335–335.

The Angiosperm Phylogeny Group. (2003). “An update of the Angiosperm Phylogeny Group classification for the orders and families of flowering plants: APG II." *Botanical Journal of the Linnean Society*, 141(4), 399–436.

The Editors of Encyclopaedia Britannica. (2017). "Manganese CHEMICAL ELEMENT." (Online) Available on https://www.britannica.com/science/manganese (19 December 2018).

Umena, Y., Kawakami, K., Shen, J. R., and Kamiya, N. (2011). "Crystal structure of oxygen–evolving photosystem II at a resolution of 1.9Å." *Nature*, 473, 55–60.

Welch, R. M. (1995). “Micronutrient Nutrition of Plants.” *Critical Reviews in Plant Sciences*, 14(1), 49–82.

White, M. C., Baker, F. D., Chaney, R. L., and Decker, A. M. (1981). “Metal Complexation in Xylem Fluid: II. THEORETICAL EQUILIBRIUM MODEL AND COMPUTATIONAL COMPUTER PROGRAM.” *Plant Physiology*, 67(2), 301–310.

Wu, S. H. (1994). "Effect of manganese excess on the soybean plant cultivated under various growth conditions." *Journal of Plant Nutrition*, 17(6), 991–1003.

Yongmanitchai, W., and Ward, O. P. (1991). "Growth of and omega–3 fatty acid production by *Phaeodactylum tricornutum* under different culture conditions." *Applied and Environmental Microbiology*, 57(2), 419–425.

Zelitch, I. (1971). *Photosynthesis, photorespiration, and plant productivity*. Academic Press, United States.

Zhang, B., Zhang, C., Liu, C., Jing, Y., Wang, Y., Jin, L., Yang, L., Fu, A., Shi, J., Zhao, F., Lan, W., and Luan, S. (2018). "Inner Envelope CHLOROPLAST MANGANESE TRANSPORTER Supports Manganese Homeostasis and Phototrophic Growth in Arabidopsis." *Molecular Plant*, 11(7), 943–954.

Zonneveld, B. J. M. (1986). "Cheap and simple yeast media." *Journal of Microbiological Methods*, 4(5–6), 287–291.

Appendices I

Results and calculate data

Unless stated otherwise all error bars are ±95% confidence limits

Table I1 Optical density 630 nm data with Microplate reader for yeast in manganese conditions (n = 6)

Time (hour)	Optical density (OD)						
	Control	**10 mmol m^{-3} Mn**	**30 mmol m^{-3} Mn**	**100 mmol m^{-3} Mn**	**300 mmol m^{-3} Mn**	**1 mol m^{-3} Mn**	**3 mol m^{-3} Mn**
0	0.074 ± 0.001	0.074 ± 0.001	0.078 ± 0.005	0.069 ± 0.001	0.088 ± 0.003	0.141 ± 0.010	0.339 ± 0.009
2	0.078 ± 0.002	0.079 ± 0.002	0.084 ± 0.005	0.074 ± 0.001	0.095 ± 0.004	0.144 ± 0.008	0.354 ± 0.015
4	0.097 ± 0.002	0.101 ± 0.002	0.101 ± 0.006	0.091 ± 0.001	0.114 ± 0.006	0.157 ± 0.007	0.363 ± 0.008
6	0.140 ± 0.004	0.150 ± 0.002	0.143 ± 0.009	0.135 ± 0.003	0.150 ± 0.008	0.185 ± 0.007	0.376 ± 0.012
8	0.227 ± 0.005	0.252 ± 0.006	0.235 ± 0.020	0.224 ± 0.009	0.228 ± 0.015	0.241 ± 0.013	0.410 ± 0.024
10	0.321 ± 0.006	0.356 ± 0.009	0.340 ± 0.024	0.318 ± 0.014	0.322 ± 0.026	0.300 ± 0.013	0.495 ± 0.019
12	0.425 ± 0.009	0.465 ± 0.013	0.448 ± 0.028	0.420 ± 0.018	0.425 ± 0.034	0.375 ± 0.016	0.566 ± 0.038
14	0.506 ± 0.011	0.549 ± 0.014	0.539 ± 0.034	0.500 ± 0.022	0.514 ± 0.041	0.445 ± 0.020	0.547 ± 0.028
16	0.568 ± 0.015	0.610 ± 0.017	0.608 ± 0.041	0.563 ± 0.028	0.583 ± 0.048	0.507 ± 0.026	0.490 ± 0.070
18	0.614 ± 0.015	0.652 ± 0.016	0.661 ± 0.49	0.609 ± 0.037	0.634 ± 0.058	0.555 ± 0.032	0.478 ± 0.088
20	0.639 ± 0.015	0.633 ± 0.016	0.695 ± 0.054	0.635 ± 0.035	0.662 ± 0.063	0.590 ± 0.039	0.455 ± 0.084
22	0.639 ± 0.014	0.657 ± 0.012	0.704 ± 0.066	0.637 ± 0.032	0.671 ± 0.076	0.606 ± 0.039	0.439 ± 0.077
24	0.642 ± 0.017	0.656 ± 0.013	0.706 ± 0.062	0.636 ± 0.032	0.674 ± 0.084	0.617 ± 0.036	0.425 ± 0.077

Table I2 Data of Exponential growth rate of yeast for manganese (n = 6)

Yeast experiment	Parameter				
	k constant (k h^{-1})	t_2 (hour)	V_0	Pearson r	P–value
Control	0.0672 ± 0.0080	10.3205 ± 1.2327	0.1542 ± 0.0238	0.9244	1.6685×10^{-102}
10 mmol m^{-3} Mn	0.0646 ± 0.0085	10.7308 ± 1.4175	0.1700 ± 0.0277	0.9094	4.2611×10^{-99}
30 mmol m^{-3} Mn	0.0693 ± 0.0084	10.0021 ± 1.2102	0.1604 ± 0.0260	0.9231	3.5250×10^{-102}
100 mmol m^{-3} Mn	0.0679 ± 0.0084	10.2114 ± 1.2563	0.1508 ± 0.0242	0.9209	1.1969×10^{-101}
300 mmol m^{-3} Mn	0.0676 ± 0.0082	10.2598 ± 1.2386	0.1588 ± 0.0249	0.9214	9.2019×10^{-102}
1000 mmol m^{-3} Mn	0.0603 ± 0.0050	11.5025 ± 0.9507	0.1659 ± 0.0156	0.9561	2.6145×10^{-112}
3000 mmol m^{-3} Mn	0.0104 ± 0.0053	66.8197 ± 34.1449	0.3887 ± 0.0311	0.4260	2.5849×10^{-49}

Table I3 Optical density 630 nm data with Microplate reader for yeast in manganese + EDTA conditions (n = 6)

Time (hour)	Optical density (OD)						
	Control	**10 mmol m^{-3} Mn**	**30 mmol m^{-3} Mn**	**100 mmol m^{-3} Mn**	**300 mmol m^{-3} Mn**	**1 mol m^{-3} Mn**	**3 mol m^{-3} Mn**
0	0.068 ± 0.003	0.074 ± 0.012	0.069 ± 0.002	0.074 ± 0.001	0.083 ± 0.003	0.109 ± 0.002	0.277 ± 0.010
2	0.086 ± 0.006	0.079 ± 0.011	0.076 ± 0.002	0.082 ± 0.004	0.092 ± 0.004	0.136 ± 0.016	0.379 ± 0.018
4	0.161 ± 0.019	0.114 ± 0.025	0.106 ± 0.003	0.112 ± 0.008	0.102 ± 0.046	0.163 ± 0.014	0.391 ± 0.018
6	0.320 ± 0.017	0.208 ± 0.066	0.180 ± 0.011	0.189 ± 0.016	0.181 ± 0.005	0.210 ± 0.016	0.411 ± 0.015
8	0.495 ± 0.012	0.385 ± 0.091	0.353 ± 0.034	0.353 ± 0.023	0.293 ± 0.009	0.277 ± 0.024	0.460 ± 0.028
10	0.660 ± 0.009	0.576 ± 0.106	0.514 ± 0.039	0.525 ± 0.032	0.429 ± 0.012	0.361 ± 0.024	0.492 ± 0.030
12	0.776 ± 0.008	0.745 ± 0.106	0.656 ± 0.038	0.691 ± 0.035	0.564 ± 0.016	0.443 ± 0.015	0.496 ± 0.040
14	0.900 ± 0.014	0.893 ± 0.103	0.798 ± 0.054	0.799 ± 0.068	0.668 ± 0.022	0.518 ± 0.017	0.533 ± 0.055
16	0.910 ± 0.016	0.922 ± 0.096	0.908 ± 0.052	0.885 ± 0.018	0.743 ± 0.028	0.571 ± 0.018	0.506 ± 0.061
18	0.937 ± 0.020	0.937 ± 0.093	0.913 ± 0.156	0.878 ± 0.033	0.751 ± 0.040	0.608 ± 0.020	0.503 ± 0.068
20	0.918 ± 0.038	0.942 ± 0.090	0.895 ± 0.180	0.879 ± 0.034	0.755 ± 0.047	0.633 ± 0.020	0.490 ± 0.059
22	0.936 ± 0.066	0.948 ± 0.087	0.886 ± 0.201	0.879 ± 0.033	0.751 ± 0.054	0.645 ± 0.022	0.486 ± 0.050
24	0.917 ± 0.113	0.947 ± 0.087	0.828 ± 0.209	0.880 ± 0.033	0.761 ± 0.066	0.649 ± 0.023	0.468 ± 0.052

Table I4 Data of Exponential growth rate of yeast for manganese + EDTA (n = 6)

Yeast experiment	Parameter				
	k constant (k h^{-1})	t_2 (hour)	V_0	Pearson r	P–value
Control	0.0558 ± 0.0095	12.4143 ± 2.1146	0.2978 ± 0.0526	0.8587	3.2328x10-90
10 mmol m^{-3} Mn + EDTA	0.0631 ± 0.0107	10.9847 ± 1.8681	0.2569 ± 0.0524	0.8633	5.0710x10-91
30 mmol m^{-3} Mn + EDTA	0.0628 ± 0.0120	11.0306 ± 2.1105	0.2393 ± 0.0546	0.8364	2.8362x10-87
100 mmol m^{-3} Mn + EDTA	0.0630 ± 0.0100	10.9994 ± 1.7520	0.2398 ± 0.0457	0.8774	3.2138x10-93
300 mmol m^{-3} Mn + EDTA	0.0626 ± 0.0091	11.0648 ± 1.6101	0.2061 ± 0.0356	0.8923	8.7816x10-96
1000 mmol m^{-3} Mn + EDTA	0.0582 ± 0.0059	11.9093 ± 1.2162	0.1879 ± 0.0209	0.9374	6.1260x10-106
3000 mmol m^{-3} Mn + EDTA	0.0141 ± 0.0041	49.0524 ± 14.1760	0.3804 ± 0.0240	0.6392	1.936x10-67

Table I5 Data & statistics on Yield with PAM of *C. vulgaris* with manganese (n = 6)

***C. vulgaris* experiment**	**Parameter**				
	Y_{max}	**Y_k**	**$Y_{0.5}$**	**Pearson r**	**P–value**
Control	0.4852 ± 0.0128	0.0109 ± 0.0005	63.5448 ± 3.1036	0.9955	2.3019×10^{-99}
1 mol m^{-3} Mn	0.5132 ± 0.0143	0.0113 ± 0.0006	61.3107 ± 3.2801	0.9946	2.2813×10^{-97}
2 mol m^{-3} Mn	0.5051 ± 0.0128	0.0107 ± 0.0005	64.7397 ± 3.1823	0.9954	4.9073×10^{-99}
3 mol m^{-3} Mn	0.4965 ± 0.0105	0.0100 ± 0.0004	69.5516 ± 2.8958	0.9968	2.1809×10^{-103}
5 mol m^{-3} Mn	0.4917 ± 0.0115	0.0097 ± 0.0004	71.6864 ± 3.3265	0.9960	8.0869×10^{-101}
7 mol m^{-3} Mn	0.4935 ± 0.0108	0.0095 ± 0.0004	73.1420 ± 3.1688	0.9966	1.2467×10^{-102}
10 mol m^{-3} Mn	0.5046 ± 0.0116	0.0096 ± 0.0004	71.9435 ± 1.6342	0.9961	3.8080×10^{-101}

Table I6 Data & statistics on ETR with PAM of *C. vulgaris* with manganese (n = 6)

***C. vulgaris* experiment**	**Parameter**			
	E_{opt}	**P_{max}**	**Pearson r**	**P–value**
Control	136.7448 ± 6.7740	93.4898 ± 1.5693	0.9772	1.1083×10^{-36}
1 mol m^{-3} Mn	145.1252 ± 7.8550	98.0627 ± 3.3616	0.9703	9.9640×10^{-34}
2 mol m^{-3} Mn	137.9001 ± 7.7456	96.0630 ± 3.6722	0.9700	1.2837×10^{-33}
3 mol m^{-3} Mn	142.6826 ± 6.8540	104.8134 ± 3.4389	0.9769	1.5507×10^{-36}
5 mol m^{-3} Mn	150.3714 ± 8.1219	102.5483 ± 3.8035	0.9693	2.3563×10^{-33}
7 mol m^{-3} Mn	151.7604 ± 8.4473	110.6171 ± 4.2319	0.9671	1.4059×10^{-32}
10 mol m^{-3} Mn	147.9831 ± 7.5110	107.8323 ± 3.7522	0.9733	6.4133×10^{-35}

Table I7 Data & statistics on NPQ with PAM of *C. vulgaris* with manganese (n = 6)

***C. vulgaris* experiment**	**Parameter**		
	NPQ_{max}	**Pearson r**	**P–value**
Control	0.3850 ± 0.0072	0.9925	9.8084×10^{-82}
1 mol m^{-3} Mn	0.3713 ± 0.0128	0.9768	3.0447×10^{-70}
2 mol m^{-3} Mn	0.3330 ± 0.0096	0.9832	1.5282×10^{-73}
3 mol m^{-3} Mn	0.3337 ± 0.0103	0.9797	1.3562×10^{-71}
5 mol m^{-3} Mn	0.3268 ± 0.0130	0.9724	1.9700×10^{-68}
7 mol m^{-3} Mn	0.3191 ± 0.0159	0.9555	2.0765×10^{-63}
10 mol m^{-3} Mn	0.3342 ± 0.0114	0.9782	6.8805×10^{-71}

Table I8 Data & statistics on absorptance & chlorophyll *a* of *C. vulgaris* with manganese (n = 4)

***C. vulgaris* experiment**	**Parameter**	
	Absorptance (%)	**Chl *a* (mg m^{-2})**
Control	61.3500 ± 1.5759	57.2760 ± 0.4186
1 mol m^{-3} Mn	62.0167 ± 2.3025	56.8292 ± 1.1092
2 mol m^{-3} Mn	58.7500 ± 4.0229	56.9883 ± 0.9781
3 mol m^{-3} Mn	61.4500 ± 1.5520	56.2878 ± 0.8650
5 mol m^{-3} Mn	57.6667 ± 4.2647	55.5418 ± 1.0866
7 mol m^{-3} Mn	60.2833 ± 3.4618	54.9739 ± 4.7005
10 mol m^{-3} Mn	58.3500 ± 1.9382	54.909 ± 0.1113

Table I9 Data & statistics on Yield with PAM of *C. vulgaris* with manganese and EDTA (n = 6)

***C. vulgaris* experiment**	**Parameter**				
	Y_{max}	**Y_k**	**$Y_{0.5}$**	**Pearson r**	**P–value**
Control	0.4116 ± 0.0147	0.0076 ± 0.0006	90.7646 ± 6.7779	0.9907	3.6341×10^{-91}
1 mol m^{-3} Mn + EDTA	0.4184 ± 0.0131	0.0075 ± 0.0005	92.8097 ± 6.1276	0.9924	2.0029×10^{-93}
2 mol m^{-3} Mn + EDTA	0.4263 ± 0.0135	0.0079 ± 0.0005	87.9770 ± 5.7875	0.9925	1.1299×10^{-93}
3 mol m^{-3} Mn + EDTA	0.4117 ± 0.0166	0.0066 ± 0.0006	105.0570 ± 9.2685	0.9870	2.5702×10^{-87}
5 mol m^{-3} Mn + EDTA	0.4221 ± 0.0150	0.0075 ± 0.0006	92.2289 ± 6.9131	0.9905	6.9235×10^{-91}
7 mol m^{-3} Mn + EDTA	0.4088 ± 0.0058	0.0083 ± 0.0005	83.6412 ± 4.5243	0.9939	5.6663×10^{-96}
10 mol m^{-3} Mn + EDTA	0.4189 ± 0.0170	0.0068 ± 0.0006	102.0209 ± 8.9471	0.9872	1.6175×10^{-87}

Table I10 Data & statistics on ETR with PAM of *C. vulgaris* with manganese and EDTA (n = 6)

***C. vulgaris* experiment**	**Parameter**			
	E_{opt}	**P_{max}**	**Pearson r**	**P–value**
Control	242.4445 ± 11.0153	57.117 ± 1.8087	0.9706	8.0553×10^{-34}
1 mol m^{-3} Mn + EDTA	220.2467 ± 11.0066	57.4432 ± 2.0125	0.9645	9.8772×10^{-32}
2 mol m^{-3} Mn + EDTA	291.4601 ± 11.2093	71.3020 ± 1.8562	0.9636	1.7971×10^{-31}
3 mol m^{-3} Mn + EDTA	241.4987 ± 10.9193	61.3561 ± 1.9343	0.9819	3.0604×10^{-39}
5 mol m^{-3} Mn + EDTA	192.8856 ± 10.2686	49.4940 ± 1.8446	0.9708	6.7098×10^{-34}
7 mol m^{-3} Mn + EDTA	293.7325 ± 13.7087	69.4317 ± 2.1786	0.9631	2.6341×10^{-31}
10 mol m^{-3} Mn + EDTA	242.4445 ± 11.0153	57.1170 ± 1.8087	0.9716	3.2922×10^{-34}

Table I11 Data & statistics on NPQ with PAM of *C. vulgaris* with manganese + EDTA (n = 6)

***C. vulgaris* experiment**	**Parameter**		
	NPQ_{max}	**Pearson r**	**P–value**
Control	0.4116 ± 0.0147	0.9907	3.6341×10^{-91}
1 mol m^{-3} Mn	0.3139 ± 0.0154	0.9627	5.6212×10^{-75}
2 mol m^{-3} Mn	0.3165 ± 0.0135	0.9646	1.3129×10^{-75}
3 mol m^{-3} Mn	0.2727 ± 0.0108	0.9702	2.0340×10^{-78}
5 mol m^{-3} Mn	0.3115 ± 0.0117	0.9755	6.0989×10^{-80}
7 mol m^{-3} Mn	0.3595 ± 0.0156	0.9581	1.3742×10^{-73}
10 mol m^{-3} Mn	0.3064 ± 0.0166	0.9551	9.2618×10^{-73}

Table I12 Data & statistics on absorptance & chlorophyll *a* of *C. vulgaris* with manganese and EDTA (n = 4)

***C. vulgaris* experiment**	**Parameter**	
	Absorptance (%)	**Chl *a* (mg m^{-2})**
Control	73.2000 ± 1.1400	150.0148 ± 9.5614
1 mol m^{-3} Mn + EDTA	73.4167 ± 2.9440	147.5982 ± 5.4888
2 mol m^{-3} Mn + EDTA	72.1333 ± 4.3344	144.8495 ± 8.4877
3 mol m^{-3} Mn + EDTA	72.9833 ± 2.1776	143.6541 ± 4.9664
5 mol m^{-3} Mn + EDTA	74.9167 ± 3.0091	147.7821 ± 3.1778
7 mol m^{-3} Mn + EDTA	75.5600 ± 2.6870	152.0825 ± 1.7468
10 mol m^{-3} Mn + EDTA	75.3167 ± 2.0814	151.6695 ± 4.5014

Table I13 Data of *L. minor* leaf number for manganese (n = 3)

***L. minor* experiment**	**Day**						
	Initial	**1st**	**2nd**	**3rd**	**4th**	**5th**	**6th**
Control	4.000 ± 0.000	6.667 ± 1.434	8.000 ± 0.000	9.333 ± 1.434	14.000 ± 0.000	17.333 ± 3.795	18.000 ± 2.484
10 mmol m^{-3} Mn	4.000 ± 0.000	6.667 ± 1.434	7.667 ± 1.434	8.333 ± 1.434	12.667 ± 3.795	16.333 ± 7.589	18.000 ± 2.484
30 mmol m^{-3} Mn	4.000 ± 0.000	6.667 ± 1.434	7.667 ± 1.434	8.333 ± 1.434	11.333 ± 3.795	14.333 ± 5.737	15.333 ± 6.252
100 mmol m^{-3} Mn	4.000 ± 0.000	6.000 ± 4.303	7.333 ± 2.868	8.000 ± 0.000	10 ± 2.484	12.333 ± 1.434	13.333 ± 1.434
300 mmol m^{-3} Mn	4.000 ± 0.000	6.333 ± 1.434	6.667 ± 2.868	9.000 ± 4.303	12.000 ± 2.484	13.667 ± 2.868	15.333 ± 3.795
1000 mmol m^{-3} Mn	4.000 ± 0.000	4.667 ± 2.868	6.667 ± 2.868	8.000 ± 0.000	8.000 ± 0.000	8.333 ± 1.434	8.333 ± 1.434

Table I14 Data of Exponential growth rate of *L. minor* for manganese (n = 3)

***L. minor* experiment**	**Parameter**				
	k constant (k h^{-1})	**t_2 (day)**	**V_0 (n)**	**Pearson r**	**P–value**
Control	0.2192 ± 0.0320	3.1627 ± 0.4617	5.2382 ± 0.8052	0.9670	1.2373×10^{-24}
10 mmol m^{-3} Mn	0.2263 ± 0.0342	3.0623 ± 0.4623	4.9787 ± 0.8220	0.9644	2.5955×10^{-24}
30 mmol m^{-3} Mn	0.1948 ± 0.0385	3.5581 ± 0.7041	5.0130 ± 0.9088	0.9375	7.9837×10^{-22}
100 mmol m^{-3} Mn	0.1756 ± 0.0273	3.9473 ± 0.6143	4.8518 ± 0.6121	0.9589	1.1077×10^{-23}
300 mmol m^{-3} Mn	0.1984 ± 0.0328	3.4938 ± 0.5775	4.9020 ± 0.7584	0.9560	2.1845×10^{-23}
1000 mmol m^{-3} Mn	0.1040 ± 0.0353	6.6637 ± 2.2637	4.9218 ± 0.7393	0.8358	3.5706×10^{-17}

Table I15 Data of *L. minor* leaf surface, Chl *a* and absorptance for manganese (n = 6)

***L. minor* experiment**	**Parameter**			**Chl *a* per Leaf SA**		
	Leaf surface (10^{-6} m^2)	**Chl *a* (µg)**	**Absorptance (%)**	**Slop (m)**	**Pearson r**	**P–value**
Control	0.1610 ± 0.0230	7.0225 ± 1.4313	58.1333 ± 6.6139	10.9288 ± 0.8367	0.9826	$6.5420x10^{-8}$
10 mmol m^{-3} Mn	0.1746 ± 0.0226	7.0341 ± 1.4235	56.9333 ± 5.5585	10.0513 ± 1.5874	0.9245	$6.6104x10^{-6}$
30 mmol m^{-3} Mn	0.1703 ± 0.0248	5.6326 ± 0.8576	59.8000 ± 8.5810	8.2454 ± 0.9382	0.9585	$9.6521x10^{-7}$
100 mmol m^{-3} Mn	0.1752 ± 0.0181	4.3811 ± 0.9287	63.1833 ± 5.6597	6.4723 ± 1.2807	0.8835	$2.8459x10^{-5}$
300 mmol m^{-3} Mn	0.1754 ± 0.0263	4.4874 ± 0.9963	51.9667 ± 12.4186	6.4081 ± 0.9856	0.9306	$5.0208x10^{-6}$
1000 mmol m^{-3} Mn	0.1727 ± 0.0214	2.4881 ± 0.5487	64.2167 ± 8.2262	3.6160 ± 0.4712	0.9504	$1.6949x10^{-6}$

Table I16 Data of Relative growth rate of *L. minor* for manganese (n = 3)

***L. minor* experiment**	**RGR (n n^{-1} d^{-1})**
Control	0.2505 ± 0.0230
10 mmol m^{-3} Mn	0.2505 ± 0.0230
30 mmol m^{-3} Mn	0.2225 ± 0.0675
100 mmol m^{-3} Mn	0.2006 ± 0.0177
300 mmol m^{-3} Mn	0.2234 ± 0.0407
1000 mmol m^{-3} Mn	0.1221 ± 0.0282

Table I17 Data of *L. minor* leaf number for manganese + EDTA (n = 3)

***L. minor* experiment**	**Day**	**Leaf number (n)**						
		Initial	**1st**	**2nd**	**3rd**	**4th**	**5th**	**6th**
Control		4.000 ± 0.000	4.667 ± 1.434	6.000 ± 2.484	7.000 ± 4.303	9.333 ± 2.868	9.667 ± 3.795	11.000 ± 4.303
10 mmol m^{-3} Mn + EDTA		4.000 ± 0.000	4.333 ± 1.434	5.333 ± 1.434	7.000 ± 2.484	8.000 ± 2.484	8.333 ± 3.795	9.667 ± 6.525
30 mmol m^{-3} Mn+ EDTA		4.000 ± 0.000	4.667 ± 1.434	6.000 ± 2.484	7.667 ± 1.434	8.667 ± 2.868	9.333 ± 2.868	12.000 ± 2.484
100 mmol m^{-3} Mn+ EDTA		4.000 ± 2.484	4.667 ± 2.868	5.000 ± 4.303	7.667 ± 2.868	8.667 ± 5.171	9.667 ± 6.252	11.000 ± 2.484
300 mmol m^{-3} Mn+ EDTA		3.667 ± 1.434	4.333 ± 2.868	5.667 ± 3.795	6.667 ±3.795	6.667 ±3.795	8.333 ±6.252	9.667 ± 7.589
1000 mmol m^{-3} Mn+ EDTA		3.667 ± 1.434	4.000 ± 0.000	4.000 ± 0.000	4.000 ± 0.000	4.000 ± 0.000	4.000 ± 0.000	4.000 ± 0.000

Table I18 Data of Exponential growth rate of *L. minor* for manganese + EDTA (n = 3)

***L. minor* experiment**	**Parameter**				
	k constant (k h^{-1})	**t_2 (day)**	**V_0 (n.)**	**Pearson r**	**P–value**
Control	0.1632 ± 0.0395	4.2476 ± 1.0287	4.3004 ± 0.7748	0.9070	5.3975×10^{-20}
10 mmol m^{-3} Mn + EDTA	0.1459 ± 0.0424	4.7509 ± 1.3823	4.1313 ± 0.7846	0.8701	2.2452×10^{-18}
30 mmol m^{-3} Mn + EDTA	0.1731 ± 0.0282	4.0033 ± 0.6525	4.1955 ± 0.5453	0.9541	3.3711×10^{-23}
100 mmol m^{-3} Mn + EDTA	0.1696 ± 0.0508	4.0866 ± 1.2232	4.1183 ± 0.9595	0.8675	2.8374×10^{-18}
300 mmol m^{-3} Mn + EDTA	0.1505 ± 0.0620	4.6042 ± 1.8952	3.9150 ± 1.0910	0.7783	4.6014×10^{-15}
1000 mmol m^{-3} Mn + EDTA	0.0089 ± 0.0122	77.8697 ± 106.7361	3.8476 ± 0.1720	0.3329	2.0627×10^{-6}

Table I19 Data of *L. minor* leaf surface, Chl *a* and absorptance for manganese + EDTA (n = 6)

***L. minor* experiment**	**Parameter**			**Chl *a* per Leaf SA**		
	Leaf surface (10^{-6} m^2)	**Chl *a* (µg)**	**Absorptance (%)**	**Slop (m)**	**Pearson r**	**P–value**
Mn + EDTA Control	0.1145 ± 0.0155	3.4297 ± 1.7868	52.0500 ± 6.7011	7.8223 ± 1.7217	0.9303	$5.0722x10^{-6}$
10 mmol m^{-3} Mn + EDTA	0.1099 ± 0.0178	5.1943 ± 2.1943	51.0000 ± 5.1802	12.0373 ± 0.9151	0.9904	$1.0483x10^{-8}$
30 mmol m^{-3} Mn + EDTA	0.1501 ± 0.0177	6.1203 ± 2.1325	54.4167 ± 4.3813	10.0334 ± 1.3279	0.9403	$3.5642x10^{-6}$
100 mmol m^{-3} Mn + EDTA	0.1559 ± 0.0326	4.1554 ± 2.7345	53.0833 ± 5.4670	6.1929 ± 1.5089	0.9728	$4.5268x10^{-6}$
300 mmol m^{-3} Mn + EDTA	0.1211 ± 0.0250	3.0278 ± 1.9670	55.0667 ± 8.1485	5.6863 ± 1.6288	0.9749	$3.7029x10^{-6}$
1000 mmol m^{-3} Mn + EDTA	0.1058 ± 0.0358	0	10.0000 ± 3.4595	0	-	-

Table I20 Data of Relative growth rate of *L. minor* for manganese + EDTA (n = 3)

***L. minor* experiment**	**RGR (n n^{-1} d^{-1})**
Control	0.1671 ± 0.0688
10 mmol m^{-3} Mn + EDTA	0.1430 ± 0.1135
30 mmol m^{-3} Mn + EDTA	0.1827 ± 0.0346
100 mmol m^{-3} Mn + EDTA	0.1717 ± 0.1125
300 mmol m^{-3} Mn + EDTA	0.1576 ± 0.1461
1000 mmol m^{-3} Mn + EDTA	0.0160 ± 0.0688

Table I21 Data & statistics on Yield with PAM of *L. minor* with manganese (n = 6)

***L. minor* experiment**	**Parameter**				
	Y_{max}	**Y_k**	**$Y_{0.5}$**	**Pearson r**	**P–value**
Control	0.5992 ± 0.0334	0.0065 ± 0.0008	106.9072 ± 13.0502	0.9719	$2.3579x10^{-78}$
10 mol m^{-3} Mn + EDTA	0.5889 ± 0.0412	0.0053 ± 0.0009	130.4767 ± 21.1193	0.9483	$4.7762x10^{-71}$
30 mol m^{-3} Mn + EDTA	0.5957 ± 0.0542	0.0063 ± 0.0013	110.6139 ± 22.2429	0.9218	$6.6338x10^{-66}$
100 mol m^{-3} Mn + EDTA	0.5482 ± 0.0528	0.0058 ± 0.0013	120.1333 ± 26.1786	0.9078	$8.6235x10^{-64}$
300 mol m^{-3} Mn + EDTA	0.5751 ± 0.0406	0.0044 ± 0.0007	159.2933 ± 27.4193	0.9384	$6.9865x10^{-69}$
1000 mol m^{-3} Mn + EDTA	0.5688 ± 0.0430	0.0052 ± 0.0009	133.7998 ± 23.5539	0.9388	$5.7218x10^{-69}$

Table I22 Data & statistics on ETR with PAM of *L. minor* with manganese (n = 6)

***L. minor* experiment**	**Parameter**			
	E_{opt}	**P_{max}**	**Pearson r**	**P–value**
Control	287.0218 ± 21.3014	211.7581 ± 10.6329	0.9224	$3.9138x10^{-23}$
10 mol m^{-3} Mn + EDTA	362.2838 ± 44.5849	272.8675 ± 20.7820	0.8492	$4.9010x10^{-16}$
30 mol m^{-3} Mn + EDTA	336.8379 ± 63.2852	289.8806 ± 34.8672	0.7015	$3.4482x10^{-9}$
100 mol m^{-3} Mn + EDTA	447.5299 ± 43.3228	324.2312 ± 17.2161	0.9318	$1.5356x10^{-24}$
300 mol m^{-3} Mn + EDTA	409.9634 ± 22.5387	332.4331 ± 10.5698	0.9722	$1.9250x10^{-34}$
1000 mol m^{-3} Mn + EDTA	421.3524 ± 48.1575	280.6232 ± 18.2495	0.8932	$1.0965x10^{-19}$

Table I23 Data & statistics on absorptance & chlorophyll *a* of *L. minor* with manganese (n = 6)

***L. minor* experiment**	**Parameter**	
	Absorptance (%)	**Chl *a* (mg m^{-2})**
Control	79.9833 ± 8.0385	98.7765 ± 8.3064
10 mol m^{-3} Mn + EDTA	82.9500 ± 10.0103	96.8099 ± 15.2686
30 mol m^{-3} Mn + EDTA	75.5167 ± 10.3769	72.8247 ± 6.8853
100 mol m^{-3} Mn + EDTA	90.5500 ± 3.8386	76.8152 ± 8.2800
300 mol m^{-3} Mn + EDTA	84.3167 ± 6.0254	79.3700 ± 15.7968
1000 mol m^{-3} Mn + EDTA	79.9833 ± 8.0385	85.0208 ± 11.3264

Table I24 Data & statistics on Yield with PAM of *L. minor* with manganese and EDTA (n = 6)

***L. minor* experiment**	**Parameter**				
	Y_{max}	**Y_k**	**$Y_{0.5}$**	**Pearson r**	**P–value**
Control	0.5992 ± 0.0334	0.0065 ± 0.0008	106.9072 ± 13.0502	0.9719	2.3579×10^{-78}
10 mol m^{-3} Mn + EDTA	0.5643 ± 0.0419	0.0037 ± 0.0007	187.3345 ± 35.3652	0.9214	7.7987×10^{-66}
30 mol m^{-3} Mn + EDTA	0.5865 ± 0.0375	0.0040 ± 0.0006	172.6984 ± 27.5107	0.9456	2.0579×10^{-70}
100 mol m^{-3} Mn + EDTA	0.5404 ± 0.0358	0.0032 ± 0.0006	215.7822 ± 37.7096	0.9278	6.6611×10^{-67}
300 mol m^{-3} Mn + EDTA	0.5362 ± 0.0437	0.0046 ± 0.0009	151.7441 ± 29.7904	0.9215	7.3961×10^{-66}
1000 mol m^{-3} Mn + EDTA	0.6795 ± 0.0478	0.0134 ± 0.0018	51.5948 ± 6.7764	0.9660	4.5403×10^{-76}

Table I25 Data & statistics on ETR with PAM of *L. minor* with manganese and EDTA (n = 6)

***L. minor* experiment**	**Parameter**			
	E_{opt}	**P_{max}**	**Pearson r**	**P–value**
Control	287.0218 ± 21.3014	211.7581 ± 10.6329	0.9224	3.9138×10^{-23}
10 mol m^{-3} Mn + EDTA	483.7879 ± 57.4078	372.1672 ± 23.0995	0.9146	4.2241×10^{-22}
30 mol m^{-3} Mn + EDTA	417.4858 ± 33.2737	332.1665 ± 15.1467	0.9457	4.8310×10^{-27}
100 mol m^{-3} Mn + EDTA	516.2103 ± 69.5240	380.6713 ± 25.8236	0.9068	3.7253×10^{-21}
300 mol m^{-3} Mn + EDTA	395.0343 ± 72.8980	233.5809 ± 25.4687	0.7730	7.4540×10^{-12}
1000 mol m^{-3} Mn + EDTA	239.1946 ± 23.6931	135.2488 ± 9.3489	0.8695	1.4682×10^{-17}

Table I26 Data & statistics on absorptance & chlorophyll *a* of *L. minor* with manganese and EDTA (n = 6)

***L. minor* experiment**	**Parameter**	
	Absorptance (%)	**Chl *a* (mg m^{-2})**
Control	79.9833 ± 8.0385	98.7765 ± 8.3064
10 mol m^{-3} Mn + EDTA	81.1833 ± 14.9834	79.2463 ± 18.2971
30 mol m^{-3} Mn + EDTA	81.2167 ± 10.9432	82.3620 ± 16.6744
100 mol m^{-3} Mn + EDTA	79.2167 ± 7.5298	80.5978 ± 17.3032
300 mol m^{-3} Mn + EDTA	74.6500 ± 15.5560	89.8796 ± 29.4364
1000 mol m^{-3} Mn + EDTA	84.7167 ± 7.1434	84.0016 ± 14.8504

Appendices II

Photo of yeast and plants

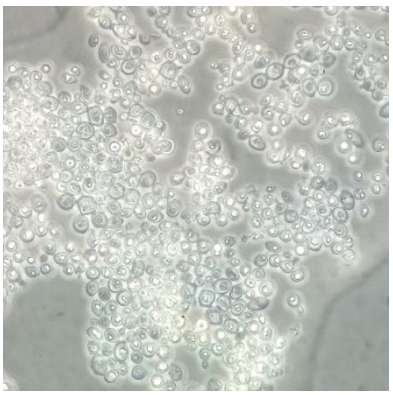

Figure II1 Yeast (*Saccharomyces cerevisiae*) (06/03/2019)

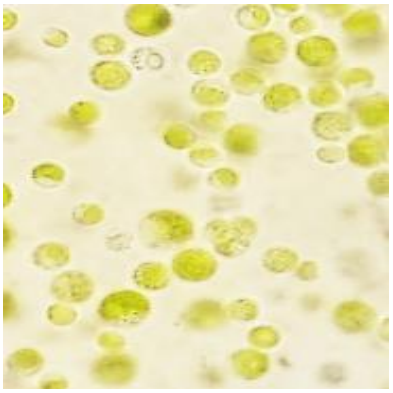

Figure II2 *Chlorella vulgaris* (06/03/2019)

Figure II3 *Lemna minor* (14/06/2017)

Appendices III

Data analysis by using ANOVA

Table III1 *Saccharomyces cerevisiae* growth rate on manganese

ANOVA based upon data entered as means, ± SE or ±95% CL & n					
	df	**SS**	**MS**	**F**	**P–value**
Treatment	6	0.0163	0.0027	52.6651	4.4530×10^{-16}
Residual	35	0.0018	5.1588×10^{-5}		
Total	41	0.0181			

Multiple comparison	**10 mmol m^{-3}**	**30 mmol m^{-3}**	**100 mmol m^{-3}**	**300 mmol m^{-3}**	**1000 mmol m^{-3}**	**3000 mmol m^{-3}**
Control	ns	ns	ns	ns	ns	*
10 mmol m^{-3}		ns	ns	ns	ns	*
30 mmol m^{-3}	ns		ns	ns	ns	*
100 mmol m^{-3}	ns	ns		ns	ns	*
300 mmol m^{-3}	ns	ns	ns		ns	*
1000 mmol m^{-3}	ns	ns	ns	ns		*
3000 mmol m^{-3}	*	*	*	*	*	

Note * = significant, ns = no significant

Table III2 *Saccharomyces cerevisiae* growth rate on manganese + 1 mmol m^{-3} EDTA

ANOVA based upon data entered as means, ± SE or ±95% CL & n

	df	SS	MS	F	P–value
Treatment	6	0.0116	0.0019	25.4837	2.0667×10^{-11}
Residual	35	0.0026	7.5646×10^{-5}		
Total	41	0.0142			

Multiple comparison	**10 mmol m^{-3}**	**30 mmol m^{-3}**	**100 mmol m^{-3}**	**300 mmol m^{-3}**	**1000 mmol m^{-3}**	**3000 mmol m^{-3}**
Control	ns	ns	ns	ns	ns	*
10 mmol m^{-3}		ns	ns	ns	ns	*
30 mmol m^{-3}	ns		ns	ns	ns	*
100 mmol m^{-3}	ns	ns		ns	ns	*
300 mmol m^{-3}	ns	ns	ns		ns	*
1000 mmol m^{-3}	ns	ns	ns	ns		*
3000 mmol m^{-3}	*	*	*	*	*	

Note * = significant, ns = no significant

Table III3 *C. vulgaris* yield rate on manganese

ANOVA based upon data entered as means, ± SE or ±95% CL & n					
	df	**SS**	**MS**	**F**	**P–value**
Treatment	6	0.0033	0.0005	4.1255	3.1015×10^{-3}
Residual	35	0.0047	1.3307×10^{-4}		
Total	41	0.0080			

Multiple comparison	**1 mol m^{-3}**	**2 mol m^{-3}**	**3 mol m^{-3}**	**5 mol m^{-3}**	**7 mol m^{-3}**	**10 mol m^{-3}**
Control	*	ns	ns	ns	ns	ns
1 mol m^{-3}		ns	ns	*	ns	ns
2 mol m^{-3}	ns		ns	ns	ns	ns
3 mol m^{-3}	ns	ns		ns	ns	ns
5 mol m^{-3}	*	ns	ns		ns	ns
7 mol m^{-3}	ns	ns	ns	ns		ns
10 mol m^{-3}	ns	ns	ns	ns	ns	

Note * = significant, ns = no significant

Table III4 *C. vulgaris* yield rate on manganese + 10 mol m^{-3} EDTA

ANOVA based upon data entered as means, ± SE or ±95% CL & n					
	df	**SS**	**MS**	**F**	**P–value**
Treatment	6	0.0015	0.0002	1.3411	0.2655
Residual	35	0.0063	$1.8071x10^{-4}$		
Total	41	0.0078			

Multiple comparison	**1 mol m^{-3}**	**2 mol m^{-3}**	**3 mol m^{-3}**	**5 mol m^{-3}**	**7 mol m^{-3}**	**10 mol m^{-3}**
Control	ns	ns	ns	ns	ns	ns
1 mol m^{-3}		ns	ns	ns	ns	ns
2 mol m^{-3}	ns		ns	ns	ns	ns
3 mol m^{-3}	ns	ns		ns	ns	ns
5 mol m^{-3}	ns	ns	ns		ns	ns
7 mol m^{-3}	ns	ns	ns	ns		ns
10 mol m^{-3}	ns	ns	ns	ns	ns	

Note * = significant, ns = no significant

Table III5 *C. vulgaris* electron transport rate on manganese

ANOVA based upon data entered as means, ± SE or ±95% CL & n					
	df	**SS**	**MS**	**F**	**P–value**
Treatment	6	1437.6769	239.6128	21.5977	1.9746×10^{-10}
Residual	35	388.3027	11.0944		
Total	41	1825.9797			

Multiple comparison	**1 mol m^{-3}**	**2 mol m^{-3}**	**3 mol m^{-3}**	**5 mol m^{-3}**	**7 mol m^{-3}**	**10 mol m^{-3}**
Control	ns	ns	*	*	*	*
1 mol m^{-3}		ns	*	ns	*	*
2 mol m^{-3}	ns		*	*	*	*
3 mol m^{-3}	*	*		ns	ns	ns
5 mol m^{-3}	ns	*	ns		*	ns
7 mol m^{-3}	*	*	ns	*		ns
10 mol m^{-3}	*	*	ns	ns	ns	

Note * = significant, ns = no significant

Table III6 *C. vulgaris* electron transport rate on manganese + 10 mol m^{-3} EDTA

ANOVA based upon data entered as means, ± SE or ±95% CL & n

	df	SS	MS	F	P–value
Treatment	6	2103.2919	350.5487	104.2259	7.7016×10^{-21}
Residual	35	117.7174	3.3634		
Total	41	2221.0093			

Multiple comparison	**1 mol m^{-3}**	**2 mol m^{-3}**	**3 mol m^{-3}**	**5 mol m^{-3}**	**7 mol m^{-3}**	**10 mol m^{-3}**
Control	ns	*	*	*	*	*
1 mol m^{-3}	ns	*	*	*	*	*
2 mol m^{-3}	*	ns	ns	ns	ns	ns
3 mol m^{-3}	*	ns	ns	ns	ns	ns
5 mol m^{-3}	*	ns	ns	ns	ns	ns
7 mol m^{-3}	*	ns	ns	ns	ns	ns
10 mol m^{-3}	*	ns	ns	ns	ns	ns

Note * = significant, ns = no significant

Table III7 *C. vulgaris* non–photochemical quenching on manganese

ANOVA based upon data entered as means, ± SE or ±95% CL & n					
	df	**SS**	**MS**	**F**	**P–value**
Treatment	6	0.0220	0.0037	29.2326	2.9893×10^{-12}
Residual	35	0.0044	1.2527×10^{-4}		
Total	41	0.0264			

Multiple comparison	**1 mol m^{-3}**	**2 mol m^{-3}**	**3 mol m^{-3}**	**5 mol m^{-3}**	**7 mol m^{-3}**	**10 mol m^{-3}**
Control	ns	*	*	*	*	*
1 mol m^{-3}	ns	*	*	*	*	*
2 mol m^{-3}	*	ns	ns	ns	ns	ns
3 mol m^{-3}	*	ns	ns	ns	ns	ns
5 mol m^{-3}	*	ns	ns	ns	ns	ns
7 mol m^{-3}	*	ns	ns	ns	ns	ns
10 mol m^{-3}	*	ns	ns	ns	ns	ns

Note * = significant, ns = no significant

.

Table III8 *C. vulgaris* non–photochemical quenching on manganese + 10 mol m^{-3} EDTA

ANOVA based upon data entered as means, ± SE or ±95% CL & n

	df	SS	MS	F	P–value
Treatment	6	0.0726	0.0121	66.2917	1.1860×10^{-17}
Residual	35	0.0064	1.8263×10^{-4}		
Total	41	0.0790			

Multiple comparison	**1 mol m^{-3}**	**2 mol m^{-3}**	**3 mol m^{-3}**	**5 mol m^{-3}**	**7 mol m^{-3}**	**10 mol m^{-3}**
Control	*	*	*	*	*	*
1 mol m^{-3}		ns	*	ns	*	ns
2 mol m^{-3}	ns		*	ns	*	ns
3 mol m^{-3}	*	*		*	*	*
5 mol m^{-3}	ns	ns	*		*	ns
7 mol m^{-3}	*	*	*	*		*
10 mol m^{-3}	ns	ns	*	ns	*	

Note * = significant, ns = no significant

Table III9 *L. minor* growth rate on manganese

ANOVA based upon data entered as means, ± SE or ±95% CL & n					
	df	**SS**	**MS**	**F**	**P–value**
Treatment	5	0.0294	0.0059	32.2495	1.4772×10^{-6}
Residual	12	0.0022	1.8212×10^{-4}		
Total	17	0.0316			

Multiple comparison	**10 mmol m^{-3}**	**30 mmol m^{-3}**	**100 mmol m^{-3}**	**300 mmol m^{-3}**	**1000 mmol m^{-3}**
Control	ns	ns	*	ns	*
10 mmol m^{-3}		ns	*	ns	*
30 mmol m^{-3}	ns		ns	ns	*
100 mmol m^{-3}	*	ns		ns	*
300 mmol m^{-3}	ns	ns	ns		*
1000 mmol m^{-3}	*	*	*	*	

Note * = significant, ns = no significant

Table III10 *L. minor* growth rate on manganese + 10 mmol m^{-3} EDTA

ANOVA based upon data entered as means, ± SE or ±95% CL & n					
	df	**SS**	**MS**	**F**	**P–value**
Treatment	5	0.0591	0.0118	40.8077	$4.0027Ex10^{-7}$
Residual	12	0.0035	$2.8971x10^{-4}$		
Total	17	0.0626			

Multiple comparison	**10 mmol m^{-3}**	**30 mmol m^{-3}**	**100 mmol m^{-3}**	**300 mmol m^{-3}**	**1000 mmol m^{-3}**
Control	ns	ns	ns	ns	*
10 mmol m^{-3}		ns	ns	ns	*
30 mmol m^{-3}	ns		ns	ns	*
100 mmol m^{-3}	ns	ns		ns	*
300 mmol m^{-3}	ns	ns	ns		*
1000 mmol m^{-3}	*	*	*	*	

Note * = significant, ns = no significant

Table III11 *L. minor* chlorophyll content *a* per leaf surface area on manganese

ANOVA based upon data entered as means, ± SE or ±95% CL & n					
	df	**SS**	**MS**	**F**	**P–value**
Treatment	5	216.4106	43.2821	41.2480	1.4671×10^{-12}
Residual	30	31.4794	1.0493		
Total	35	247.8900			

Multiple comparison	**10 mmol m^{-3}**	**30 mmol m^{-3}**	**100 mmol m^{-3}**	**300 mmol m^{-3}**	**1000 mmol m^{-3}**
Control	ns	*	*	*	*
10 mmol m^{-3}		*	*	*	*
30 mmol m^{-3}	*		ns	*	*
100 mmol m^{-3}	*	ns		ns	*
300 mmol m^{-3}	*	*	ns		*
1000 mmol m^{-3}	*	*	*	*	

Note * = significant, ns = no significant

Table III12 *L. minor* chlorophyll *a* content per leaf surface area on manganese + 10 mmol m^{-3} EDTA

ANOVA based upon data entered as means, ± SE or ±95% CL & n					
	df	**SS**	**MS**	**F**	**P–value**
Treatment	5	519.7239	103.9448	65.4476	3.1736×10^{-15}
Residual	30	47.6464	1.5882		
Total	35	567.3703			

Multiple comparison	**10 mmol m^{-3}**	**30 mmol m^{-3}**	**100 mmol m^{-3}**	**300 mmol m^{-3}**	**1000 mmol m^{-3}**
Control	*	ns	ns	ns	*
10 mmol m^{-3}		ns	*	*	*
30 mmol m^{-3}	ns		*	*	*
100 mmol m^{-3}	*	*		ns	*
300 mmol m^{-3}	*	*	ns		*
1000 mmol m^{-3}	*	*	*	*	

Note * = significant, ns = no significant

Table III13 *L. minor* relative growth rate on manganese

ANOVA based upon data entered as means, ± SE or ±95% CL & n					
	df	**SS**	**MS**	**F**	**P–value**
Treatment	5	0.0342	0.0068	30.2657	2.0921×10^{-6}
Residual	12	0.0027	2.2631×10^{-4}		
Total	17	0.0370			

Multiple comparison	**10 mmol m^{-3}**	**30 mmol m^{-3}**	**100 mmol m^{-3}**	**300 mmol m^{-3}**	**1000 mmol m^{-3}**
Control	ns	ns	*	ns	*
10 mmol m^{-3}		ns	*	ns	*
30 mmol m^{-3}	ns		ns	ns	*
100 mmol m^{-3}	*	ns		ns	*
300 mmol m^{-3}	ns	ns	ns		*
1000 mmol m^{-3}	*	*	*	*	

Note * = significant, ns = no significant

Table III14 *L. minor* relative growth rate on manganese + 10 mmol m^{-3} EDTA

ANOVA based upon data entered as means, ± SE or ±95% CL & n					
	df	**SS**	**MS**	**F**	**P–value**
Treatment	5	0.0578	0.0116	7.4338	2.1803×10^{-3}
Residual	12	0.0187	1.5543×10^{-3}		
Total	17	0.0764			

Multiple comparison	**10 mmol m^{-3}**	**30 mmol m^{-3}**	**100 mmol m^{-3}**	**300 mmol m^{-3}**	**1000 mmol m^{-3}**
Control	ns	ns	ns	ns	*
10 mmol m^{-3}		ns	ns	ns	*
30 mmol m^{-3}	ns		ns	ns	*
100 mmol m^{-3}	ns	ns		ns	*
300 mmol m^{-3}	ns	ns	ns		*
1000 mmol m^{-3}	*	*	*	*	

Note * = significant, ns = no significant

VITAE

Name **Mr. Wannapisit Thammakul**

Student ID **5930221005**

Educational Attainment

Degree	Name of Institution	Year of Graduation
Bachelor of Science (Fisheries, Fishery Biology)	Kasetsart University	2015